THE DEVELOPMENT OF AN EXPERIMENTAL TECHNIQUE FOR UG-2 ORE FLOTATION

By

Taswald Llewelyn Moodley

A thesis submitted in fulfilment of the academic requirements for the degree of Master of Science in Engineering in the School of Chemical Engineering

University of KwaZulu-Natal

School of Chemical Engineering

University of KwaZulu-Natal

Durban

February 2013

ABSTRACT

Production of platinum and associated metals is a major source of revenue for South Africa. Significant losses occur in the concentrating stage (10 to 15 per cent) and this research is focused on optimising platinum flotation. Research begins by conducting laboratory batch flotation tests. However, subsequent pilot-plant tests often produce different results. It is believed these differences arise from the artificial nature of laboratory techniques. This project was focused on improving flotation techniques in the laboratory.

The largest source of platinum in South Africa is the UG2 reef and two samples of this ore were used for testing: 'good' and 'bad' ore. These had different characteristics with regards to the recovery of PGMs and the presence of talc. The latter is an unwanted floatable mineral, which must be depressed to prevent excessive recovery.

The conventional laboratory test procedure makes use of batch tests in various sizes of flotation cells. The procedure was made more realistic, by using four stages of flotation, rather than just two, to mimic a typical platinum flotation plant. The use of four stages made it possible to separate the fast-floating and slow-floating stages and to control froth conditions accordingly. Attention was also given to the fact that in laboratory tests, water is often added to the 'cleaner' stage of flotation, to make up the level. Experiments showed that this dilution, which does not take place in practice, had a significant impact on overall efficiency.

A method of measuring frother concentration was developed and used to determine the realistic level of frother in cleaning tests. Tests at these levels of frother concentration showed that significant improvements could be made to plant performance, by making use of a thickener to reduce the frother concentration in the cleaning stages.

The improved test procedure was used on both good and bad ores, and the effect of regrinding was also tested. A combined solids recovery of 2 % over both cleaners was targeted for all test work. At this recovery, the regrinding of the bad ore increased the PGM recovery from 67 to 76 per cent at the cost of an additional 8 g/t depressant.

An investigation of the effect of frother concentration in the cleaning stage, using good ore, demonstrated that that rejection of chromite could be improved significantly by reducing frother concentration. The tests mimicked the use of a thickener to separate some of the water with a high concentration of frother. Tests conducted on the good ore showed that use of two thickeners, as opposed to none, reduced the Cr_2O_3 content of the final concentrate from 4.2 to 3.2 per cent for the equivalent concentrate mass and PGM recovery. The depressant requirement was also reduced from 67 to 55 g/t. These tests provided insight on how to improve performance on a platinum flotation plant, particularly when floating the bad ore.

PREFACE

I, Taswald Llewelyn Moodley declare that unless indicated, this thesis is my own work and that it has not been submitted for a degree at another University or Institution.

_____

Taswald Llewelyn Moodley

As the candidate's supervisor, I, Prof BK Loveday, approve this thesis for submission.

_____

Prof B.K Loveday

ACKNOWLEGEMENTS

I would like to thank my Lord and saviour Jesus Christ for the strength he gives me every day. None of this work would be possible without Him.

I would also like to thank the following individuals:

- Prof B.K Loveday for his steadfast support and assistance throughout the duration of my project.
- My parents, Sherine and Truter and sister, Sean for always encouraging and believing in me.
- The technical and support staff at the UKZN Chemical Engineering department for assisting me whenever necessary.
- Mintek, for both financial and technical support.
- The congregation and leadership at the Evangelical Bible Church Ladysmith, who have supported and mentored me through all my endeavours.
- Astin, Terrence, Ash, Surekha, Dookie, Damian and Manogran for their constant support and help throughout my studies.

CONTENTS

LIST OF FIGURES

LIST OF TABLES

NOMENCLATURE

SYMBOL	DESCRIPTION	UNITS
v_a	SUPERFICIAL FLUX VELOCITY	$m.min^{-1}$ or $m^3.m^{-2}.min^{-1}$
γ	SURFACE TENSION	$N.m^{-1}$
θ	DIAMETER	mm
θ	CONTACT ANGLE	degrees [^{o}]
h	LIQUID HEIGHT	cm
ρ	DENSITY	$kg.m^{-3}$
g	UNIVERSAL GRAVITATIONAL CONSTANT	$m.s^{-2}$
r	RADIUS	mm
η	VISCOSITY OF THE LIQUID	$kg.m^{-1}.s^{-1}$
x	MILLING TIME	minutes
y	CUM. % PASSING 75 µm	%
E_r	PERCENTAGE ERROR	%

1 INTRODUCTION

Wills and Napier-Munn (2005) stated "*Flotation is undoubtedly the most important and versatile mineral processing technique, and both its use and application are continually being expanded to treat greater tonnages and to cover new areas.*"

Prior to understanding what froth flotation is, it is important to point out exactly where it fits into the entire process on a typical platinum concentrator plant. The objective in any concentrator plant is to separate valuable minerals, in this case platinum and other metal sulphide minerals, from gangue or waste material. The process description given will be based upon UG-2 ore, a typical platinum bearing ore in South Africa:

The beneficiation process shown in Figure 1 contains four stages in the following order: Mining, concentrating, smelting and refining. Froth flotation is part of the concentrating stage. At each stage, the ratio of PGMs to gangue minerals is increased thus improving the overall concentrate grade. UG-2 ore typically contains a mass percentage of 0.0005% PGMs (Jones, 1999). In terms of head grade, this is about 5 g/t.

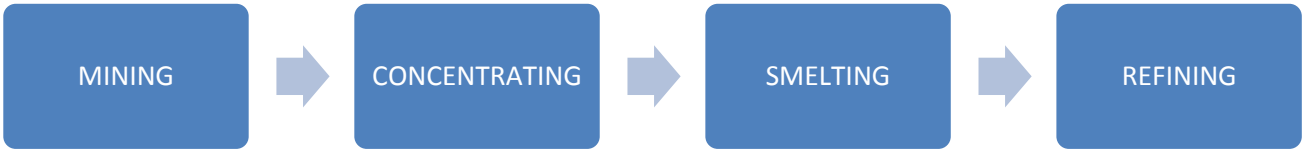

Figure 1: Flow sheet of a typical PGM concentration process

This mined ore is initially crushed and milled to liberate the PGMs by reducing the particle size. This serves as the feed to the flotation process. There is an upgrading of the concentrate at each stage of the flotation process to produce a final PGM concentrate grade of 0.01 to 0.04% (or 0.015% PGMs). The concentrate is then dried, smelted and finally hydrometallurgy is used separate the valuable minerals from the base minerals to obtain a final concentration of approximately 99.9% PGMs (Jones, 1999).

At each upgrading stage, there is an inadvertent loss of PGMs in an effort to separate them from the gangue minerals. However, the losses incurred during the mining and concentration stages account for the largest PGM losses. The cumulative PGM losses are about 15% after the flotation stage. The remaining stages have combined PGM losses of less than 5%. Thus, most of the research in the mineral beneficiation industry is focused on finding ways of improving the recovery and reducing the losses of PGMs in the mining and concentration stages, in particular the flotation stage.

Froth flotation is a process in which valuable and gangue minerals are separated from each other. This separation is based on the differences in surface properties of the various minerals. The ore is ground in the presence of water to a size at which adequate liberation of the valuable minerals from the gangue minerals has been achieved. The water-ore mixture is

referred to as the pulp. The laboratory procedure involves placing the pulp in a flotation cell and adding reagents to alter the surface properties of the particles, rendering the valuable minerals hydrophobic. The pulp is then agitated by means of a stirring device whilst air is simultaneously bubbled through it. The particles are then carried to the surface of the pulp where they form a mineralized froth, which migrates to the edge of the vessel (known as the launder). Thus, the process is referred to as froth flotation (Jan, 1982).

There are two main performance factors that describe the flotation process viz. the concentrate recovery and grade. The concentrate refers to the minerals obtained from the froth, usually removed by scraping in laboratory tests. The recovery of valuable minerals obtained in the concentrate is measured as a percentage of the valuable minerals present in the feed. The concentrate grade is the concentration of valuable minerals in the concentrate. Both the recovery and grade depend on chemical properties (pH, reagents etc.) and hydrodynamic conditions (agitation, aeration etc.) within the cell (Çilek and Yılmazer, 2003). The aim of any flotation process is to obtain the maximum possible concentrate grade and PGM recovery.

Froth flotation has been successfully employed as a separation technique in the mining, mineral, metallurgical and chemical industries. Its major applications are in the minerals processing industry where it accounts for about 95% of the world base metal production annually. Processing of crushed ore via this technique totals approximately two billion tonnes annually (Ives, 1984).

It was initially used to concentrate the sulphides of copper(Cu), lead(Pb) and zinc(Zn) but nowadays it is used to process the sulphides of platinum (Pt) and nickel(Ni) and gold(Au) (Wills and Napier-Munn, 2005).

South Africa is responsible for the bulk of the world's platinum group metal (PGM) production (Deglon, 2005). Platinum is a major source of income and 80% of the world's platinum reserves are found in South Africa. Moreover, South African mines supply 74% of the world's platinum demand (Jones, 1999). The focal point of South African production is the Bushveld Igneous Complex (BIC) – a very large ore body containing several layers (reefs) in which iron, chromium and platinum minerals are concentrated. There are three main types of PGM bearing reefs namely; the Merensky Reef, the Platreef and the UG-2 chromitite layer (Xiao and Laplante, 2004). Due to the diminishing supplies of Merensky Reef and the scarce locations of Platreef, most recent flotation research has been focused on improving the recovery of PGM's from UG-2 ore (Jones, 1999).

The valuable base metals contained within UG-2 ore account for less than 0.1% of the mass of the reef whilst the primary gangue minerals account for approximately 26% (Xiao and Laplante, 2004). The PGM's contained within the UG-2 ore are difficult to recover due to the high talc content (1-3 wt. %), high chromite content (75 wt. %) and known liberation problems due to composite particles compared to Merensky ore (Hay and Roy, 2010).

The initial work in this thesis was performed on a sample of UG-2 ore, of unknown origin, known to possess poor flotation characteristics. This was termed 'bad ore'. A new laboratory

test procedure was developed to simulate conditions on a plant and tests on the 'bad ore' were used to illustrate how platinum recovery could be optimised. The test procedure was then applied to a UG-2 ore which possessed favourable flotation characteristics, termed 'good ore'.

According to Deglon (2005), "*most South African platinum concentrators use mechanically agitated flotation cells"* These cells have both a stator and a rotor to suspend the pulp minerals. Compressed air is dispersed through the pulp via the stator. It is delivered via a pipe through the shaft of the rotor (Jan, 1982). Industrially, these machines are arranged in series alongside each other. This is referred to as a cell bank. There are weirs placed between the impellers to create the bank series of cells. In the absence of these weirs, it is referred to as "open-flow" or "free-flow" flotation (Wills and Napier-Munn, 2005).

A significant amount of gangue mineral is recovered in a single flotation stage and several stages are required to improve the separation, similar in principal to multistage distillation. Conventional laboratory work is normally performed in two stages viz. a rougher followed by cleaner stage. This two-stage process is used to simulate industrial process conditions. There are many different types of circuits designed to optimise both the recovery and grade of the flotation process (Wills and Napier-Munn, 2005). Industrially however, there are multiple flotation stages with pulp recycles between certain stages in order to recover the maximum amount of PGM's and depress floatable gangue minerals. In order to simulate this, a simplified 4 stage circuit consisting of a rougher, scavenger and two separate cleaning stages was proposed. This circuit separated the concentrates into two different grades viz. high and low, or 'fast floating' and 'slow floating'.

This circuit allowed each stage to be evaluated and optimised separately. For example, a re-grind of the rougher tailings was tested to improve the liberation of PGM's contained within the composite particles. The difficulty of this circuit configuration was that experimental conditions needed to be optimised in each cell individually and then the circuit needed to be optimised as a whole.

According to Wiese et al. (2011) "*Batch flotation tests have long been used to optimise reagent performance for application to large scale plants*."

The objective of this study was to perform batch flotation tests using improved experimental techniques to recover the largest possible amount of PGM's in an economically viable concentrate mass. It is believed these improved techniques will make batch flotation tests more realistic and hence make them more effective for testing reagent and circuit changes. The differences in the recoveries of PGMs between laboratory and industrial scale is due to the differences in how the froth phase influences the PGM's recovery via true flotation (Martyn P, 2010). The investigation focused on the cleaner stages where the effect of depressant dosage, impeller speed and other factors on the flotation recovery and grade were examined.

2 LITERATURE REVIEW

2.1 PRINCIPLE OF FROTH FLOTATION

Froth flotation is commonly used in the minerals industry for the extraction of valuable minerals (Koh and Smith, 2011). This is a selective process and the separation is based upon the surface property differences between the minerals involved. These differences can either be "*naturally occurring or induced by the addition of surfactants*" (Muganda et al., 2011).

Laboratory flotation can either be performed in a batch or continuous mode. Laboratory test work is usually performed in a batch mode. This test work is said to provide the basis for the design of commercial plants. This description for laboratory froth flotation is summarized in Figure 2 below:

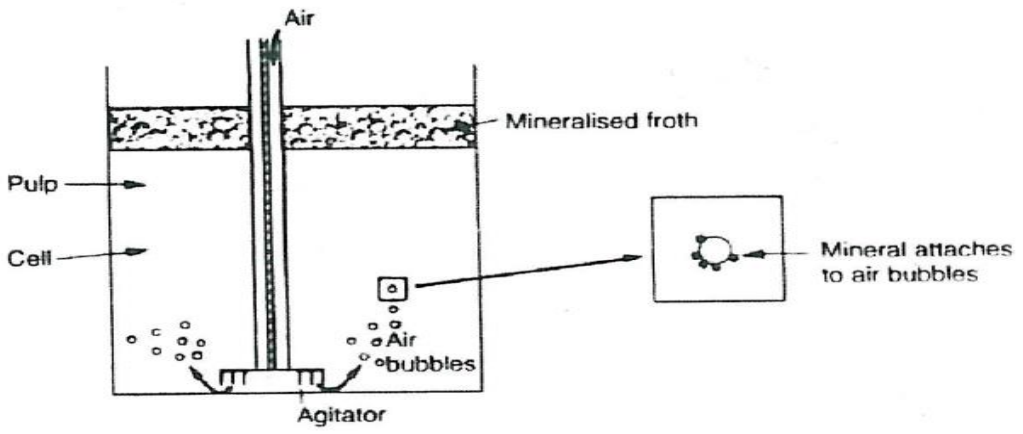

Figure 2: Diagram depicting the froth flotation mechanism (Wills and Napier-Munn, 2005)

UG2 ore is a mixture of both valuable and gangue minerals. The first beneficiation step is to liberate some of these valuable minerals from gangue using a suitable grind (Ives, 1984). Flotation can only be applied to relatively finely ground ore (Wills and Napier-Munn, 2005). However, fine grinding is expensive and there is an economic trade-off between the amount of grinding used and the PGM recovery obtained.

The ore is normally ground in the presence of water and then transferred to a flotation cell, before adding chemicals. Compressed air, regulated via a flow measurement device, is drawn through a shaft. A rotating impeller disperses this air forming fine bubbles. The hydrophobic particles attach to air bubbles that are dispersed through the mixture. These particles are then carried to the surface of the mineralised froth where they are scraped off manually (Wills and Napier-Munn, 2005, Jan, 1982).

The process of PGM recovery and upgrading in froth flotation comprises of two primary focus areas namely;

1. Pulp phase
2. Froth phase

2.2 PULP PHASE

The pulp phase is primarily concerned with the recovery of valuable minerals (Wiese et al., 2011). This is achieved by creating the physico-chemical environment to *"promote bubble-particle collision, successful attachment of the valuable hydrophobic particles and the transport of these mineral laden bubbles to the froth phase*" (Bradshaw et al., 2005).

The two sub-processes that occur in the pulp phase are;

- Bubble-particle collision.
- Transportation of the attached particle to the froth phase.

Good chemical and hydrodynamic conditions are required for the selective attachment of PGM's to air bubbles. Chemical conditions are responsible for the collection of particles whilst hydrodynamic conditions ensure effective solids suspension within the pulp (Van der Westhuizen and Deglon, 2007).

Chemical reagents (or surfactants), which alter the surface properties of either the valuable or unwanted mineral, are added to condition the pulp. The surface properties are altered to achieve the desired effects, with the particles becoming either hydrophobic (incompletely wetted by water phase) or hydrophilic (completely wetted by the water phase).

Wills and Napier-Munn (2005) noted that the degree of hydrophobicity (or wettability) of a particle surface plays an important role in the adsorption of particles onto the surface of bubbles. This is measured by the contact angle (θ). According to Muganda et al. (2011) the "*attachment of a particle to a bubble is influenced by the contact angle…".* This is the angle is measured on the liquid phase side, between the solid surface and the tangent to the liquid surface at the contact point of the three interface's viz. solid, liquid, air (Jan, 1982).

The contact angle is determined by the interfacial tensions of these three interfaces (Ives, 1984). These tensions are shown in Figure 3 and are the surface energies between solid and air ($\gamma_{s/a}$), solid and water ($\gamma_{s/w}$) and water and air ($\gamma_{w/a}$). The greater the contact angle, the greater the forces of adhesion between the bubble and the solid. Thus, hydrophobic particles generate higher contact angles compared to hydrophilic particles (Wills and Napier-Munn, 2005). This means that hydrophobic particles are more selectively recovered in the froth at the expense of hydrophilic particles.

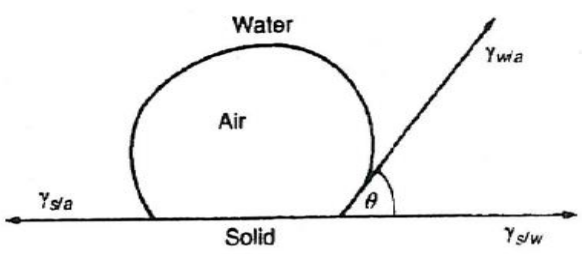

Figure 3: Contact angle between bubble and particle in aqueous medium (Wills and Napier-Munn, 2005)

The equilibrium force balance of the above figure is;

$$\gamma_{s/a} = \gamma_{s/a} + \gamma_{s/a} \cos\theta$$

The surfaces of valuable minerals are chemically altered such that they become hydrophobic and hence selectively attach to air bubbles and are carried to the surface of the froth phase. This mechanism, known as "true flotation", is the preferred transport mechanism within the pulp. However, there is a strong possibility of the recovery of both gangue and valuable minerals in the production concentrate. This is the non-selective mechanism of entrainment and entrapment within and between the streamlines of the rising bubbles respectively (Wills and Napier-Munn, 2005).

2.2.1 COLLECTORS

Collectors are organic compounds which react with the surfaces of valuable minerals, making them water repellent. They can either be ionising compounds that dissociate completely in water or non-ionising compounds that are insoluble in water (Wills and Napier-Munn, 2005).

Time is needed for the action between the collector and the particle surface to occur (Wills and Napier-Munn, 2005). This is achieved by either chemically or physically bonding to the surface of the mineral. In the latter, the bonding is weak and reversible. This means that as the concentration of collector in the cell decreases, the collector will desorb from the mineral surface. The bonding in the former is irreversible and limited to a small area on the active sites of the mineral surface (Crozier, 1992). These active sites on the particles refer to "kinks and ledges, emerging dislocations and lattice defects" on the surface of the particles (Jan, 1982).

Figure 4 below illustrates that collectors consist of both a polar and non-polar group. The former reacts with the mineral surface whilst the latter repels the water to create the hydrophobic surface (Lotter and Bradshaw, 2010).

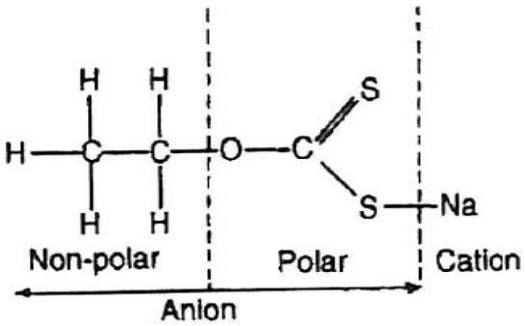

Figure 4: Structure of sodium ethyl xanthate collector (Wills and Napier-Munn, 2005)

Lotter and Bradshaw (2010) stated that sulphide minerals are semi-conductors viz. "*they can either accept or donate electrons in an electrochemically active system*". Collectors bond to the solid surface with their polar groups. These bonds can be electrical, physical or chemical as stated before. The non-polar group is orientated towards the solution and, in this way, the

particles become hydrophobic (Wills and Napier-Munn, 2005). This is depicted in Figure 5 below:

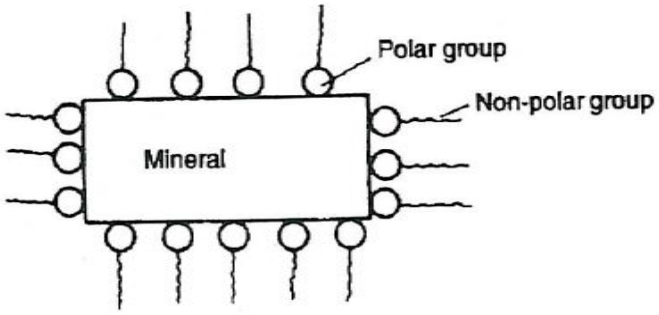

Figure 5: Collector adsorption on mineral surface (Wills and Napier-Munn, 2005)

Anionic collectors are widely used in mineral flotation. These are classified according to the structure of the polar group in the molecules as either oxyhydral or sulphyhydral. Wills and Napier-Munn (2005) stated that "the xanthates are the most important for sulphide mineral flotation and they are the most widely used thiol collectors. The collector used in this investigation was Sodium Isobutyl Xanthate (SIBX).

SIBX belongs to the group of thiol collectors known collectively as xanthates. They are classified as sulphyhydral based on the bivalent sulphur present the molecular structure. Typical examples of xanthates used include ethyl, isopropyl, isobutyl and hexyl types. They are named after the non-polar hydrocarbon group 'R' that consists of hydrocarbon groupings with one to six carbon atoms (Wills and Napier-Munn, 2005). The length of this 'R' group affects the behaviour of the collector. Lotter and Bradshaw (2010) gave the following sequence of increasing collector stability, with reference to the 'R' group in xanthate collectors:

Methyl< ethyl< n-propyl< n-butyl< isopropyl

Lotter and Bradshaw (2010) stated that "an increase in the length of the chain reduces the concentration of collector needed for effective flotation." It was also found that the orientation of the collector molecules on the surface of the minerals varied according to the length of the "R" groups. Shorter chained "R" groups lie perpendicular to the mineral surface whilst longer chained "R" groups lie horizontal to the mineral surface (Lotter and Bradshaw, 2010).

2.2.2 THE EFFECT OF COLLECTORS ON SULPHIDE MINERAL FLOTATION

The concentration of collector in the pulp is an important variable in the flotation of sulphide minerals. It is generally acceptable practise to minimise collector addition. A thin monomolecular layer of collector on the particle is optimal. This will not hinder the non-polar group that makes the particle surface hydrophobic. The use of excess collector reduces the selectivity of the process. A larger concentration of collector implies multiple monomolecular layers on valuable minerals. This reduces the proportion of non-polar groups of the collector molecule that are oriented towards the liquid phase. Thus, the recovery of valuable mineral in

the concentrate is reduced (Wills and Napier-Munn, 2005). Excess dosages of collector tend to coat the surfaces of unwanted particles and make them hydrophobic. These particles are then recovered in the concentrate thus reducing the overall grade. There is also the increased cost of using a higher collector dosage (Wills and Napier-Munn, 2005).

It is difficult to remove an anionic collector from the surface of the particle due to the strong bonding involved particularly when chemical bonds are formed. A generally acceptable practise is to use longer chain (referring to the length of the "R" group) collectors to impart hydrophobicity to particles. A lower concentration of longer chain collectors is equivalent to a higher concentration of shorter chain collectors. The longer chained collectors thus require smaller dosages to achieve the same recovery of mineral (Wills and Napier-Munn, 2005).

It is important to consider the particle properties before a collector is selected for flotation. In some cases, a long chained collector is used initially to float all the valuable minerals. The longer chained collectors produce higher recoveries but lower grade concentrates (Crozier, 1992). They are usually used in the rougher stages, thereafter a short chained collector, of high concentration, is used to recover the particles that are difficult to float. In this way, the overall selectivity of the process is ensured (Wills and Napier-Munn, 2005).

The use of excess collector has also been shown to have a negative effect on the movement of solids in the froth to cell launder, due to froth weakening. The increased particle hydrophobicity results in the froth being dry and immobile (Ata, 2012).

Composite particles comprise a valuable mineral attached to the surface of an unwanted mineral. Thus these minerals behave as a complex particle with varying surface properties. Composite particles are a result of ineffective mineral liberation during grinding. These pose a significant problem during flotation. The selective collectors merely attach to the surface of the valuable mineral in the complex. The effectiveness of the collector action depends on the way in which the valuable mineral is orientated in the particle complex. That portion coated with collector, usually the exposed surface of the valuable mineral, will behave as hydrophobic. The remainder of the uncoated particle surface will behave hydrophilically. Thus the probability of flotation of these particles is largely dependent on the proportion of the exposed surface containing the valuable mineral. The flotation of this composite particle will depend on the impact point of the bubble on the particle. It must strike the particle at the exposed surface of the valuable mineral, where it is hydrophobic, so that it can attach. This collision period is short so the particle must quickly attach to the bubble in order to be carried to the froth.

2.2.3 FROTHERS

These heterophilic surface active reagents can be divided into two categories, those that are slightly soluble or those that are completely soluble in water (Crozier, 1992, Wills and Napier-Munn, 2005). Examples of frothers that are partially soluble in water include aliphatic alcohols, alkoxy paraffin's and natural oils like eucalyptus. Polyglycol and polyglycerol ethers are examples of frothers that are completely miscible in water. Crozier (1992) stated that these glycols produce "*compact, long lasting froths*" that disintegrate quickly once in the

launders. Glycols produce more selective froths compared to their slightly soluble counterparts.

Frothers manufactured by the Dow Chemical Co. are named according to their molar weights. For example, the frother used in this thesis was Dowfroth 200 (DOW200), which has a molar weight of 206 g/ mol (Crozier, 1992). These polyglycol frothers are the strongest surface active frothers that are used and have been found to be very effective. This means they can support the masses of larger particles and high grade feed materials (Wills and Napier-Munn, 2005). It has been stated that a good performing frother should have negligible collecting properties. When they are similar to ionic collectors, like oleates, frothers form froths that are far too stable to allow for sufficient transport of valuable mineral. The froth becomes too stable thus causing a problem in further processing. The froth should be just stable enough to transport the valuable mineral to the launder, then disintegrate quickly thereafter (Wills and Napier-Munn, 2005).

Frothers play an important role in flotation. They stabilize the bubble formation in the pulp to allow for selective drainage of entrained gangue minerals by stabilizing the froth phase to a certain extent (Wills and Napier-Munn, 2005).

2.2.4 MECHANISM OF FROTHER-BUBBLE INTERACTION

It is important to note that natural residual charges are present on the particle surface that exists at the instant of collision. Jan (1982) said that it is due to the "high degree of heterogeneity of the particle surfaces". It was also stated that another role of a frother is to replace the natural repulsive forces at the bubble-particle interface, with those of attraction. This is accomplished by frothers aligning their dipoles correctly at the instant of collision. This ensures bubble-particle adhesion at the instant they collide.

Frothers are organic reagents that are adsorbed on the air-water interface. They consist of a polar and non-polar group. The polar groups combine with the water phase and the non-polar groups, which are hydrophobic, are pushed into the air phase. These molecules form around the air bubble, with their polar groups orientated outside the air bubble towards the water phase, with their non-polar groups situated on the surface of the air bubble. They stabilize the air bubbles by reducing the surface tension between the water and the bubble surface (Wills and Napier-Munn, 2005).

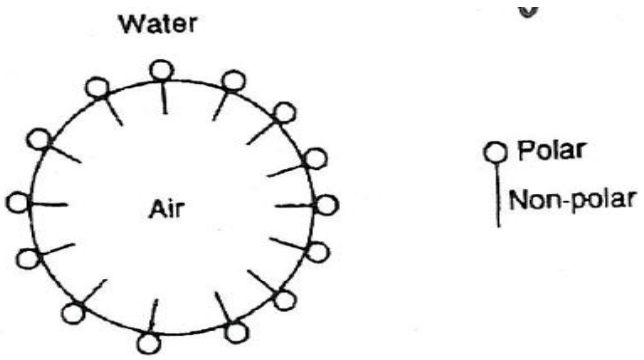

Figure 6: Attachment of frother molecules on bubble surface (Wills and Napier-Munn, 2005)

There are a number of features which must be considered in selecting a particular frother. It usually starts by assessing the PGM recoveries obtained by using a sample set of five different frothers (Dowfroth 200, pine oil etc.) (Jan, 1982). A frother must be selected so that a suitable froth is formed, ensuring the selectivity of the process is maintained without affecting the overall recovery of valuable minerals (Ekmekçi et al., 2003).

2.2.5 DEPRESSANTS

Depressants are used to selectively reduce the recovery of certain gangue minerals that are recovered in the concentrate (Bradshaw et al., 2005), by making them hydrophilic. This means that those particles will not be able to attach to the surface of the air bubble. In this way, the overall selectivity of the process is improved. There are many types of inorganic and organic depressants (Wills and Napier-Munn, 2005). Examples of inorganic depressants include sodium cyanide, zinc sulphate, sulphuric acid etc. These are used when the properties of two or more particles are so similar that a collector can't selectively adsorb onto the surface of the valuable particle. Lime and cyanide are the most widely used inorganic depressants (Crozier, 1992). Cyanide reacts with most sulphide minerals under alkaline conditions, to form a stable metal-cyanide layer, which prevents formation of the metal xanthate precipitate on the surface of the particle. It can also displace an existing xanthate layer on a mineral. Cyanide is very toxic and has been shown to dissolve Gold and Silver (Wills and Napier-Munn, 2005).

Natural polysaccharides (i.e. tannic acid, starch and glues etc.) or synthetically produced polyglycols can be used to depress minerals that have natural hydrophobicity. There is a growing popularity for the use of polymeric organic depressants. They are less hazardous than some inorganic depressants. Carboxymethyl cellulose (CMC) and modified guar gum (guar) are popular polymeric depressants used in the South African PGM industry (Corin and Harris, 2010). The structural units for each of these types of depressants are shown in Figure 7:

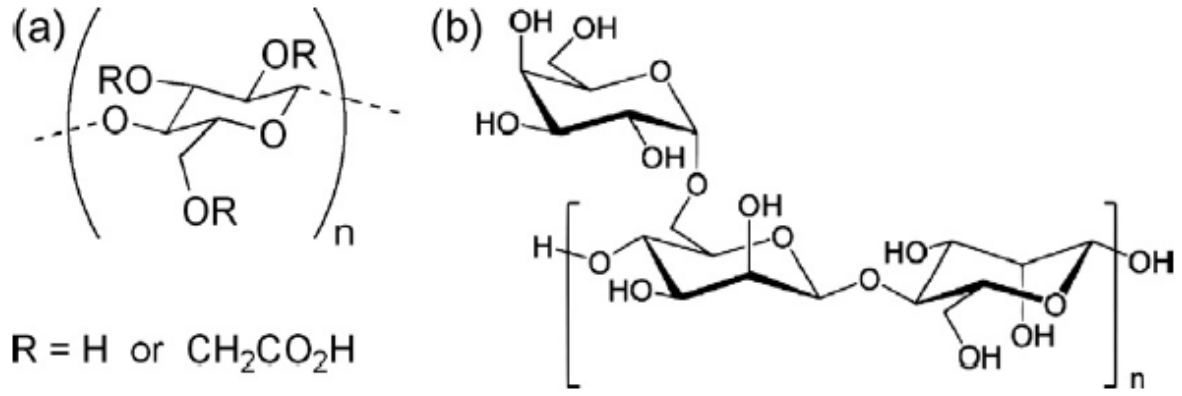

Figure 7: Structural units of (a) CMC (b) guar (Corin and Harris, 2010)

These depressants both adsorb onto the surfaces of talcaeous gangue minerals, making the surfaces hydrophilic thereby reducing their recovery in the concentrate. The branched structural units of guar type depressants (shown in (b) above) possess more hydroxyl groups

compared to the straight chained CMC type (shown in (a) above) thus are very soluble in water and don't possess any charge once adsorbed. CMC type depressants ionise in solution and have a negative charge. Thus for CMC type depressants, a charge is passed onto the mineral when it is adsorbed and particularly at high dosages, these surfaces repel each other (Bradshaw et al., 2005). This is due to the presence of a large number of carboxylic groups (shown as R in Figure 7(a)). The substitution of the hydroxyl groups by carboxylic groups is known as the degrees of substitution (DS).This reflects the average number of carboxylic acid groups per glucose unit (Oudhoff K.A et al., 2004). The DS value can range between 0 and 3 due to the molecular structure. This value depends on various factors including the molecular weight of the anhydrous glucose unit, substituent group etc. CMC depressants have a DS of 0.7 (Corin and Harris, 2010) compared to guar depressants which have very low DS.

Guar depressants adsorb more strongly onto talcaeous minerals but require large dosages compared to CMC. Thus a CMC type depressant, KU5, was selected for these experiments. It is known that increased charge can cause froth destabilising effects and thus reduce the recovery of gangue particles.

2.2.6 MECHANISM OF BUBBLE FORMATION

The nascent bubble flotation mechanism is widely regarded as an accurate representation of bubble-particle interaction. It is governed by the interaction of both frother and collector molecules at selective points on the surface of the mineral. This mechanism is only valid at low reagent dosages as is the case in sulphide mineral flotation (Crozier, 1992).

Smaller bubbles (micro-bubbles) are thought to form at these points of frother-collector interaction. Secondary bubbles are thought to form simultaneously on the surface between the frother and collector molecules. These bubbles are attached to the naturally hydrophobic gangue minerals, as is the case with talc embedded in the grains of pyroxene. The minerals then nucleate micro-bubbles, which act as transport links for the formation of bigger bubbles. These can also attach to other bubbles recirculating in the cell (Crozier, 1992).

In the case of a batch flotation cell, formation of bubbles occurs in two steps. The initial cavitation induced air bubbles form at the impeller blades. These then break up into the micro air bubbles described by Crozier (1992). This is shown in Figure 8 below:

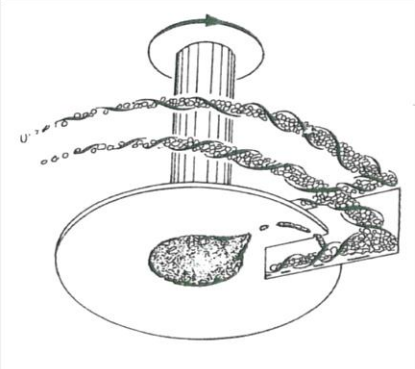

Figure 8: Bubble vortex format ion (Ives, 1984)

Once a particle has been attached to the surface of a bubble it is carried to the surface of the froth. As the bubble rises, it forms streamlines around it. A thin film of liquid surrounds the bubble and the collected particles are held within this film. Obviously, larger particles with a higher mass have higher momentum compared to smaller particles. This increases the probability of them piercing through the streamlines surrounding the bubble. The buoyancy of the bubble then lifts the attached particle to the surface where it is collected in the froth phase (Jan, 1982).

The Grainger-Allen theory of bubble formation states that air cavities are formed behind the obstruction to the flow (i.e. the impeller). The edge of the cavity is then sucked into the blades of the impeller, thus creating finer bubbles from the cavity. This edge of the air cavity is known as the "wake" (Ives, 1984). This is shown in the Figure 9. The particles tend to accumulate here due to their gravity. Once this tail becomes saturated with material, the particles begin to detach from it.

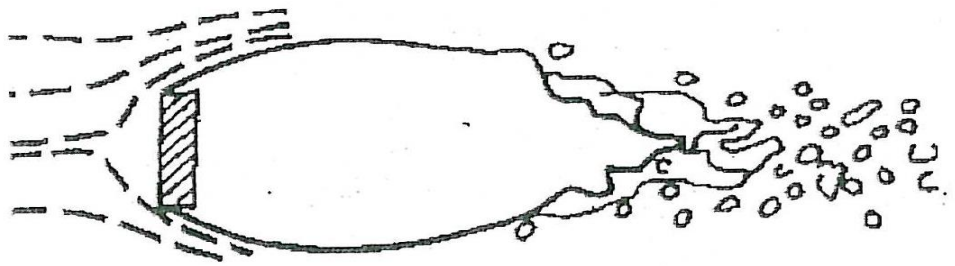

Figure 9: Cavitation mechanism of bubble formation (Crozier, 1992)

2.3 FROTH PHASE

The froth phase is responsible for the *"upgrading of the valuable materials reporting to the concentrate without loss of valuable materials*" (Bradshaw et al., 2005).

As the bubbles rise through the mineralised froth, the film between the bubbles becomes thinner and coalescence occurs, thus altering the bubble size and proportion of water. This implies that these two factors vary at different froth heights. The liquid fraction is generally higher at the froth-pulp interface compared to higher portions of the froth. This results in the bubbles themselves becoming distorted as they rise. They can enter the froth-pulp interface as spherical in shape and become polyhedral at the top layer of the froth (Ata, 2012).

As the water drains, the bubble Plateau borders (or distance between the bubbles) becomes smaller. This thinning of these borders increases the chances of bubble coalescence. The drainage in froth is a function of the viscosity of the liquid. The less viscous the liquid surrounding the bubbles, the greater is the rate of drainage of the liquid layers between the bubbles (Jan, 1982).

2.3.1 MECHANISM OF FROTH DRAINAGE

Plateau borders are the curved regions that separate the thin films of the bubbles from the bulk pulp (Ives, 1984). The thinning of the liquid film occurs initially by drainage due to gravity of the liquid, then by movement of the liquid within the film itself (Jan, 1982). These films can be either fast or slow draining depending on the properties of the air-water interface (Crozier, 1992). The plateau borders are shown in Figure 10:

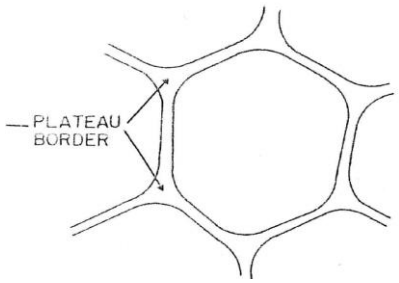

Figure 10: Plateau borders (Jan, 1982)

This bubble coalescence, along with bubble bursting and froth overloading, is responsible for the detachment of hydrophobic particles originally attached to the bubbles. This bubble bursting occurs only at the surface of the froth layer. A portion of these hydrophobic and gangue particles is entrained into the froth via the wake of the bubbles (Ross, 1997).

The detached particles can re-attach to other rising bubbles or be drained all the way back into the pulp phase. It is assumed that the amount of detached particles recovered in the froth phase far outweighs those recovered by rising bubbles in the pulp phase (Ross, 1997). The hydrophilic particles are less likely to re-attach compared to the hydrophobic particles. The interstitial liquid, constantly being drained, also contains a large amount of entrained gangue minerals. Thus the overall selectivity of the flotation process is improved by a well-drained froth. This implies that more hydrophobic, valuable minerals are recovered compared to gangue minerals.

Hydrophobic particles, in addition to froth liquid fraction have been shown to cause bubble coalescence and rupture. When a particle channels the gap between two adjacent bubbles, it will move to a central position until a contact angle condition is met.

There exists a critical degree of wetting which enables the prediction of whether or not the particle will cause bubble coalescence. This is based on the contact angle that the bubble forms. If this angle (θ) is less than 90^0, then it is deemed below this critical degree of wetting and the bubbles will not coalesce. This is shown in A in Figure 11. However, if it is greater than 90^0 then the particle will penetrate both sides of the liquid films resulting in bubble coalescence. This is shown in B in Figure 11.

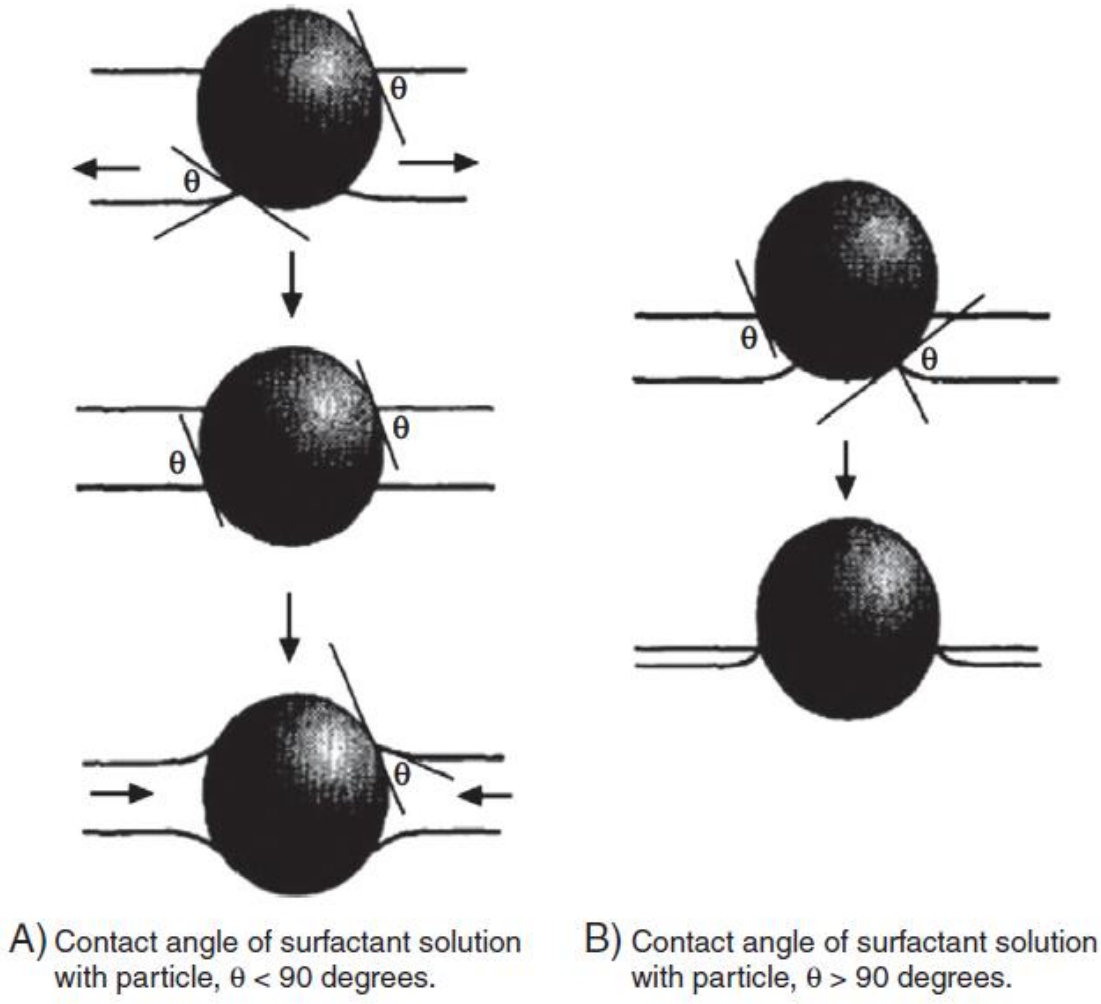

Figure 11: Particle behaviour in bubble coalescence (Ata, 2012)

Hence extremely hydrophobic particles ($\theta > 90^0$) are not easily recovered in the flotation concentrate due to bubble coalescence and rupturing. The majority of particles recovered in the flotation concentrate have contact angles between 30^0 to 50^0 as these particles are assumed to attach to and be transported through the froth without penetrating the lamella (Ata, 2012).

Bubble coalescence causes the froth to reach a maximum particle carrying capacity (or froth loading). This means that the froth becomes saturated with particles thus any further particle recovery is not possible. When bubbles coalesce, the oscillations between the bubbles can cause particles to detach. Larger particles, due to their higher mass and momentum detach more readily than smaller particles. Furthermore, it has been found that if a bubble is coated with more particles (high particle loading) prior to the coalescence, then particle detachment after coalescence is reduced (Ross, 1997).

2.4 MECHANICAL FACTORS

Mechanical impellers and induced air flow are factors responsible for efficient gas dispersion, particle suspension and flotation within the cell (Deglon, 2005). Yang and Aldrich (2006) stated "*Aeration rate and impeller speed are important operational variables in flotation and*

the controlling of them is significant for improving the flotation performance." The impeller imparts energy to the contacting pulp. This energy is responsible for the creation of pulp movement and flow within the float cell.

2.4.1 HYDRODYNAMICS

Hydrodynamics refer to the bulk flow of pulp in the cell according to Deglon (2005). The rotation of the impeller creates a certain flow pattern within the cell. This is also known as an average path of the bulk pulp flow. The dimensions of the flotation cell (viz. size, shape) and impeller properties (geometry, rotational speed) affect these flow patterns.

The fluid is dispersed by the impeller in three directions viz. radial, axial and tangential. These form fluid jets that disperse into the bulk of the pulp. These fluid jets carry kinetic energy, which is transferred to the pulp translating into turbulence within the cell. The fluid is then circulated back to the impeller to be redistributed to the pulp. Thus the flow patterns of the fluid within the cell are continuous (Deglon, 2005).

2.4.2 TURBULENCE

Turbulence is responsible for basic sub processes like *"bubble-breakup, particle dispersion and bubble-particle contacting."* The phenomenon responsible for converting the kinetic energy possessed by the fluid into turbulence is called "vortex stretching" (Deglon, 2005). The modelling of this turbulence is done with the use of Navier Stokes equations relating to the formation of physical vortices within the cell volume (Deglon, 2005). There are two main types of eddies that have been shown to influence the sub processes of flotation namely "*inertial sub range eddies*" and "*viscous dissipation eddies."* Modelling of the turbulence in the cell is beyond the scope of this project.

Çilek and Yılmazer (2003) stated that the hydrodynamics occurring within the cell can be described using dimensionless groups such as Reynolds number, Froude number and Air Flow Number (AFN). These ratios are based on physical variables occurring within the cell viz. aeration rate, impeller speed, pulp density etc. These physical variables are directly related to gangue entrainment and water recovery in the concentrate.

Improved drainage can be achieved by increasing the air flow rate and impeller speeds, for example. An increase in these variables causes an increase in the overall number of bubbles present in the system. This causes a crowding effect, thus the bubbles push against one another. The "squeezing" of the bubbles decreases the thickness of the plateau borders between each bubble. This phenomenon, together with the natural gravity of the draining liquid, causes the velocity of the draining liquid to increase (Jan, 1982).

2.5 ENTRAINMENT

As bubbles rise, the thickness present between the respective bubbles films allow for the transport of fine particles into the froth phase. This transport process is known as particle entrainment (Wiese et al., 2011).

It has been shown by Çilek and Yılmazer (2003) that mechanical entrainment is a non-selective process. This means that both valuable and gangue minerals are recovered in the

water. This idea has forced researchers to use this realistic problem of mechanical entrainment to the benefit of the overall flotation. Research done by Çilek and Yılmazer (2003) and Schubert (1999) showed that the turbulence within a cell, affects the overall grade and recovery of gangue minerals and the water recovery. Thus, different flow patterns were created within the cell by use of baffles, and the water and gangue recovery investigated. These baffles are placed at different positions within the cell to change the orientation of the flow patterns within the cell. This is shown in Figure 12:

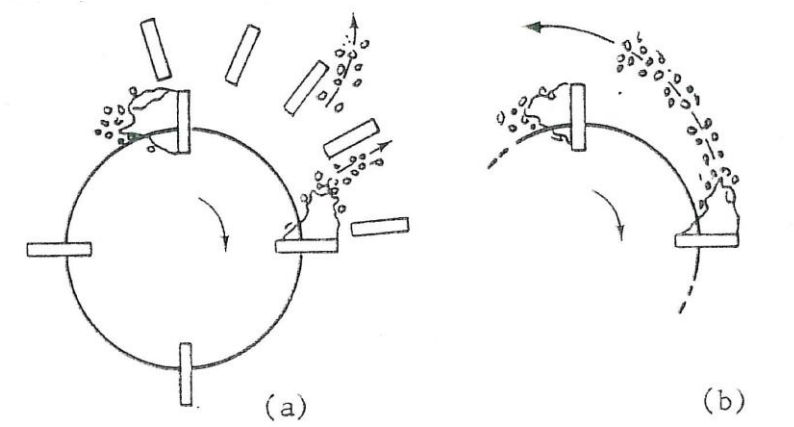

Figure 12: The effect of baffles on flow patterns (Ives, 1984)

The effects of baffles are shown in Figure 12(a) whilst in Figure 12(b) no baffles were used. The use baffles clearly disperse the fluid in different directions as shown by the arrowheads. This changes the hydrodynamics within the cell.

Particle entrainment can be reduced by spraying wash-water over the froth. This water moves downwards through the Plateau borders as the bubbles rise. It tends to promote increased drainage of particles, which are mainly hydrophilic gangue minerals, back into the froth phase. The water must be carefully dispersed such that it does not cause the rupture of the rising bubbles that contain valuable minerals. This idea cannot be successfully used in mechanical cells however due to the shallow nature of the froths, which limit natural drainage (Ata, 2012).

2.6 THE BUSHVELD IGNEOUS COMPLEX

South Africa contains 89% of the world's PGM reserves (Jones, 1999). These are concentrated in layers in the Bushveld Igneous complex, an igneous intrusion which also accounts for the world's largest reserves of both vanadium and chromite ore. In South Africa, platinum-group metals (PGMs) are the primary product whilst base metals are obtained as by-products of concentration operations (Jones, 1999).

The six PGMs are ruthenium (Ru), platinum (Pt), palladium (Pd), iridium (Ir), rhodium (Rh) and osmium (Os) (Wagner, 1973). Together with gold (Au) and silver (Ag), these are collectively known as precious metals (Xiao and Laplante, 2004).

The minerals of the platinum group metals in the Complex occur as cooperite, stibiopalladinite or sperrylite. The majority of the base metal sulphides occur as chalcopyrite, pentlandite and pyrrhotite. These account for a minor mass portion of the complex i.e. 0.1 wt. %. The remainder of the reef (99.9 wt. %) comprises of gangue minerals (chromite, pyroxene, feldspar and talc) (Ekmekçi et al., 2003).

Table 1 shows that South Africa produces 74 % of the world Platinum supply, but that most of the Palladium supply (66%) comes from Russia. South Africa produces 60% of the world Ruthenium supply. This table validates the need for finding more exploitable reserves in South Africa to supply the demands for Platinum and Palladium specifically. Table 2 shows the quantity and market value (at February 1999) of PGMs contained within each layer:

Table 1: Supply and demand figures for 1997 worldwide in millions of ounces (Moz) (Jones, 1999)

	Pt	Pd	Rh	Ru	Ir	Os	Total Pt, Pd, Rh	PGM reserves (Moz)
SA Supply	3.7	1.81	0.377	0.49*	0.8*	0.016*	5.9	2030
Russia Supply	0.9	4.8	0.24				5.9	199
Canada Supply	0.16	0.28	0.012				0.5	10
USA Supply	0.08	0.27					0.4	23
Other Supply	0.13	0.10	0.003				0.2	23
Total World Supply	4.97	7.25	0.632				12.9	2280
Total World Demand	5.2	7.46	0.460	0.357	0.127	0.005#	13.1	
SA as % of world supply	74	25	60				46	89

***** *The estimated figures for South African production of Ru, Ir and Os was based on doubling 1984 production figures, as has happened with platinum production over the period.*

 # The figure for world demand of osmium is based on a 1993 estimate.

The prices shown in Table 2 are out of date. The boom in the world economy followed by major downward adjustments in 2003 and 2008, resulted in significant price movements. Several new mines were opened in the boom, followed by mine closures. Nevertheless, Table 2 provides an overview of the relative contributions of the precious metals.

There are three types of exploitable PGM layers currently in the Bushveld Complex. These are the Platreef, Merensky Reef and the Upper Group 2 (UG-2) chromitite layer (Jones, 1999).

Table 2:Average grades (grams per tonne) of the precious metals in the Merensky, UG-2 and Platreef ores (Jones, 1999)

	$/oz	Merensky ore			UG2 ore			Platreef ore		
		g/t	$/t	mass %	g/t	$/t	mass %	g/t	$/t	mass %
Pt	379	3.25	39.54	59	2.46	29.98	41	1.26	15.35	42
Pd	350	1.38	15.47	25	2.04	22.96	34	1.38	15.53	46
Rh	860	0.17	4.56	3	0.54	14.93	9	0.09	2.49	3
Ru	37	0.44	0.52	8	0.72	0.86	12	0.12	0.14	4
Ir	395	0.06	0.70	1	0.11	1.45	1.9	0.02	0.30	0.8
Os	400	0.04	0.57	0.8	0.10	1.31	1.7	0.02	0.23	0.6
Au	287	0.18	1.62	3.2	0.02	0.22	0.4	0.10	0.94	3.4
Total PGM + Au		5.5	62.99	100	6.0	71.70	100	3.0	34.99	100

From Table 2 it can be clearly seen that UG-2 ore contains the highest collective value of precious metals per tonne of ore (71.70 $/t). Merensky ore has the highest value of Platinum at 39.54 $/t. It can also be deduced from this table that Platreef ore contains almost exclusively Platinum and Palladium reserves (88% of the reef) compared to the Merensky (84%) and UG-2(75%) ores. However it accounts for the least collective value (30.88 $/t) compared to the Merensky (55.01 $/t) and UG-2(52.94 $/t). This is because it is mined exclusively in one location (Potgietersrus Platinum by Anglo) and the reserves are much lower than those for the other two reefs.

The copper and nickel sulphide content of the UG-2 ore is much lower than that found in the Merensky reef. Most of the precious minerals are found within copper and nickel sulphide minerals. These base metal sulphides therefore assist in the flotation and smelting of trace amounts and they are valuable co-products. The lower base metal production from the UG-2 reef (Xiao and Laplante, 2004) is therefore a disadvantage when processing UG-2 ore. Table 3 shows the quantity and market value (at February 1999) of base metal sulphides contained within each layer:

Table 3:Base metal content of the Merensky and UG-2 reef (Jones, 1999)

	$/lb	Merensky ore			UG2 ore		
		% in ore	$/t	mass %	% in ore	$/t	mass %
Ni	2.25	0.13	6.44	62	0.07	3.47	80
Cu	0.66	0.08	1.16	38	0.018	0.25	20
Total Base metals		0.21	7.61	100	0.09	3.72	100

Due to the rapid depletion of exploitable Merensky reserves, the next best option to improve the production of Platinum and Palladium was to concentrate the UG-2 ore body (Jones, 1999). In fact it was stated by Bryson (1998) that a substantial quantity of PGM production will be coming from the UG-2 ore body in the coming years. The test work in this thesis was conducted using UG-2 ore.

The majority of PGMs within UG-2 ore occur within base metal sulphides, which are associated with silicates. Examples of these PGM sulphides include cooperite, braggite, laurite etc (Hay and Roy, 2010). The main gangue minerals, including chromite, are pyroxene, feldspar and talc.

Chromite and talc are siliceous gangue minerals that affect the flotation process (Megraw, 1916). They pose problems in concentration and subsequent smelting of UG-2 ore (Mailula et al., 2003).

2.7 TALC

Talc accounts for between 1 to 3 % of the mass of the reef (Hay and Roy, 2010). Aplan and Fuerstenau (1962) cited in Liu et al. (2006) stated that talc crystals are naturally hydrophobic gangue minerals. Contact angle measurements of talcaeous minerals have proved difficult and thus the exact degree of hydrophobicity is unknown. It is known however that these minerals have froth stabilising characteristics (Lotter et al., 2008, Bradshaw et al., 2005). Talc particles are physically flat sheets. Each sheet typically consists of brucite Mg (OH) sandwiched between two layers of silicates tetrahedral. Ionic bonds hold the atoms within the layers in place.

It is located within the grain boundaries of the base metal pyroxene. The talc is responsible for interfering with the flotation of the slower floating species viz. pyrrhotite, pentlandite and composite particles. This is because the talc is fast floating compared to the aforementioned species; hence it enters the froth before them, causing a stabilizing effect in the froth. It is recovered in the concentrate at the expense of these minerals, lowering the grade of the concentrate (Wiese et al., 2010).

When a talc particle is broken, it forms two very distinct surfaces viz. edges and planes. The edges are charged whilst the planes are uncharged (Lotter et al., 2008). The edges form due to the breaking of the intermolecular ionic bonds whilst the planes are formed by the brittle layers that are easily ruptured. Due to the abovementioned properties, planes are hydrophobic whilst edges are hydrophilic in nature (Bradshaw et al., 2005). The depressant thus adsorbs onto the planes, and the ionic groups reduce hydrophobicity, reducing recovery of talc, and in so doing, it increases the grade of the final concentrate.

2.8 CHROMITE

Chromite is a naturally hydrophilic mineral hence it cannot be transported to the concentrate via true flotation. It is usually recovered via entrainment thus has a strong correlation with the amount of water recovered in the concentrate. Ekmekçi et al. (2003) showed that the recovery of chromite in the concentrate is directly proportional to the water recovery. They also demonstrated that the chromite recovery decreases with increased froth height as described in the entrainment section previously. Hay (2010) showed that the relationship between the chromite and water recovery was independent of the scale of operation viz. the same type of relationships exist at plant scale operations.

The UG-2 reef is a chromitite. A small amount of adjacent material is mined to ensure maximum recovery of PGMs ore and to provide sufficient height for mining. Hence, the feed to the processing plant has relatively high chromite ($FeO.Cr_2O_3$) content of up to 75% by mass (Hay and Roy, 2010). The UG-2 chromitite has a chromium oxide (Cr_2O_3) content of between 40-50% (Hay and Roy, 2010). The percentage of original PGMs associated with chromite can vary from as little as 2% to about 10% depending on the properties of the UG-2 ore (Hay and Roy, 2010).

However, upon the addition of certain chemical reagents, the surface of the chromite minerals can be altered making them hydrophobic. This means that chromite can also appear in the concentrate by means of true flotation. Studies conducted by Wesseldijk et al. (1999) and Mailula et al. (2003) showed that chromite recoveries in the concentrates were increased by the addition of copper sulphate ($CuSO_4$) activator at certain pH values. Wesseldijk et al., (1999) stated that $CuSO_4$ forms a link between the surface of the chromite mineral and the xanthate collector. Thus $CuSO_4$ causes the xanthate collectors to adsorb onto the surface of chromite mineral thus they are recovered via true flotation.

The smelting process is designed to separate the gangue minerals from valuable PGMs associated with the Cu and Ni sulphides. This process takes place in electrical furnaces that operate at temperatures of above 1600^0C for UG-2 ore (Jones, 1999). Two distinct phases are

formed during this process viz. The matte phase of molten base metal sulphide (and associated with the PGMs), and the slag phase associated with the silicate minerals. The separation relies on the density difference between matte and slag.

Chromite and magnetite form stable spinel's that have intermediate densities compared to the matte and slag. This affects the separation of the two phases thus reducing the overall grade of the product. Thus, the maximum allowable chromite content for a typical UG-2 concentrate grade of 400g/t is about 3% by mass (Jones, 1999). This constraint is applied to minimise the effect of the accumulation of chromite during the smelting stage of the overall concentration process (Hay and Roy, 2010).

2.9 COMPOSITE PARTICLES

Composite particles comprise of a valuable mineral attached to the surface of an unwanted mineral. Thus these minerals behave as a complex particle with varying surface properties. Composite particles are a result of ineffective mineral liberation during grinding. These pose a significant problem during flotation. The selective collectors merely attach to the surface of the valuable mineral in the complex. The effectiveness of the collector action depends on the way in which the valuable mineral is orientated in the composite particle. That portion of the particle surface which reacts with the collector, (the sulphide mineral) will be coated by collector and it will be hydrophobic. The remainder of the (uncoated) particle surface will behave in a hydrophilic manner. Thus the probability of flotation of these particles is largely dependent on the proportion of the exposed surface containing the valuable mineral. The flotation of this composite particle will depend on the impact point between particle and bubble. It must strike the particle at the exposed hydrophobic surface, so that it can attach. This collision period is short so the particle must quickly attach to the bubble in order to be carried to the froth.

2.10 FLOTATION CIRCUITS

Flotation circuits are designed to optimise both the recovery and grade of the final concentrate. Single stage batch tests cannot achieve the same results as circuits since circuits incorporate recycling certain tailing and concentrate products. A simplified circuit, shown in Figure 13, consists of banks of cells arranged in the following series to simulate the various stages of flotation viz.

- Rougher stage
- Scavenger stage
- Cleaner stage
- Re-cleaner stage

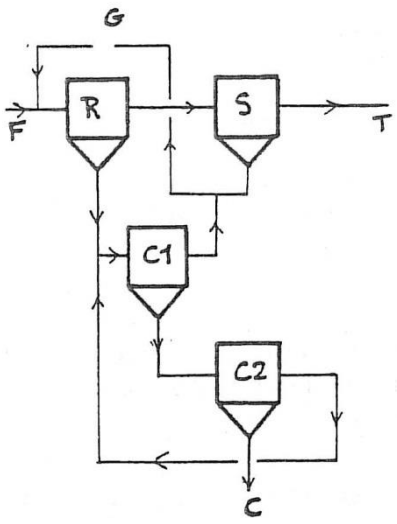

Figure 13: A simplified flotation circuit (Ives, 1984)

In Figure 13, C and T refer to the concentrate and tailings respectively. R, C1, C2 and S refer to the rougher, cleaner and scavenger stages respectively. Each box represents a bank of cells. This circuit is used to concentrate one product. 'G' denotes a grinding stage. In this case there is only one grinding stage however more complex circuits involve additional grinding stages.

Generally the number and sizes of the cells within these banks varies according to the quantity of ore being treated and the economics of the plant. Larger cells are used in the initial rougher banks of cells and relatively smaller sized cell used in the cleaner banks. Most banks can consist of anywhere between 4-20 cells depending on the requirements of the process (Ives, 1984).

The rougher and cleaner stages usually recover the fast floating minerals. In PGM flotation, these are chalcopyrite, pentlandite and include naturally floating talc. The tailing from the rougher is transferred to another flotation stage known as the scavenger. The grade of concentrate resulting from the rougher and cleaner stages is generally higher than that of the scavenger stages. This is due to the reduced amount of floatable sulphide and platinum minerals that report to the scavenger banks. There are also cleaning stages associated with the concentrates from the scavenging stage. The slow floating and composite minerals are also found in these banks.

The use of multiple stages of flotation is a crucial factor in the success of circuits. This ensures that the maximum possible recovery and grade can be achieved from the ore. However, there are certain consequences associated with recycling. One such effect is recycling of frother, depressant and collector (Ives, 1984). It should also be noted that the frother molecules are concentrated at the air/water interface and hence the water associated with flotation concentrates will have a higher frother concentration than that of the feed. Therefore, addition of frother to roughing and scavenging stages, to achieve adequate froth stability, may have the effect of producing undesirable froth stability in the subsequent cleaning and re-cleaning stages.

A two-staged mill/float circuit is employed in the PGM industry. This is known as the MF2 circuit. It has a coarser primary grind of between 30-40% passing 75µm. This size is said to effectively reduce overgrinding of chromite and reduce overall entrainment. This allows certain PGMs to be captured initially without the need of overgrinding thus reducing downstream milling costs. The finer secondary grind, between 65-85% passing 75µm, effectively liberates fine PGMs trapped within silicate minerals (Hay and Roy, 2010).

For UG2 ore, the average grain sizes of the PGMs are 12µm depending on the associated mineral (Hay and Roy, 2010). However, it should be noted that the PGMs are often associated with base metal sulphides and that the grain size of these minerals becomes important for recovery of the PGMs. In order to liberate these minerals from the ore, the ore must be ground to an appropriate size fraction for the flotation process. In the case of UG-2 ore, it has to be ground to about 80% passing 75µm for economic recovery of the PGM minerals (Jones, 1999).

2.11 THE EFFECT OF FROTHER ON FLOTATION OF PLATINUM FROM UG2 ORE

Ekmekçi et al. (2003) used hand-scraped batch rougher tests on UG2 ore, (obtained from the Crocodile River mine), to evaluate various types of frothers. The key variables manipulated were the froth height and frother type. Five different frothers were used, namely SF6005, SF6008, SF9325 (all proprietary blends (Senmin)), DOW200 and TEB (1, 1, 3-Triethoxybutane).The frother dosage was fixed at typical plant dosage of 60 g/t for all tests. The froth heights varied from 1, 2 and 3 cm. The dosages of SIBX collector and KU5 depressant were constant for all the frother types.

SF6005, SF6008, SF9325 and DOW200 were shown to exhibit consistent froth behaviour producing high water recoveries at all froth heights as compared to TEB. The TEB has a much lower water solubility compared to the other highly water soluble frothers. Due to frother similarities, SF6005, SF6008, SF9325 and DOW200 were labelled as Group A type frothers whilst TEB was labelled as a Group B type frother.

Based on the water, mass and chromite recoveries, Group A frothers were classified as strong and stable frothers. Group B produced a brittle froth resulting in low water recoveries. At high froth heights, the recovery of water decreased due to the increased drainage resulting in an improvement of the selectivity of valuable minerals in both groups.

The selectivity's of the frothers were also investigated. It was found that the DOW200 had a higher mass recovery than the TEB at all froth heights. This was due to the more stable froth phase and also a result of the higher water recoveries. It was shown that the cumulative grade of chromite that reported to the concentrate was less than 3% for froth heights 2 cm and 3 cm. This was true for the Group A frothers. Group B had a cumulative chromite grade less than 3% at all froth heights. The Group B frother produced significantly lower mass recoveries at all froth heights. The mass of chromite present in the final concentrate decreased as the froth height increased. This is due to the increased natural drainage as the froth height is increased (Ekmekçi et al., 2003).

It was concluded that the group A frothers produced more stable froths with larger bubbles allowing for better drainage compared to Group B. The mass recovery of both water and minerals using TEB was far too low. The use of Group A frothers was recommended based on their good flotation characteristics at froth depths that result in suitable drainage. These frothers were able to achieve reasonable mass recoveries compared to the lower mass recoveries of Group B frothers. It was also recommended to increase the froth height to reduce the grade of chromite present in the concentrate (Ekmekçi et al., 2003).

2.12 CASE STUDIES INVOLVING THE USE OF DEPRESSANTS TO SOLVE THE TALC PROBLEM

Depressant are the most expensive of all reagents utilized in the platinum flotation industry (Shortridge et al., 2000), and hence there has been a significant investment in research on mechanisms for depression of Non-floatable gangue (NFG) minerals (Parolis et al., 2008, Corin and Harris, 2010). In particular, Corin and Harris (2010) showed that there is no benefit of blending both CMC and guar type depressants. This was based on the fact that similar PGE recoveries were obtained for both the blended and pure depressants.

Talc is a naturally hydrophobic, silicate mineral present in gangue in the South African platinum ore bodies (Shortridge et al., 2000). It has a unit structure of $Mg_3(Si_2O_5)_2(OH)_2$ and is very difficult to separate from valuable mineral. It has been known to be easily recovered and thereby reduces the overall grade of the concentrate (Beattie et al., 2006).

A significant amount of research has been invested in the field of talc depression. Liu et al., (2006) found that the adsorption of CMC type depressants onto talc is independent of the pH of the pulp. Beattie et al. (2006) did research on the adsorption characteristics of various polymeric depressants. The depressants used were either natural or synthetic with a wide range of degrees of substitution (DS) to allow for a wide range of chemical properties. The contact angle of the adsorbed talc and the thickness of the adsorbed depressant layer on the particle were the two primary factors that influenced the depressant effectiveness.

Shortridge et al. (2000) investigated the use of CMC and modified guar depressants (at a range of molecular weights) and their ability to depress naturally hydrophobic talc. The CMC average DS was 0.8 whilst the guar average was 0.1. The CMC possess a high charge compared to the low charge guar depressant. A salt solution of 10^{-3} M potassium nitrate (KNO_3) solution was used in the micro flotation tests.

It was shown that maximum depression of talc by guar occurs at a dosage of 20 g/t, with no further depression noted at higher dosages. CMC depressant showed poor depression characteristics at the same dosage. The poor depression could be due to the electrostatic repulsion between the talc surface and the negatively charged CMC depressant.

Guar molecules have an extended adsorbed layer on the talc, forming a tail extension on the adsorbed molecule. The CMC adsorbs flat on the surface, with no tail sticking out into the pulp. Even though the CMC molecules occupied a 1000 times greater surface area on the talc

surface compared to the guar, the guar shows a greater depressing action. The tail structure was presumed to provide an extended shielding to the air bubble thus ensuring no adhesion.

The results found by Shortridge et al. (2000) showed that the higher the molecular weight of the guar, the better the depressing action. The CMC showed no improvement in depressing action, even as the molecular weight of the depressant was increased at a fixed KNO_3 dosage. They concluded that the ionic strength of the KNO_3 solution impacted negatively on the adsorption of the CMC type depressants.

(Parolis et al., 2008) found that certain metal cations in solution promoted the adsorption of CMC onto talc. These were Ca^{2+} and Mg^{2+} cations. These divalent cations caused greater coiling of CMC chains on the talc surface compared to the monovalent K^+ cations. This coiling improved the effectiveness of the CMC adsorption onto talc. K^+ cations were found to negatively impact the adsorption of CMC onto talc. This result was similar to that observed by Shortridge et al. (2000).

2.13 THE EFFECTS OF COLLECTORS AND FROTHERS ON THE PERFORMANCE OF DEPRESSANTS

Wiese et al. (2010) performed batch flotation tests using Merensky ore. They were investigating the effects of varying DOW200 frother dosages on the performance of CMC and guar depressants. This flotation performance was based upon the recovery of Cu and Ni sulphides. The frother dosages ranged from 40 to 70 g/t whilst the depressant dosages ranged from 0 to 500 g/t. All other factors, including air flow rate, froth height, SIBX collector dosage etc. were kept constant.

Their results showed that the water recovery increased as the frother dosage was increased from 40 to 70 g/t across all depressant dosages. It was also apparent that the use of frother displayed little selectivity due to the effect on the concentrate grade. Both the Cu and Ni grades decreased as the frother dosage increased. This was due to the increased gangue entrainment as a result of the increased froth stability. It was also observed that froth stability was improved by increasing the frother dosage, particularly for CMC depressant at 500 g/t. The CMC produced brittle froth at this dosage due to its dispersing characteristics and the removal of talc from the froth.

The use of high frother dosages was demonstrated to improve the recovery of Cu and Ni sulphides however it reduced the overall grade of the concentrate. The use of high dosages of depressant was found to increase the grade of the concentrate however the overall recovery of Cu and Ni sulphides was lower. This was considered to be due losses in the recovery of composite or partially liberated sulphide particles. Thus one must find and optimum balance between increasing both the frother and depressant dosage.

Bradshaw et al. (2005) performed flotation tests on Merensky ore. They were investigating the effect of SEX and SIBX collectors on the recovery of Cu and Ni sulphides at various depressant dosages. Depramin 186 and Depramin 158 were the depressants used at dosages ranging from 100 to 500 g/t. The Depramin 186 is highly charged compared to Depramin

158. These depressants were used to simulate the behaviour of CMC and guar type depressants respectively.

The SIBX collector has a longer chain length compared to SEX collector and thus produces particles with a greater degree of hydrophobicity. This implies that the use of SIBX generates particle-bubble aggregates with larger contact angles compared to SEX. Thus one would expect higher recoveries using SIBX collector.

This increased hydrophobicity has an impact on the froth phase. The SIBX coated particles caused increased bubble coalescence thus producing bigger bubbles as well as a brittle froth structure compared to those coated with SEX. Thus the use of SEX collector produced higher mass and water recoveries compared to SIBX at all depressant dosages.

The grades of concentrate from the SEX were lower than those obtained with the SIBX collector. This was due to the lower natural drainage that occurs in a more stable froth. This means that SEX froth structure allowed more gangue to be entrained compared to SIBX. This reduced the grade of the concentrate.

The use of both types of depressant lowered the non-floatable gangue (NFG) recovery in the concentrate for both collectors. However, it was found that both depressants reduced the recoveries of sulphide minerals as the dosage increased. Depramin 186 exhibited higher recoveries of NFG but also displayed higher overall concentrate grades. This was due to the increased bubble sizes which facilitated improved natural drainage which reduces gangue entrainment. The Depramin 158 exhibited lower recoveries of NFG compared to the Depramin 158. This implies that it adsorbed more strongly onto the NFG surfaces.

2.14 THE EFFECTS OF HYDRODYNAMIC VARIABLES ON THE FLOTATION OF PLATINUM ORES

Hadler and Cilliers (2009) performed studies on a flotation bank of 4 rougher cells at a platinum mine in South Africa. The objective was to investigate the influence of air flow rate and froth stability on the rougher bank performance. This performance was measured by a variable known as the ‘air recovery’. It is defined as the fraction of air entering the cell that overflows into the launder as unburst bubbles. The authors had previously demonstrated a relationship between the air recovery and mineral recovery in batch tests.

Initial results showed that an increase in air flow rate increases the air recovery. However at higher air flow rates, the air recovery decreases. This meant that the froth structure became more brittle at higher air flow rates due to an increase in bubble size (i.e. the impeller has a limited capacity to disperse bubbles. It was deduced that there an optimum air flow rate exists that will lead to a peak in air recovery.

In terms of the concentrate grade and PGM recovery there were mixed results. An increase of the air flow rate increased the PGM recovery and lowered the concentrate grade. The reduction in grade was due to increased entrainment. However, the studies did show that the maximum PGM recovery occurred at the peak in air recovery without significant loss in concentrate grade.

Studies were performed by Deglon (2005) on the influence of agitation on platinum ore flotation. Results showed that an increase in agitation increases the particle-bubble attachment for both finer and coarser particles.

The grades and recoveries of platinum ores for two different cell volumes (viz. 60 and 150 litre) were recorded at different impeller speeds. These cells were part of a pilot plant, operating with a continuous feed. The assumption was that the higher the impeller speed, the turbulence within the cell. It was shown that both the recoveries and grades of the ore increased as the impeller speed increased in the 60 litre cell.

The effects of two different froth types were observed for this cell namely a shallow froth and a deep froth. The shallow froth is a consequence of an average air flow rate and the deep froth stems from a high air flow rate. The Platinum recoveries for both froth types increased linearly with impeller speed. The recoveries at all impeller speeds were constantly higher in the shallow froth compared to the deep froth. This is due to the larger drainage of gangue minerals in the deeper froth compared to the shallow froth.

The 150 litre cell was used to investigate two different grades of material viz. a lower grade rougher feed ore and a cleaner tails ore. The feed ore sizes were a 40% passing 75 microns feed for the rougher ore and a 90% passing 75 microns for the cleaner ore. The effects of different impeller speeds on the platinum recovery were monitored. It was observed that the recovery increased linearly with the impeller speed for the cleaner tails ore. However, for the rougher tails ore, it was found that the recovery increased linearly to a maximum of 55% at 950 rpm, then decreased thereafter. The recovery at 780 rpm was about 52% and the recovery at 1050 rpm was 53%. These results show an optimum speed at 950 rpm for the flotation of this ore.

Deglon (2005) explained that increasing the impeller speed resulted in an increase in the bubble-particle contact resulting in higher concentrate recoveries. However, at high impeller speeds, the particle-bubble detachment in the pulp is likely to increase and the froth phase likely to become unstable. There will be an optimum impeller speed and air flow rate combination for coarser particles. This will be dependent on the feed properties. A rougher tails ore has weak flotation behaviour compared to the cleaner ore due to the size of its particles. Thus it responds less favourably to the increase in impeller speed.

The effects of aeration rate and impeller speed on the flotation of sulphide ore were investigated by Yang and Aldrich (2006). The investigation involved using impeller speeds of 1200, 1500 and 1800 rpm respectively. The aeration rates used ranged from 2 to 8 litres per minute (l/min). The effects of the grade of sulphur were reported via rate plots for a flotation time of 8 minutes. Their results showed the grade of sulphur in the concentrate generally decreased as the aeration rate increased for each of the three impeller speeds up until 360 seconds. Thereafter it can be seen that there was an optimum impeller speed between 1800 and 1200 rpm for the sulphur grade. Further investigations showed that an air flow rate of 4 l/min and an impeller speed of 1500 rpm optimised the recovery and the grade

of sulphur. These investigations incorporated factors like water recovery and gangue entrainment.

It is difficult to compare the results obtained by Deglon (2005) to laboratory results simply due to the large difference in cell volumes. Standard laboratory flotation cell volumes were used in this project, ranging from 1 to 8 litres. Obviously one cannot simply conduct experiments at the same air flow rates used by Deglon (2005) since they utilized much larger cells viz. 60 and 150 litres.

Thus the idea of a superficial air flux velocity (v_a) must be introduced. This velocity is a measure of the flow rate of the air relative to the surface area of the cell and has units of $m^3.m^{-2}.s^{-1}$(or $m.s^{-1}$). This flux thus incorporates the size of the cell used thus is an important factor in scaling air flow rates between laboratory and industrial flotation cells.

2.15 CIRCUIT OPTIMISATION

Loveday and Hemphill (2006) used simulation to optimise the design of an existing multistage platinum flotation plant. The circuit consisted of four stages namely the rougher, cleaner, scavenger and re-cleaner stages. There were several flotation cells within each stage. Included in this circuit was a re-grinding of the rougher tails. There were three recycle streams within the cleaning stages in an effort to improve the separation between the gangue and the PGMs.

A high degree of gangue entrainment occurs during single stage flotation. This necessitates multiple concentration stages where gangue entrainment is reduced and concentrate grade is improved. In some cases, recycles within certain stages are necessary to improve the separation of the gangue minerals from the PGMs.

The concentrate streams were separated into two grades viz. the higher and lower grade concentrates. It is assumed that the higher grade concentrate primarily consists of fast floating minerals. The lower grade concentrate is assumed to consist of slower floating minerals. It was shown by both Wiese et al. (2011) and Bradshaw et al. (2005) that depressant dosages influence the recoveries of Cu and Ni differently. Cu is generally associated with fast floating minerals whilst Ni is associated with slower floating species. Hence, by separating the material into fast and slow floating species, suitable additions of depressant can be selected.

The flow sheet of the plant which was simulated by Loveday and Hemphill (2006) is shown in Figure 14.

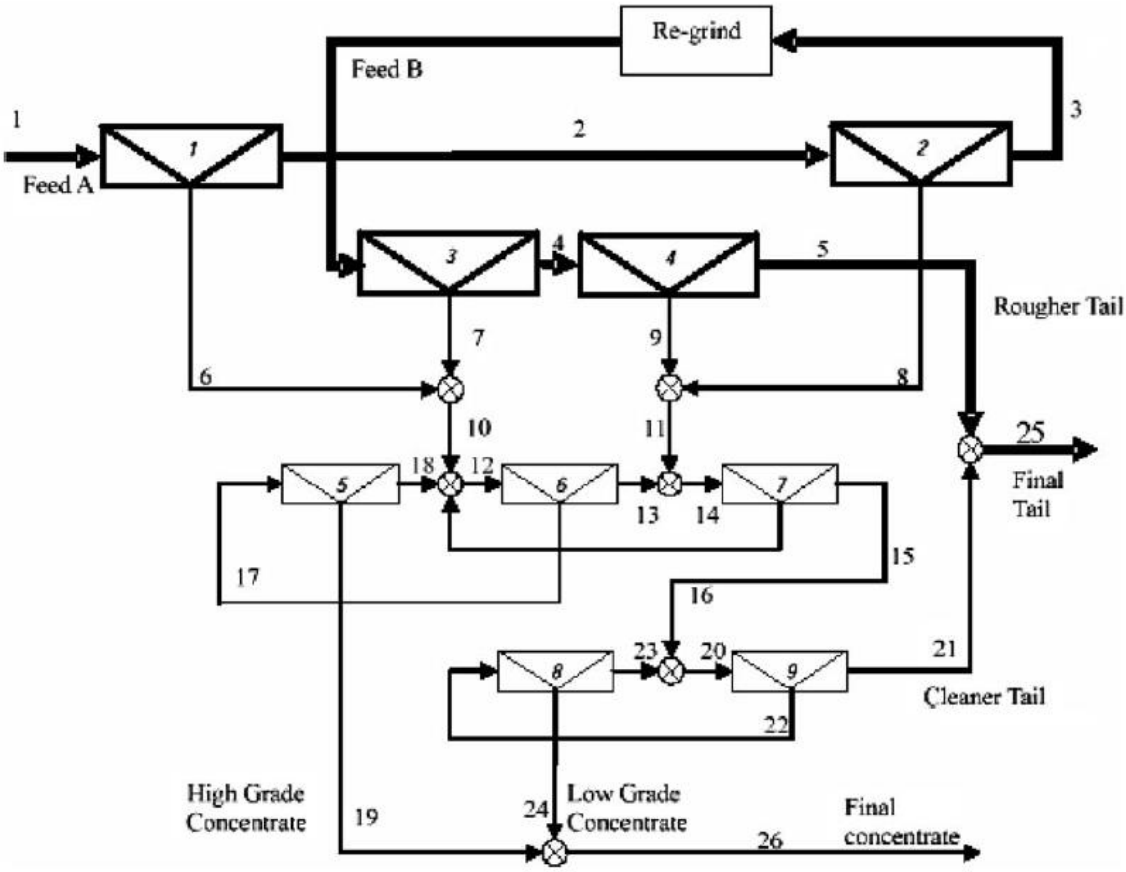

Item number	Description
1, 2	Primary roughers
3, 4	Scavengers
5, 6	HG cleaners
7, 8, 9	LG cleaners

Figure 14: Flow diagram of platinum flotation plant circuit (Loveday and Hemphill, 2006)

2.16 INVESTIGATING THE DOWNSTREAM EFFECTS OF FROTHER ADDITION

It was stated by Wiese et al. (2010) that "*increased frother dosages may lead to downstream problems in a concentrator".* These problems are due to the impact that frother dosages have on froth stability. It is known that the froth stability has a huge impact on both the PGM grade and recovery.

As discussed earlier, frother molecules adsorb onto the surface of air bubbles. These bubbles rise through the pulp and form the froth phase. Thus frother molecules are concentrated in the froth phase. The concentrate, which is recovered from the froth phase, contains both solids and liquid. Frother molecules, unlike depressants and collectors, do not adsorb onto the surface of solids. Hence they are largely associated with the liquid containing collapsed

bubbles. Hence, the frother concentration in the water is increased by all stages, relative to the feed to that stage.

In industry, the process of flotation is continuous and tank levels are controlled, for example, by use of dart valves. A batch laboratory test relies on a liquid top-up to maintain the flotation cell operating level. This liquid is usually fresh water. However, on plants, the cells are operated continuously and pulp level is controlled, using dart valves (for example), to regulate the tailings flow. Laboratory tests should therefore be designed to mimic plant conditions as much as possible.

Water is recycled on plants as much as possible, bearing in mind the residual reagents in the water and salts in solution build up to saturation levels. Some fresh make-up water is added. Ores from the Bushveld complex are ultra-basic and react with water to produce a relatively high pH of about 9.

Launder sprays are used in some cases, where the concentrate does not flow well. However, launder sprays cause dilution and the consequent loss of cleaner residence time. Most of the recycle water (from the tailings dam) and fresh make-up water is therefore added to the milling circuit.

The cell levels in a laboratory test are controlled by using fresh water top-up. This means that the cell is being artificially diluted. The result is that the frother concentration is being reduced. Hence, the complete circuit must be considered when doing laboratory tests, particularly the effects of increasing frother concentration.

In order to investigate the downstream effect of frother concentration, one would need to have a simple way of measuring frother concentration in the presence of other organic chemicals. No convenient on-site method for the determination of frother concentration was found in the literature. Gas chromatography and calibrations of bubble size and gas holdup vs. frother concentration have been employed as means of frother measurements. Finch and Gelinas (2005) used a colorimetric technique to measure the concentration of methyl isobutyl carbinol (MIBC) and DOW250 in solution. The frothers were extracted in an organic solvent and analysed by means of UV–visible spectrophotometry. The frother concentration was predicted with an error of less than 6% and showed good repeatability. This method required a short determination time, could be performed on-line and was relatively cheap. These factors were incorporated into the design of a device capable of measuring the frother concentration. Two methods of measuring frother concentration in water are described later.

2.17 SURFACE TENSION AND CAPILLARY ACTION

As mentioned earlier, one of the primary functions of frother is to reduce the surface tension between air and water. This means that the bubbles are less likely to burst upon particle-bubble collisions. Thus there exists a relationship between the surface tension of a liquid and the frother concentration. Initially, it was decided to quantify the frother concentration by using the relationship between the surface tension and capillary action of solutions.

Surface tension is defined as the "*the property of the surface of a liquid that slows it to resist an external force, due to the cohesive nature of its molecules*" (Survey, 2012b). In an open tube filled with water, there exists a natural force of cohesion between all the water molecules. The molecules lining the surface have no molecules above them thus exhibit stronger forces of attraction between the molecules alongside. This attraction between the surface water molecules creates a strong barrier between the atmosphere and water. This surface barrier is known as the surface tension and is shown in Figure 15 (Survey, 2012b).

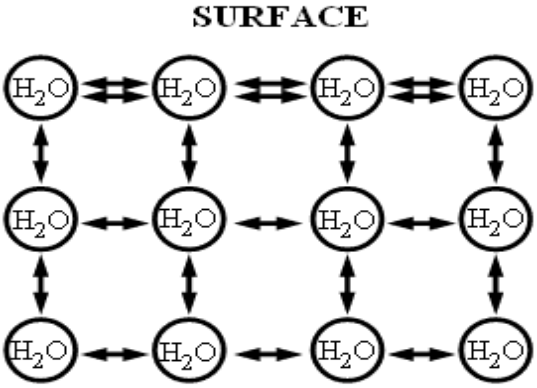

Figure 15: Forces of cohesion between water molecules (Thorpe, 2002)

A capillary tube is a length of piping, usually of narrow diameter. A glass capillary tube was used for this investigation. It is used to demonstrate the capillary action of liquids. Capillary action is defined as *"the movement of water within the spaces of a porous material due to the forces of adhesion, cohesion and surface tension"* (Survey, 2012a).

When a capillary tube is placed in a liquid solution, the water exhibits forces of adhesion towards the sides of the glass and cohesion between the molecules themselves. This adhesion causes the water to rise up the tube. This height is exaggerated at the sides of the glass since the surface tension causes the surface to stay intact (Sophocleous, 2009). The forces of adhesion are greater than those of cohesion. This causes a net upward rise of water in the tube. The shape that the water forms at the surface is called a meniscus. This is shown in Figure 16:

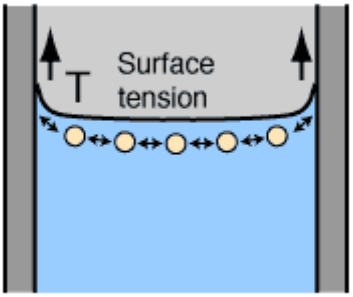

Figure 16: Meniscus formed by water in a capillary tube (Nave, 2012)

There are various factors that influence the liquid rise viz. gravity due to liquid mass, surface tension, tube diameter etc. The relationship between these factors is summarized in the

following equations taken from the fundamental equation of dynamics for pure liquids (Zhmud et al., 2000):

Equation 1: For a viscous, non-compressible liquid in a long cylindrical capillary; Newton's dynamic law is as follows:

$$\rho[hh'' + (h')^2] = \frac{2}{r}\gamma \cos\theta - \frac{8}{r^2}\eta h h' - \rho g h$$

assuming the Poiseuille flow profile throughout the capillary

Where h – height to which the fluid rises in the capillary tube

γ- liquid/air surface tension

θ- contact angle between the liquid and air

ρ- density of the liquid

g- universal gravitational constant

r- radius of the tube

η- viscosity of the liquid

The fluid will rise to a final static level h_∞ after the forces of capillarity and gravity cancel out. This is given by the following equation:

Equation 2: Static liquid height

$$h_\infty = \frac{2\gamma cos\theta}{\rho g r}$$

The equation above implies that $h_\infty \propto \gamma$. Surfactants, like DOW200 frother reduce the surface tension of liquids. Hence one would conclude that the rise of water in a capillary tube would be a simple, practical way of measuring the air/water surface tension and hence the effective frother concentration.

2.18 CONCLUSIONS FROM RESEARCH

Work done by Deglon (2005) gave rise to the idea of an optimised set of air flow rate and impeller speed combinations. These describe the hydrodynamic behaviour of the cell. There has been much work done in the recording of such data in the form of ratios and graphs, the former referring to an "Air Flow Number (AFN)" and the latter to an "Air-Impeller" envelope. The AFN is the ratio of the air flow to the impeller speed for certain ore types. The "Air-Impeller" envelope is a series of data points for optimum impeller speeds and air flow rates combinations, represented on a graph. These points, once plotted, form an "envelope-like" shape. An example of a single data point would be the 4 l/min and 1500 rpm obtained by Deglon (2005).

It is important to note that these ratios and graphs are mere guidelines in the selection of optimised conditions. Çilek and Yılmazer (2003) showed that the hydrodynamic variables of flotation cells are effective design and scale-up criteria. Work similar to that done by Yang and Aldrich (2006) will have to performed, in order to find optimised air flow rate and impeller combinations. This would require large amounts of sample and is not within the scope of this project. Their results will be used as guidelines in the selection of suitable air flow rate- impeller combinations.

It is apparent that one cannot simply consider the optimisation of a flotation process by simply considering the reagents and experimental conditions individually. All the reagents have primary and secondary effects. In the case of collectors, their function is the coating of particles that render the surfaces hydrophobic. This is the primary effect and has a positive outcome in that particles are able to attach easier to bubbles. The other induced or secondary effect of collector dosage is that increased particle hydrophobicity affects the froth phase. Bubble coalescence is promoted by hydrophobic particles which causes a decrease in froth stability reducing the overall PGM recovery. In order to optimise the PGM recovery or concentrate grade, one needs to consider both the primary and secondary effects of any chosen reagent dosage.

It was shown by Wiese et al. (2011) that changing any one reagent in a flotation process has an effect, either positive or negative, on the froth stability thus has an overall effect on the grade and recovery of PGMs. Bradshaw et al. (2005) concluded that reagents should not be considered independently of each other, and that the effects of combinations of reagents on both the pulp and froth phases should be considered.

In the past, laboratory batch flotation tests were used to find optimum experimental conditions, including reagent suites, which could be subsequently applied to larger scale operations like pilot plants. However, in most cases, the results in batch flotation tests do not correlate well with those obtained from pilot scale operations. Batch tests often produce higher recoveries and grades compared to larger scale operations. According to Wiese et al. (2011), it is believed that these differences result from the effects of reagent suites on froth stability.

The circuit used by Loveday and Hemphill (2006) displayed how concentrates are separated into different grades thus enabling one to optimise them independently. Due to their dissimilar PGM and gangue contents, these concentrates might not respond in a similar manner when subjected to identical depressant dosages. Hence it is beneficial for the purpose of this study to separate these concentrates. This influenced the design of a circuit capable of separating concentrate into two grades viz. high and low. The four stage circuit proposed for this test work, shown on Page 43 Figure 35, consisted of rougher, scavenger, high grade and low grade cleaning stages.

The downstream processing problems highlighted by Wiese et al. (2010) could only be addressed if one was able to quantify the frother concentration of any stream. Common analytical techniques are laborious, expensive and at times cannot be used online in a plant

situation. A practical and efficient method of measuring the frother concentration was sought after. The frother is concentrated in solution hence it was decided to investigate the use surface tension as a means of measuring this concentration. Later on it was discovered that the froth height generated by bubbling air through frother solutions could be used to effectively quantify the frother concentration.

This thesis is aimed at addressing some of these laboratory practises which may reduce the PGM recovery/ concentrate grade differences between laboratory and pilot scale operations.

3 EQUIPMENT

The following chapter details the equipment used to perform the experimental work in this thesis. This chapter has been divided into three sub-sections namely; Milling, flotation and frother investigation.

3.1 MILLING

A fixed speed rod mill, operating at 75 r.p.m, was used to grind the sample. It had an internal volume of 10 litres and an internal diameter of 200mm. It was fitted with four 5mm high lifters, as shown in Figure 17, which ensured that the rods did not slip.

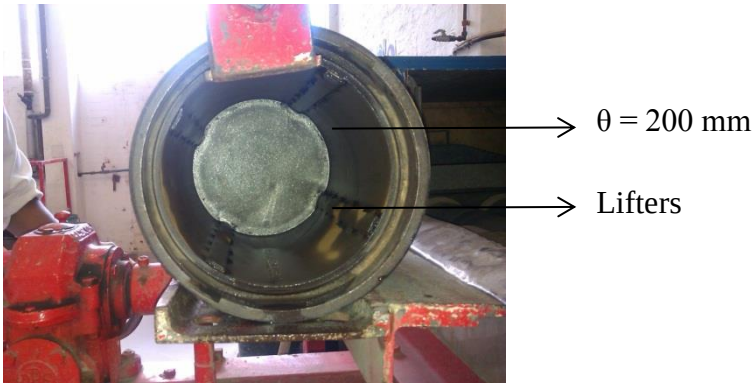

Figure 17: Internals of the mild steel rod mill

A mild steel conical funnel was used to aid in the un-loading of sample into a collection bucket. The aim of this was to reduce mass losses during the transferring process from the mill to the flotation cell. This mill setup is shown below:

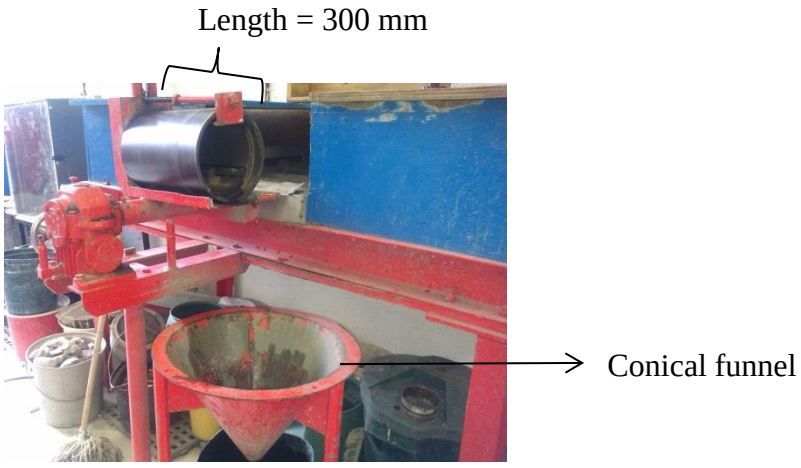

Figure 18: Milling setup

Stainless steel rods, with diameters ranging from 10 to 20 mm, were used to perform the grinding. These were all 290 mm in length. The rods together with their mill orientation are shown in the figures below:

Figure 19: Steel rods of 20, 15 and 10 mm diameter respectively (from left to right)

Figure 20: Orientation of rods in the mill

Figure 21 shows the vibrating screen which was used for wet screening of the sample at 75 microns, prior to dry screening of the oversize. These tests were required to determine the grinding time.

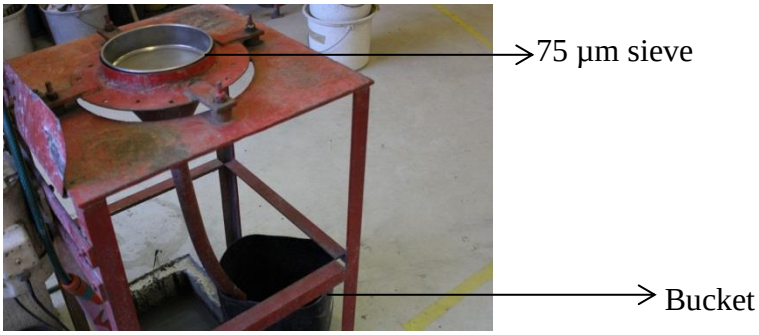

Figure 21: Wet screening apparatus

Figure 22: (from left to right) bad ore; good ore

The dry samples of good ore and bad ore, shown above were sub-sampled using a riffle. The riffle was also used for wet splitting of the rougher tailing sample for repeat assays. The total dry mass of samples was used as a measure experimental accuracy.

Figure 23: Riffle splitter apparatus

Figure 24 shows the pressure drum filter, operated at 5 bar (abs), to filter wet ore samples. Compressed air was delivered via a tube. A bucket was placed underneath to collect the filtrate or as a sample safety mechanism in the event of filter paper failure.

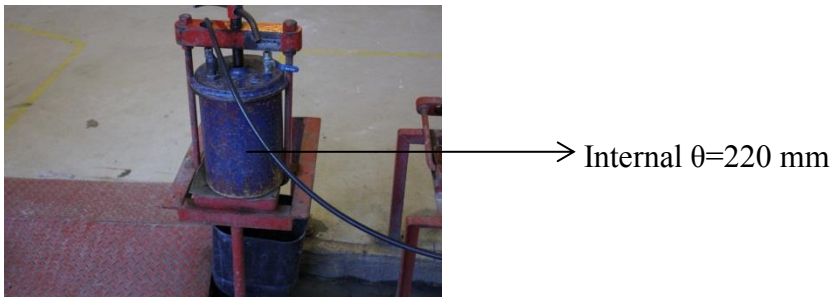

Figure 24: Pressure filtering apparatus

The samples of plus 75 micron material obtained by wet screening, were dried in an oven and analysed for a size distribution, using a sieve shaker. This was used to generate a size distribution of the particles above 75 microns. The apparatus consisted of a √2 series of sieves arranged on a vibrating screener. The sieve sizes ranged from 75 to 250 µm. The amplitude and frequency of the vibrations were constant.

Figure 25: Sieve shaker

3.2 FLOTATION EQUIPMENT

Three standard Denver flotation cell sizes were used in this work. These were the 1, 2.5 and 8 litre cells respectively. These values refer to the approximate volume occupied by the contents within the cell. The cells were provided together with a new Denver flotation mechanism, but were modified by cutting a narrow window on one side and attaching a Perspex strip, as shown in Figure 26. The window was used to monitor pulp level.

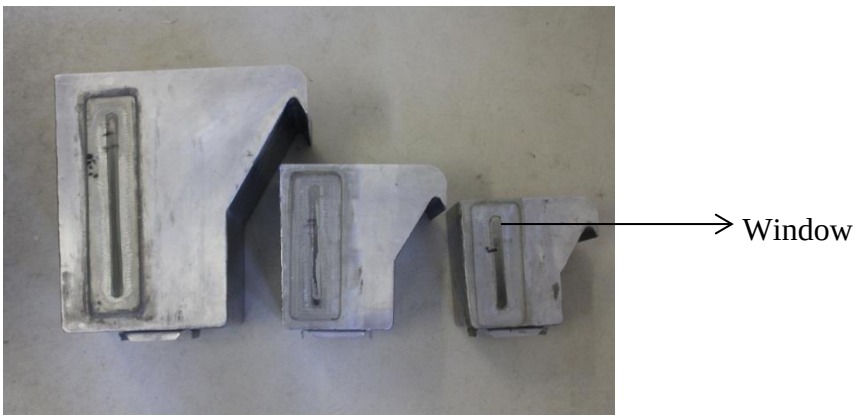

Figure 26: Standard Denver cells 8, 2.5 and 1 L sizes (left to right)

The scrapers for the flotation test work were cut, in duplicate, from Perspex glass. These were sized according to the froth depth requirements and were constrained by the cell dimensions.

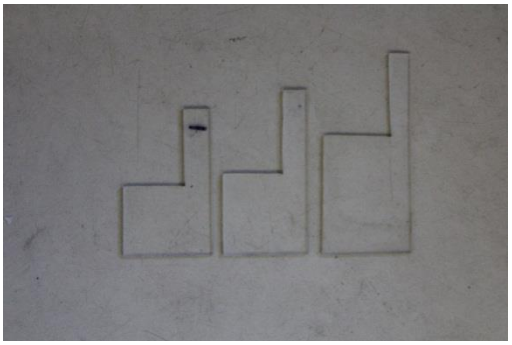

Figure 27: Scrapers for 1, 2.5 and 8 L cells respectively (from left to right)

Two Denver flotation mechanisms were available to perform test work. The new one, which has digital speed control, was used to perform test work in combination with the old one. The air flow was supplied from a compressed air main and it was set using a rotameter. The old cell, together with the two control devices are shown in Figure 28:

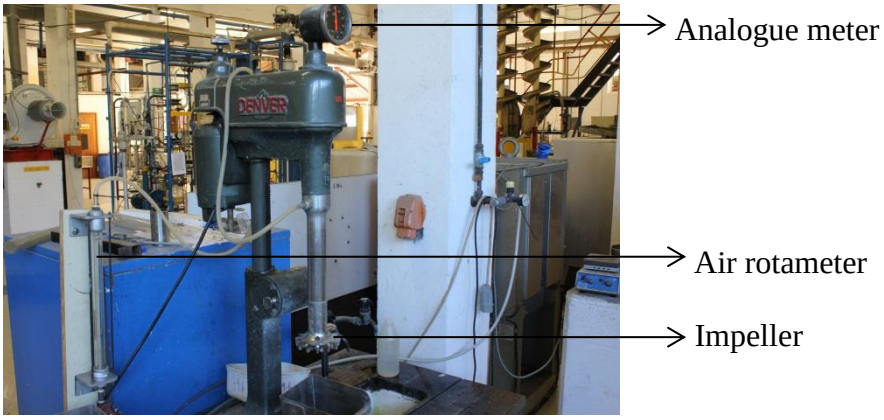

Figure 28: Denver Flotation Cell with subsidiaries

This work involved the use two different impeller sizes viz. small and large. The diameters of the impellers are shown below together with the outer shaft casings.

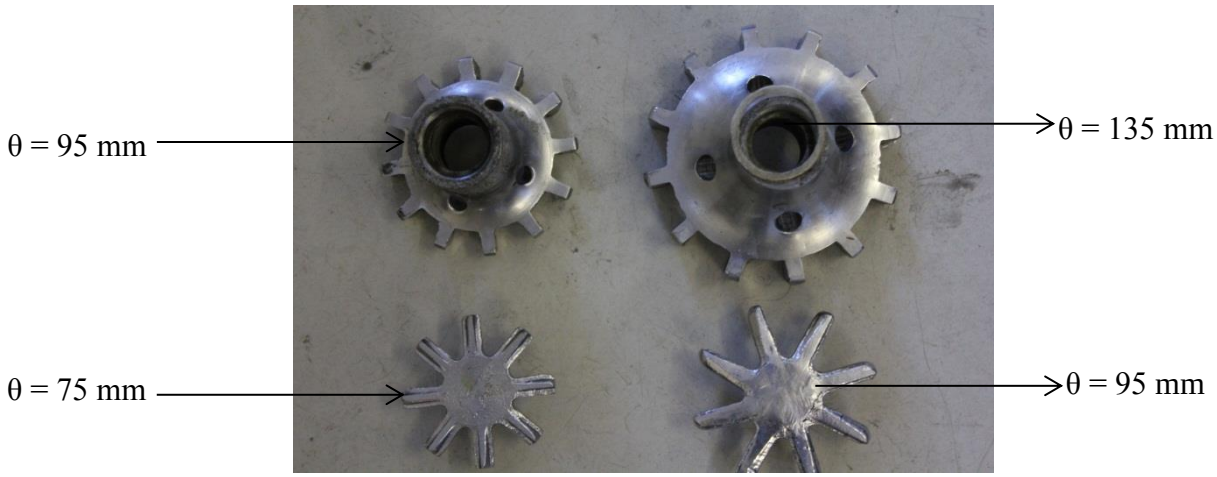

Figure 29: Impeller sizes/Shaft casings: Small and Large (from left to right)

The reagents in this work were prepared as 1 % solutions by mass in distilled water. The collector used was SIBX, which is a yellow powder in its solid form. DOW 200, a clear liquid solution, was the frother used in this work. KU5, which appears as a cream powder prior to dilution, was the depressant used. The reagents, in solution form, are shown below:

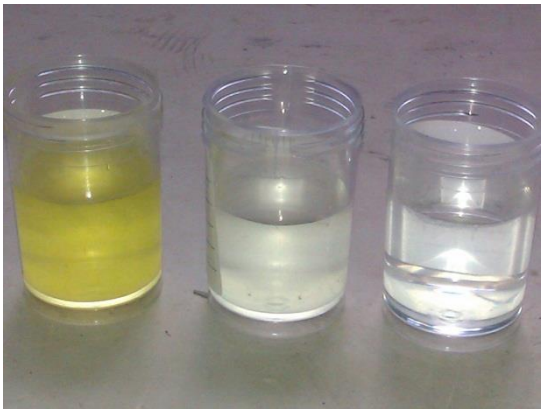

Figure 30: SIBX, KU5 and DOW 200 solutions respectively (from left to right)

3.3 FROTHER INVESTIGATION

A 1 mm (ID) glass capillary tube, together with a glass vial was used in the initial stages of this investigation. An attempt was made to quantify the frother concentration using the rise of liquids in capillary tubes, shown in the image below, but the rise in level was too small with typical samples of concentrate water.

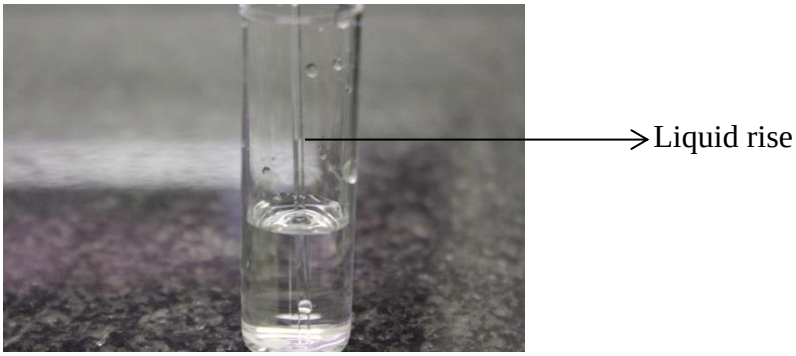

Figure 31: Capillary tube setup

The next method to be tested was to bubble air through a filtered solution and to measure the froth height, using a vertical tube (20 mm internal diameter), which had a sintered disc of fine glass sand, fitted to the bottom of the tube (See Figure 33). The perforations in the disc created sufficient pressure drop to ensure the air was evenly distributed throughout the tube. A tape measure, fixed to side was used to measure froth height.

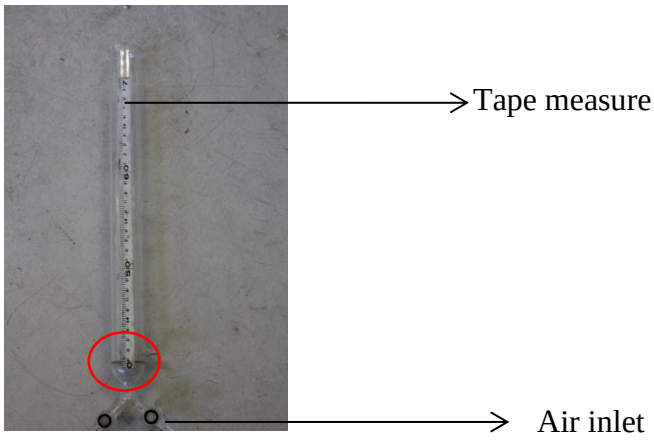

Figure 32: Sintered disc tube apparatus

Upon magnifying the highlighted section, a clearer picture of the 5 mm thick sintered disc is obtained and shown below:

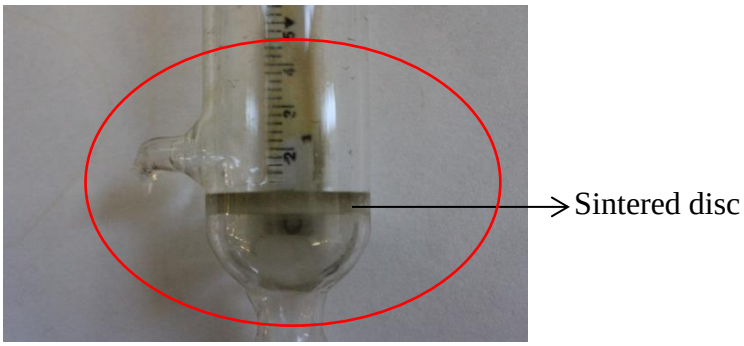

Figure 33: Magnified section showing the sintered disc

The experimental setup for both the flotation tests and frother investigation are shown below. A large rotameter delivers air to the flotation cell whilst a smaller rotameter delivers air to the frother apparatus:

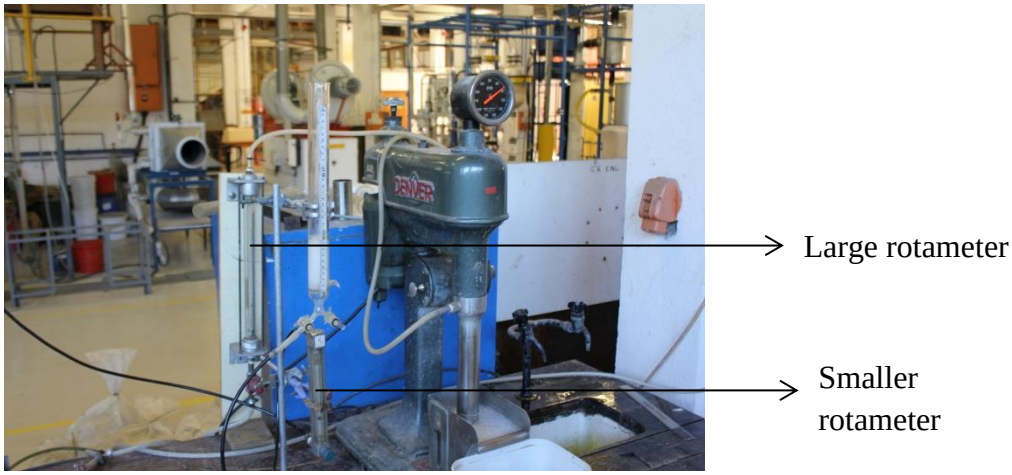

Figure 34: Flotation experimental setup

4 EXPERIMENTAL PROCEDURE

The following chapter summarizes the experimental procedure for different phases of the laboratory test work. Following the format of the previous chapter, this chapter has also been split into three sections viz. the milling, flotation and circuit procedure.

4.1 MILLING

This section will detail the procedure for milling the UG-2 ore sample. Initially, a target grind for the sample was selected, for example 80%-75µm. A fixed mass of sample was charged into the mill together with a selection of 316 SS rods. Tap water was subsequently added to create slurry within the mill. The mass of rods and volume of water were based on the operating volume within the mill. The ore was then milled for a certain time. Wet followed by dry screening was subsequently performed to determine the percentage of the sample passing 75µm. Wet screening is performed using water to create a slurry that allows the fine material to pass through the sieve, shown in Figure 21. The remaining sample was then dried overnight in the oven. Dry screening of this sample was performed using the apparatus shown in Figure 25. This allowed one to determine the additional amount of sample passing 75µm. The results from both the dry and wet screenings were combined to determine a final percentage passing 75µm. The above process was repeated at various times until the required target grind was achieved. The results were then represented in the form of milling curve. A milling curve was required to determine the milling time to achieve the target grind.

4.2 FLOTATION

SIBX, DOW 200 and KU5 were the reagents used to perform test work. Solutions of these were prepared using distilled water. The concentration of the reagents was 1 % by mass (or 1 gram per 100 ml solution). The MINTEK standard procedure was used to perform flotation tests. A brief summary of this method is given:

Once the milled sample has been transferred to the flotation cell, the cell contents were topped up to a static operating level using water. The impeller motor was then switched on whereupon the contents form a new dynamic operating level. The reagents, where necessary, were added in the following order; SIBX, DOW 200 and KU5. Conditioning time was allowed for the reagents to function in the system. The air was then turned on to allow the froth to build up to an acceptable level to perform flotation.

Upon the commencement of the test, hand scraping was used to skim the froth at 15 second intervals. The concentrate obtained from this scraping was collected by means of a tray placed below the cell launder. Water was used to maintain a constant dynamic operating pulp level for the duration of the test. However, due to certain findings later on, synthetic frother water was used. In an effort to maintain constant froth stability, the air flow was incremented at various stages of the test. Rate or bulk concentrates were collected at the end of the test and prepared for analysis.

4.3 PULP LEVEL AND FROTH DEPTH CONTROL

The pulp levels for the respective cells were constant for both ore types. The pulp level was defined as the distance from the launder lip to the pulp-froth interface at the initial dynamic operating conditions. The pulp levels are listed in Table 4 below for the various cells.

Table 4: Pulp levels at dynamic operating conditions

Cell	Pulp level/[cm]
Rougher	3.5
Scavenger	3.5
HG cleaner	3
LG cleaner	4

The froth depth was defined as the distance between the pulp-froth interface and the bottom of the scraper at dynamic operating conditions. This means that it is the height of the remaining froth once a scrape has been performed. Initially all tests on the bad ore were performed using water top-up. The froth depths of the various cells are listed in Table 5 below:

Table 5: Froth depth for initial tests performed with water top-up

Cell	Froth depth/[cm]
Rougher	2
Scavenger	2
HG cleaner	1
LG cleaner	1

However, as a result of certain findings, tests on both the good and bad ores were subsequently performed using synthetic top-up. The scrapers used in the cleaner cells were made smaller to facilitate an increase of the froth depth of the cleaner cells. The froth depths of the various cells are listed in Table 6.

Table 6: Froth depths for subsequent tests performed with synthetic top-up

Cell	Froth depth/[cm]
Rougher	2
Scavenger	2
HG cleaner	2
LG cleaner	2

4.4 CIRCUIT DESCRIPTION AND PROCEDURE

The basic structure of the plant circuit in Figure 14 was simplified and adapted for the current laboratory tests. The circuit used in this work is shown in Figure 35 below, consisting of four different stages namely; rougher, high-grade (HG) cleaner, scavenger and low-grade (LG) cleaner.

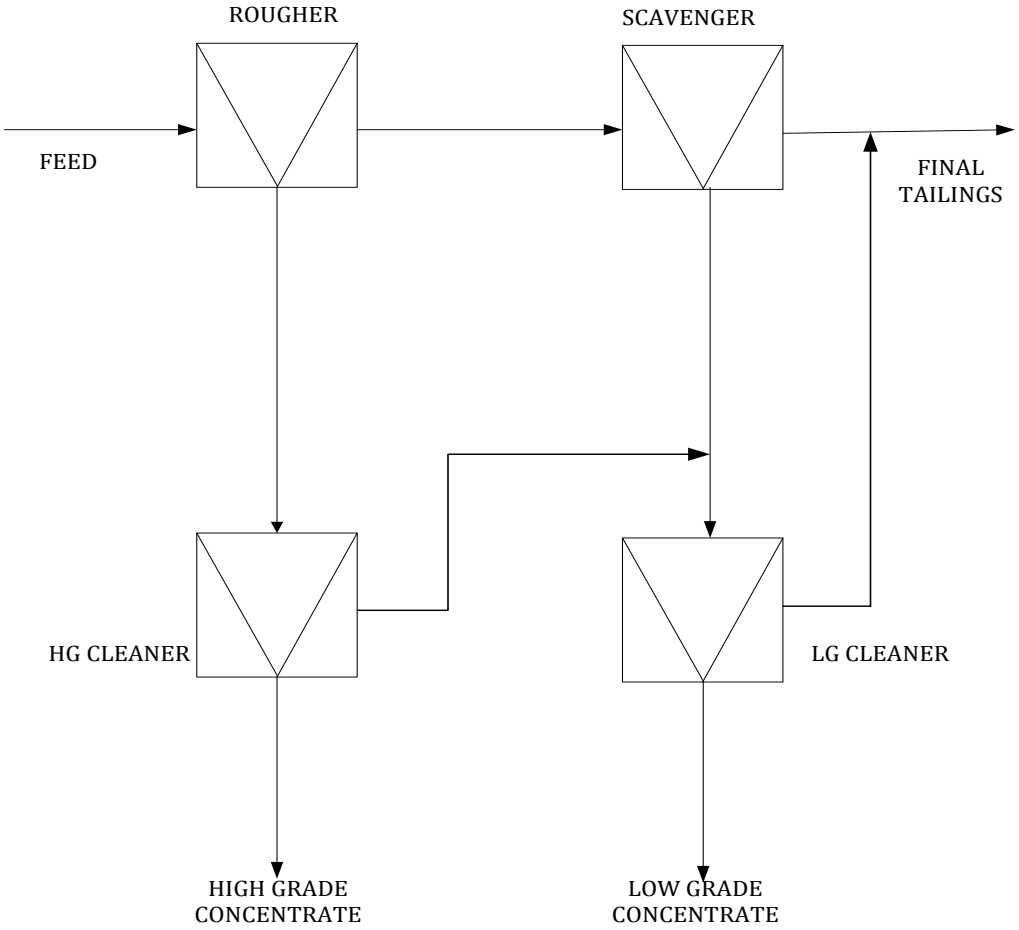

Figure 35: Circuit used for this work

The above four stage circuit was used to optimise both the recovery and grade of PGMs from UG-2 ore. This was the circuit utilised in the initial investigation stages however certain structural adjustments were made at a later stage. These adjustments were done with the intention to improve either the PGM recovery or concentrate grade. Examples of these include the insertion of a regrinding stage for the rougher tails and the application of thickeners in both the cleaner feed streams.

4.4.1 CIRCUIT DESCRIPTION

A rougher cell was used to split the PGMs into two different grades of material. The concentrate from this stage contained most of the HG material (including NFG) whilst the tailings contained the LG material (including chromite and composite particles). The rougher tailing was transferred to the scavenging stage whilst the concentrate reported to the HG cleaner.

The function of the scavenger cell was to extract as much of the remaining ‘difficult’ PGMs including the slow floating particles and those associated with composite particles. Frother was used in an attempt to facilitate the recovery of these ‘difficult’ minerals.

The LG and HG cleaning stages were used to upgrade the material. This was done either by the use of depressant and/or thickeners. The use of a thickener arose from interpretation of the research data and it will not be discussed at this stage.

The use of this circuit enables one to optimise both the PGM recovery and concentrate grade based on the quality of material it contains viz. low and high grades. This renders the ability to change process conditions on any of the units individually, and monitor the effects those changes have, not only on the unit itself, but on the circuit as a whole. This posed some difficulties due to the primary and secondary effects of reagents which were described earlier. These are known as downstream effects. The frother additions had significant downstream effects.

4.4.2 CIRCUIT PROCEDURE

This section details the procedure followed for the flotation circuit shown in Figure 35. The rougher test was performed initially followed by the scavenger test. The 8 L cell was used to perform both the rougher and scavenger flotation tests. The concentrate from the rougher cell was collected in a tray, and the test was continued as a scavenger stage, collecting the scavenger concentrate in the LG cleaner cell. The rougher concentrate was then washed into the HG cleaner cell (1L). After collection of the HG concentrate from this cell, the HG tailings were then filtered to remove all water. This was performed using the pressure drum filter. This wet filter cake was then added to the LG cleaner cell. Hence the need to use a 2.5L cell for the LG cleaner stage.

5 EXPERIMENTAL WORK

This chapter details the experimental work undertaken using three types of UG-2 ore. They were labelled according to their flotation characteristics. The good ore has favourable flotation characteristics whilst the opposite is true in the case of the bad ore. A 3rd type of ore was used in preliminary test work. This ore possessed similar characteristics to the bad ore.

5.1 PRELIMINARY TEST WORK

It was important to develop methods of controlling the dry mass of the various concentrates, prior to sending sample for analysis. A UG-2 sample of unknown origin was used for these tests. The work was primarily focused on understanding the basic mechanisms involved in the flotation process.

5.1.1 EXPERIMENTAL DETAILS: PRELIMINARY WORK

A feed grind of 80%-75µm was targeted. The rod distribution utilised is shown in Table 7:

Table 7: Rod distribution for preliminary ore

Rod Diameter/ [mm]	No. of Rods
20	12
15	12
10	12
5	12

The rod distribution selected was based on a fractional media loading within the mill. The detailed calculation is shown in Appendix A, Page 97.

Separate 2 kg samples were milled for 10, 20 and 30 minutes. Wet screening, followed by dry screening was performed. A size distribution analysis was undertaken. This data allowed one to determine the percentage of material passing 75 microns. The results of both these types of screening were combined for each milling time and the total % passing 75 microns is shown in Figure 36 for the UG-2 ore used for preliminary tests.

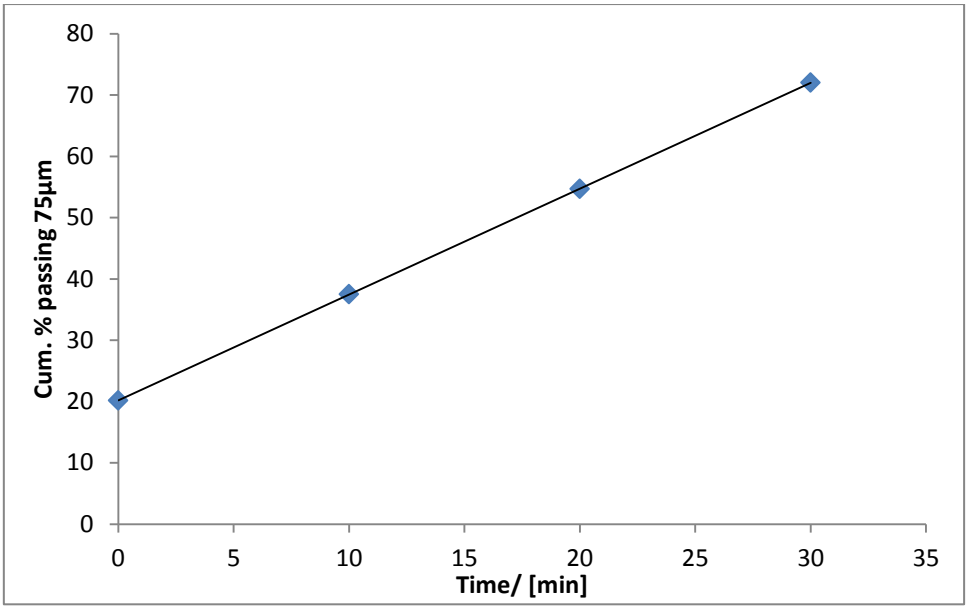

Figure 36: Milling calibration curve for preliminary ore

The linear regression shown in Figure 36 had an R-squared value of 0,999, and hence this was more than adequate for calculating the time for achieving the target grind. Similar tests were done on the other ore types.

5.1.2 INITIAL BATCH FLOTATION TESTS

Single stage batch flotation tests were done using the standard Denver 5L cell, with the larger impeller. The experimental details of this work are shown in Table 8:

Table 8: Experimental conditions for preliminary sample

SIBX	g/t	150
DOW200	g/t	20
KU5	g/t	30
AIR FLOWRATE	$m.min^{-1}$	0.51
IMPELLER SPEED	Rpm	1200

A rougher flotation test was performed and a bulk sample was collected after 20 minutes. The word ‘bulk’ means that a single concentrate was collected at the end of the allotted test time. The results for this test are summarized in Table 9.

Table 9: Bulk test results for preliminary sample

Test Type	Solids Recovery / [%]
Original	8.80
Duplicate	8.89

The recoveries above shown as a percentage of the amount present in the feed. This test was performed in duplicate. The fact that the recoveries were similar showed good repeatability.

It was noted during the test that the froth stability was reduced over time. This was due to the reduction in the amount of floatable solids. However the constant air flow could be responsible for the relatively low froth stability. The froth literally 'collapsed' after ten minutes and this meant that the recovery of solids was drastically reduced. It was decided that a steady increase in air flow could be used to improve the solids recovery in the scavenging stage.

In the first few minutes of the test, the fast floating minerals associated with PGMs and talc were recovered. This caused a stabilizing effect in the froth. In the latter stages of the test, after the recovery of the aforementioned particles, the remaining particles are difficult to recover and it was assumed that some of these particles were composite particles.

It was decided to investigate the effect of steadily increasing the air flow rate to maintain constant froth stability. A rate test was conducted over a period of 20 minutes. The experimental conditions were similar to Table 8. The air flow however, was varied from 0.41 $m.min^{-1}$ (at time 0 min) to 1.18 $m.min^{-1}$ (at time 20 min) (See Table 31, Appendix B, and Page 103). The results of this duplicate test are shown in Figure 37:

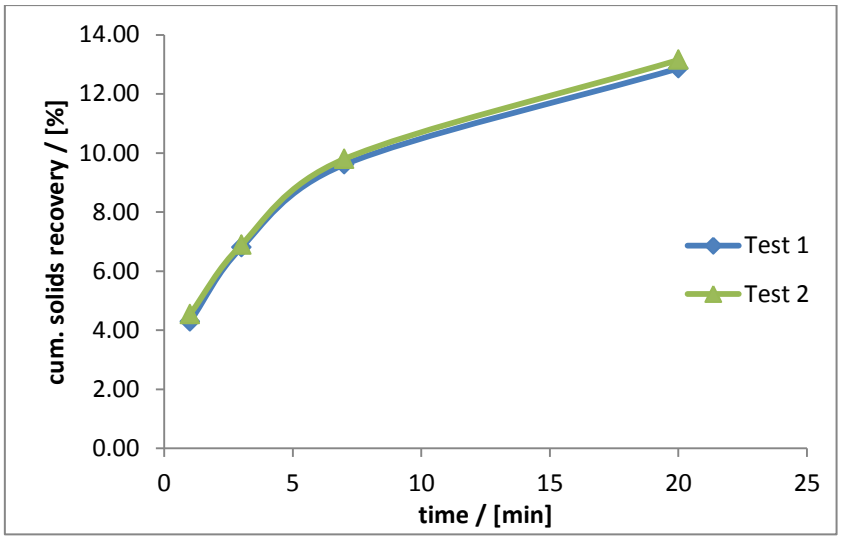

Figure 37: Cumulative solids recovery for preliminary sample

Tests 1 and 2 in the above figure refer to the original and duplicate tests respectively. The cumulative solids recovery at the end of the test 1 was approx. 13%. This is higher than the recovery of approx. 8% achieved in earlier tests shown in Table 9. This increase is due to the steady incremental increase of the air flow at each time.

One way to improve the recovery of particles is to increase the air flow. Larger air flows are necessary to maintain constant froth stability. It is known that low froth stabilities result in brittle froths that reduce solid recoveries. The increase of air flow produces greater amount of air bubbles in the pulp. These air bubbles act like 'vehicles' to transport solids. This means that there are more transport 'vehicles' to carry hydrophobic particles to the surface of the froth. Hence one obtains a greater recovery of solids. The mere presence of a larger amount of solids in the froth stabilizes the froth. The data for these tests are available in Appendix B, Table 63 and Table 64, and Page 120.

It was decided to employ this technique for all further tests involving both the good and bad ores, using targets for the various stages of flotation.

5.2 TESTS ON BAD ORE

The work has been separated into two parts. In the first part of the investigation, work was done using the circuit shown in Figure 35. The second part involved the use of a second stage of grinding, to improve liberation.

Table 10: Rod distribution for bad ore

Rod Diameter / [mm]	No. of rods
20	16
15	16
10	16

In an effort to improve the grinding properties, the smaller 5 mm rods were not used for all subsequent milling of both the good and bad ores. The details of the calculations for this new rod distribution are shown in Appendix A, Page 98.

5.2.1 PART ONE

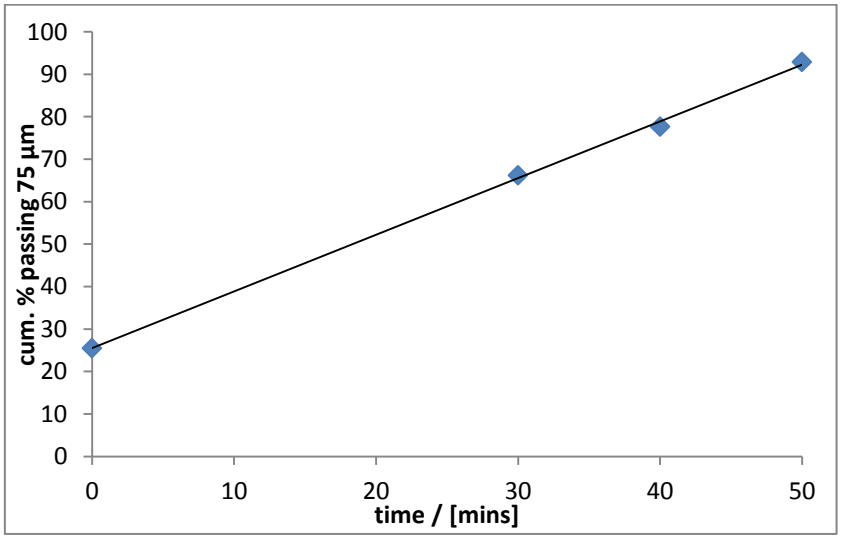

Figure 38: Bad ore milling curve

The linear regression was used to calculate the milling time (41 min) for the tests on bad ore.

5.2.2 ROUGHER FLOAT

The following experimental conditions were used for the rougher float:

Table 11: Experimental conditions for the bad ore rougher float

SIBX	g/t	150
DOW200	g/t	20
KU5	g/t	30
AIR FLOWRATE	$m.min^{-1}$	0.73
IMPELLER SPEED	Rpm	1200

The first task was to separate the material into two different grades viz. high and low grade. The benefits of doing this have been discussed earlier. This separation was performed in the rougher cell. The PGMs associated with high grade material are fast floating minerals that are rapidly recovered in the concentrate. These are generally recovered in the initial period of the test. PGMs associated with low grade material are slow floating minerals which are difficult to recover. Hence they are, if at all, recovered later in the flotation test.

The high grade material is largely associated with talc. This is because talc is also a fast floating gangue mineral. Hydrophobic particles cause bubble coalescence in the froth phase. This results in the formation of larger bubbles and produces a slower moving, stickier froth.

Slow moving froths pose difficulty industrially since the froth slowly migrates to the cell launders. This causes a reduction in the rate of solids recovery. In an effort to solve this issue, KU5 depressant was added until the froth behaviour was deemed suitable for flotation. The role of depressant was to reduce the talc recovery in the concentrate. It also had the effect of reducing the contact angle on the talc, thereby preventing excessive coalescence of the bubbles. The structures of the froth at various depressant dosages are shown in the images below:

Figure 39: Bad ore rougher froth structure at 10 g/t KU5

Figure 40: Bad ore rougher froth structure at 20 g/t KU5

Figure 41: Bad ore rougher froth structure at 30 g/t KU5

From Figure 39, Figure 40 and Figure 41 it can be seen that as the depressant dosage increased, the relative bubble sizes at the froth surface decreased. The depressant selectively attaches to the surface of the talc and hence inhibits the natural hydrophobicity of these particles. The amount of talc mineral present in the froth was reduced and hence bubble coalescence was reduced. It was observed that as the depressant dosage was increased, the froth began tipping off the lip more readily.

It was decided that the proportion of clusters of small bubbles at the start of the test would be useful indicator that there was sufficient depressant. It is easy to switch the air off and add more depressant.

30 g/t represented the froth structure most favourable for flotation based on the froth behaviour. It was decided not to try any further depressant additions in the rougher cell since the primary purpose of this cell, in addition to the separation of the high and low grade material, is to recover as much of the PGMs as possible. Further depressant addition was not feasible due to the risk of losing PGMs. The froth structure becomes more unstable as the presence of hydrophobic particles is reduced.

The next step involved the separation of the high and low grade material. Initially, the froth was dark in colour with big bubbles as shown in Figure 41. The dark colour is the result of the presence of hydrophobic solids, particularly talc. This is shown in Figure 42 and Figure 43, which show the froth colour with and without solids present. The mineralised froth here is much more brittle and much lighter in colour compared to the previous Figure 41. This shows the importance of particles in stabilizing the froth structure.

As the froth is skimmed off, there is a removal of those solids present in the froth. These are subsequently replaced in the froth by more solids which are captured by rising bubbles. However, there is a limited amount of recoverable hydrophobic particles in the pulp. The result of this is that there is a decrease in the rate of solids recovery as the test is performed. This net effect of this is that the froth becomes steadily lighter in colour as time passes. Figure 42 was taken after the first colour change was seen in the froth viz. after 3 minutes:

Figure 42: Rougher froth structure after 3 minutes

Figure 43: Froth structure with no solids

It is apparent from Figure 42 that this froth has a different structure compared to that of Figure 41. Firstly the presence of smaller bubbles is indicative of less bubble coalescence. The froth is a lighter shade in colour indicating the presence of less solids.

It was assumed that, after 3 minutes, most of the talc and fast floating hydrophobic minerals were recovered in the concentrate. These fast floating PGM minerals constituted the high grade material. This represented a solids recovery of about 4 % of the feed material.

The next phase of the investigation involved optimising the scavenger and HG cleaner cells. Due to the structure of the circuit, these cells are independent of each other and hence independent adjustments were possible.

5.2.3 SCAVENGER

Table 12: Experimental conditions for scavenger cell

SIBX	g/t	0
DOW200	g/t	0 – 16
KU5	g/t	0
AIR FLOWRATE	$m.min^{-1}$	0.73 – 1.24
IMPELLER SPEED	Rpm	1200

The purpose of the scavenger cell was to recover as much of the remaining difficult material as possible. This includes composite particles and other slower floating species. Frother was used to improve the recovery of solids. The progressive increase in air flow was based on visual observations of the froth, and hence, as the frother concentration increased, smaller air flows were required to sustain a desirable froth flow (See Table 32, in Appendix B, page 103). Figure 44 shows the effect of frother addition (expressed as g/t of original feed) on the solids recovery in the scavenger stage (same cell):

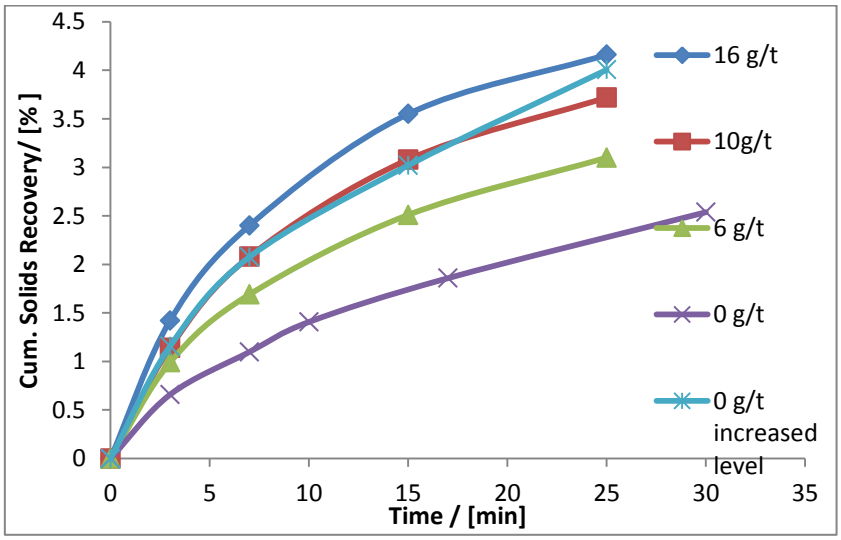

Figure 44: Cumulative solids recovery at various frother dosages in scavenger cell- bad ore

Figure 44 shows that as the frother dosage increased from 0 to 16 g/t, the cumulative recovery of solids increased. The frother molecules reduce the air/water surface tension hence air bubbles are less likely to rupture or coalesce. This results in the presence of a larger proportion of smaller bubbles in the froth. These bubbles have a superior surface area per unit volume compared to larger bubbles. This means that a group of smaller bubbles with the same volume as a single large bubble will carry significantly more solids to the froth overflow. Hence the recovery of solids increased.

At 16 g/t, the froth comprises of smaller bubbles hence has a greater stability compared to 0 g/t. However, the brittle froth obtained at 0 g/t had benefits, namely improved drainage of entrained particles. Thus higher solids recoveries were obtained when the frother dosage was increased.

Another effect of increasing the frother dosage was the reduction in flotation time. At 0 g/t, it takes approximately 30 minutes to recover approximately 2.5% of the solids initially present in the feed. It takes 15 minutes to achieve the same solids recovery at 6 g/t. This 'time' translates into residence time used in the design of industrial cells. Thus an increase of frother improves the production rate of solids. However, it should be noted that due to the entrainment contribution to the overall solids recovery, this does not necessarily imply an improved grade in the LG cleaner concentrate.

The effect of froth height on solids recovery in the scavenger stage was evaluated at 0g/t frother addition. The laboratory procedure was based on a 2 cm froth depth, but in view of the negative effects of adding additional frother, the froth depth was reduced to 1 cm, as a way of increasing solids recovery. This is denoted on the key as '0 g/t at increased level' with reference to the increased pulp level. This increase resulted in a reduction of the froth height by 1 cm. At 0 g/t it can be seen that the reduction in froth height resulted in a 1.5% increase in solids recovery after 20 minutes. As the froth height is reduced, there is a reduction in drainage of hydrophilic particles. This implies that there is an increase in the recovery of solids via entrainment hence an overall increase in the solids recovery.

It can be seen from the shape of the graph with the lower froth height, that a close to linear relationship exists between solids recovery and time. This type of relationship implies that the non-selective process of entrainment is dominant over true flotation and as such, this idea was scrapped.

Samples were sent for analysis of total PGM's. It was decided that 16 g/t produced the targeted solids recovery of 4 % in 23 minutes. This 4% mass accounted for approximately 15% of the PGMs originally present in the ore. Industrially, no more than 40 g/t of frother is added over both the rougher and scavenger stages. Having already added 20 g/t in the rougher, this brings the overall frother addition to 36 g/t - still within industrial standards.

5.2.4 HG CLEANER

The operating volume of the HG cleaner cell was approximately one litre. This is the pulp level necessary to ensure successful flotation. The feed, or rougher concentrate, occupied half of this volume. The remaining volume was provided using fresh tap water.

Table 13: Experimental conditions for bad ore HG cleaner

SIBX	g/t	0
DOW200	g/t	0
KU5	g/t	0 – 10
AIR FLOWRATE	$m.min^{-1}$	0.41 – 1.65
IMPELLER SPEED	Rpm	1000

The HG cleaner was used to improve the grade of the rougher concentrate. This was achieved by reducing the gangue content of the concentrate, primarily consisting of talc. KU5 depressant was used to reduce the talc content by suppressing its natural hydrophobicity. The effects of depressant addition on the PGM recovery and the concentrate grade were

evaluated. The data for air flux velocity is found in Table 33, Appendix B, and Page 103. The results are presented in Figure 45 and Figure 46. Recoveries are based on rougher feed.

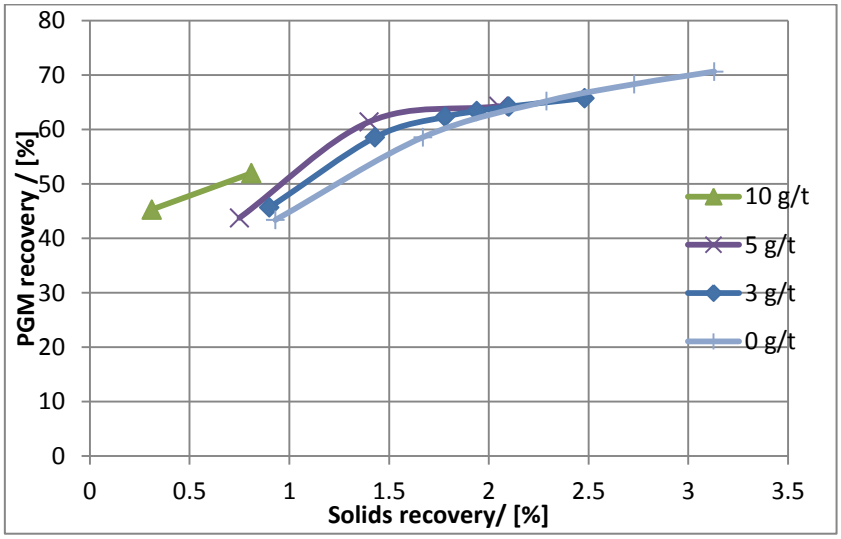

Figure 45: PGM recovery vs. solids recovery at various KU5 dosages for bad ore HG cleaner

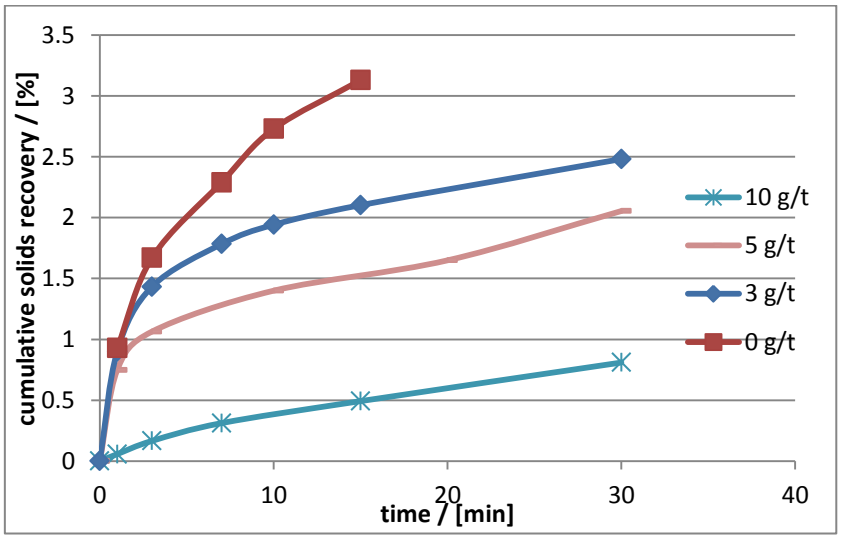

Figure 46: Cumulative solids recovery at various KU5 dosages for bad ore - HG cleaner

From Figure 46, as the depressant dosage increased from 0 to 10 g/t, the cumulative recovery of solids gradually decreased. The depressant reduced the amount of talc that is recovered in the concentrate. Talc stabilizes the froth; hence it increases the entrainment of other gangue minerals including the talc itself.

The ore is very sensitive to depressant addition. This can be observed when comparing the 5 and 3 g/t graphs. For a mere 2 g/t depressant increase, the solids recovery decreased by approximately 0.5 % after 30 minutes. The solids feed to the HG cleaner is 4 % of the original mass. Thus a solids recovery of 0.5 % represents 12.5 % of the initial amount present in the cell.

Generally, in ores with poor flotation properties, depression of the talc comes at a cost to the overall process. This 'cost' refers to the effect on the overall PGM recovery. It can be explained using Figure 45. This is a plot of the cumulative PGM vs. solids recovery at depressant dosages ranging from 0 to 10 g/t.

Ideally, one would like to remove all the talc from the ore, whilst not losing any PGMs. Hence, one would prefer for any curve to lie in the upper left hand region of the graph in Figure 45. This is where the PGM recovery is at its highest whilst the overall solids recovery at its lowest.

However this graph showed that as the mass of solids was reduced, there was an inherent loss of PGMs. The increase in depressant dosage was responsible for a reduction in cumulative solids recovery. This implied the depressant had an adverse effect on the PGM recovery.

This was due to the froth stabilizing nature of talc. Due to its natural hydrophobicity, talc particles cause bubbles to coalesce. When these bubbles coalesce, they form a sticky and stable froth. As talc particles are prevented from being recovered, the froth becomes more brittle. This causes reduction froth stability. Due to this reduced froth stability, there is a loss of entrained particles.

Ores that present difficulty floating usually have mineral liberation issues. This is due to the presence of a large amount of composite particles. These particles consist of talc, PGMs and other gangue minerals. When the talc on the surface of a composite is depressed, the chances of this particle being captured via a bubble are reduced. This means that this particle, along with the PGMs it possesses, might not be recovered hence the overall PGM recovery will decrease.

The largest cumulative PGM recovery, of roughly 70% occurs at 0 g/t. It is observed that the solids mass is reduced significantly from when 5 g/t depressant is used, whilst there are insignificant PGM losses. However, at 10 g/t it is observed that the overall solids mass has been reduced; the PGM content has decreased by roughly 15% compared to the 5 g/t curve. This is the unavoidable side effect of over-depressing the ore.

Thus it was decided that to target a cumulative PGM recovery of 60% in the HG cleaner. From Figure 45, it can be seen that a dosage of 5 g/t corresponds to the lowest solid mass recovery whilst retaining at least 60% of the PGMs. This was the KU5 dosage selected for all further test work involving this cell.

5.3 FROTHER TEST WORK

Work performed on the HG cleaner showed the effect of using a tap water top-up on the froth structure. Due to the relatively low amount of feed to the cell, the contents were made up to the operating level using fresh water. Industrially, apart from a minor flow of launder water, no significant dilution of the frother takes place. There was dilution of the frother in these laboratory cleaner tests. This dilution affects the froth structure resulting in lowered stability. Thus it accounts for differences in both the PGM recoveries and concentrate grades compared to larger scale operations. This dilution affects the overall froth structure and thus affects both

the recovery of PGMs and the concentrate grade. The concentration of frother in the cell was lowered, but there was no way of measuring the new concentration of frother within the cell.

In order to investigate this concept of dilution, it was necessary to quantify the frother concentration. It is assumed that, of the three reagents that are present within the cell, only frother itself is concentrated in the froth phase. The other two, namely depressant and collector are assumed to adsorb completely onto the solids surfaces and do not affect the frother concentration.

This chapter details attempts which were made to quantify the frother concentration in liquid solutions. Two methods were proposed. The first method relates the capillary action to the surface tension of liquids. The second method relates the froth height with no solids present.

5.3.1 METHOD ONE

The experimental setup for this method was shown in paragraph 3.3 (Figure 31). This involved the use of a capillary tube (1mm ID – 100 mm length) together with a glass vial. A brief summary of the experimental procedure follows:

Standard solutions of DOW200 in distilled water were prepared. The solutions ranged from 0 to 1.2 % by mass. It was expected that all operating frother concentrations would lie in this range. 10 ml aliquots of each solution were pipetted into the glass vial. The weight of the capillary tube was recorded before it was inserted into the solution. The weight of all the contents within the vial was subsequently recorded. The liquid capillary action was observed.

Initially, it was decided to relate the capillary liquid height to the surface tension. The properties are related via Equation 2 shown in the theory section. The surface tension is directly related to the frother concentration. A veneer calliper was used for accurate measurements of capillary height. The height was recorded three times for each solution and the arithmetic mean at each concentration and is shown in Figure 47 below:

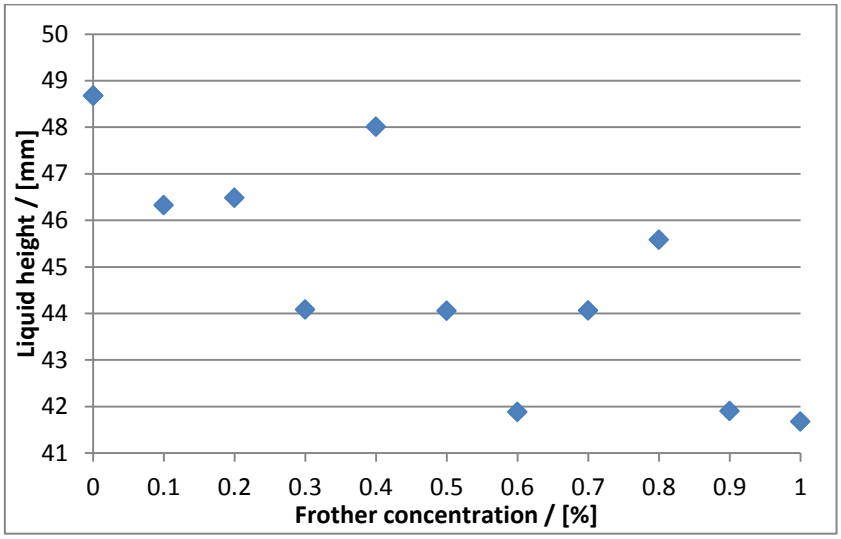

Figure 47: Liquid heights at various frother concentrations

The largest height, 48.5 mm occurred at the lowest frother concentration viz. pure water. The lowest height, 41.5 mm, occurred at the highest frother concentration viz. 1 %. Frother reduces the surface tension of the liquid. Since surface tension is directly proportional to liquid height, according to Equation 2, the liquid height should decrease as the surface tension is reduced.

The graph showed no general trend in liquid height for concentrations ranging between 0.3 – 0.8 %. The significant scatter was perplexing. Possible reasons for this could involve the method of measurement. There was a degree of uncertainty since the calliper could not measure changes less than a millimetre. Differences in height between concentrations were seen to be millimetres. Due to this inconsistency, an adjustment to the apparatus was required.

It was decided that mass measurement should be used to determine the volume and hence the level of solution in a vial, prior to insertion of the capillary tube. Once the liquid has reached a level in the tube, a finger was placed over the top end of the tube, and the tube was withdrawn. Surface liquid was allowed to drip off. The change in mass was used to measure the volume of liquid inside the capillary.

The data used to generate Figure 47 is available in Table 42, Appendix B, and Page 108.

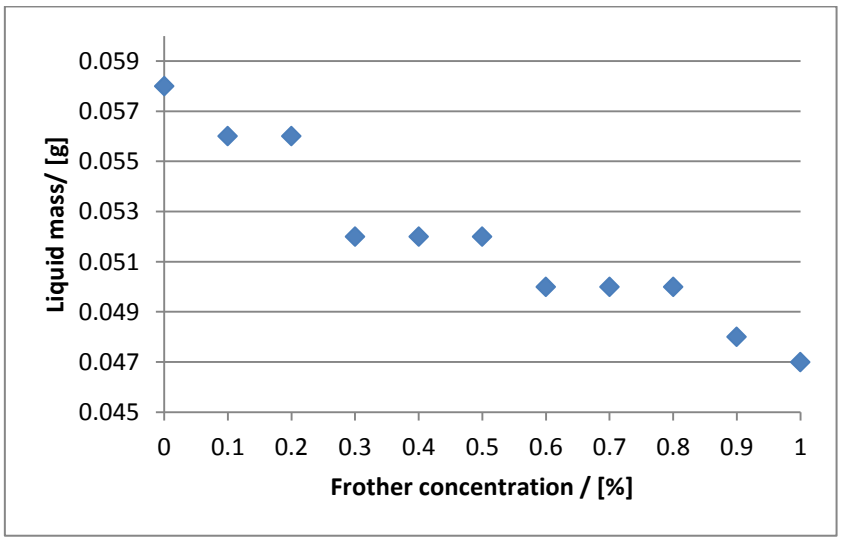

Figure 48: Liquid masses at various frother concentrations

Figure 48 showed a definite trend in the relationship between the liquid mass and the frother concentration. An increase in frother concentration resulted in a decrease in liquid mass. This type of result agrees with theory. This is due to the frother, which reduces surface tension, thereby reducing the amount of liquid within the capillary tube.

However certain frother concentrations, for example 0.1 and 0.2 per cent, produced indistinguishable liquid masses. This indicated that the method was not sensitive enough to detect slight changes in mass, which are particularly prevalent in the dilute concentration regime. The data from Figure 48 is tabulated in Table 43, Appendix B, and Page 109.

It was decided to investigate this method using a more dilute range of frother solutions. This is shown in Figure 49 below.

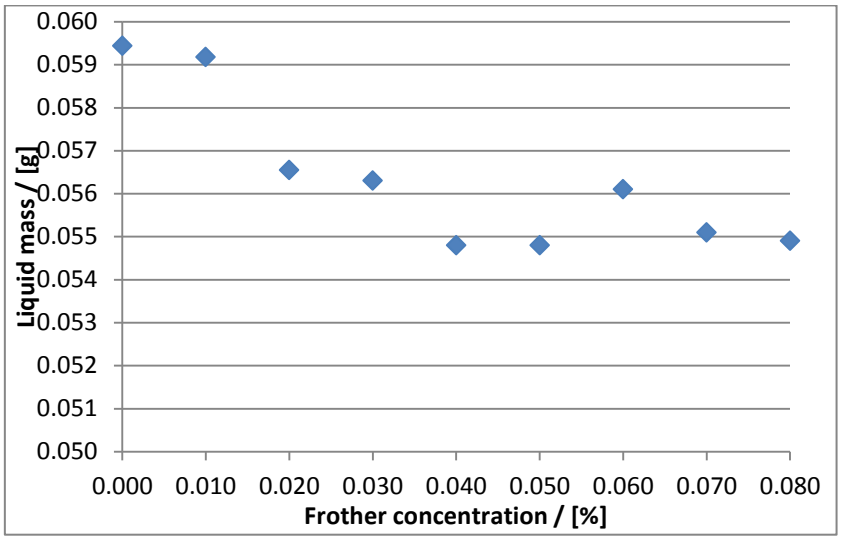

Figure 49: Liquid masses at various dilute frother concentrations

Figure 49 also shows there were several frother concentrations which produced near identical masses, for example - concentrations 0.04 & 0.05 %. This verifies that the method is not reliable for measuring small changes in liquid masses.

The mass of liquid at the initial concentration of 0 % is 0.0594 g. According to Figure 48, the mass at the corresponding initial concentration is 0.0580 g. This shows an inconsistency in the ability to replicate results using this method. A possible reason for this uncertainty in mass is the wetting of the outside of the tube. The liquid mass on the outside of the capillary affects the calibration and cannot be quantified. The data in Figure 49 is tabulated in Table 43, Appendix B, and Page 110.

Thus this method was not suitable for either dilute or concentrated frother solutions. A different approach was deemed necessary to solve the frother concentration conundrum.

5.3.2 METHOD TWO

The flotation experiments were conducted, using increments in air flow to maintain a suitable froth depth. During the concentrate removal process via scraping, the frother concentration in the cell gradually reduces. In the absence of solids, there is also a relationship between the froth height, frother concentration and the aeration rate in a vertical tube. As the aeration rate or frother concentration increase, the froth height increases. It was decided to use this simple measure of the effect of frother concentration on froth height to measure frother concentration in a simple, practical way. One consideration was the limited volume of water that could be recovered from concentrate samples by filtration.

A constant air flow rate was maintained. It was passed through a sintered disc at the bottom end of a glass tube, to create a cloud of bubbles. The concentration of frother had an effect on bubble size, as expected. The pressure in the air line leading to the sintered disc was measured, to ensure that no progressive blockage was occurring. The pressure was also used

to correct the reading on the rotameter. A fixed amount of liquid was placed inside. Thereafter the froth height was recorded after a minute.

10 ml aliquots of frother solutions were pipetted, ranging from 0 to 0.1 g/L, into the tube apparatus. This apparatus was nicknamed the ‘bubbler’ due to the bubbling nature of the froth at higher air flows.

The air rate was then turned up to 2.5 L/min, which remained constant for all subsequent concentrations. This air flow was selected due to the ability to distinguish the froth heights at various frother concentrations. The solution was then pipetted and timer started. The froth height was subsequently recorded after a minute. This height was determined with the aid of a tape measure attached the side of the bubbler. The air was turned on prior to pipetting the solution, to prevent seepage through the sintered disc thereby affecting the reliability of results. Figure 50 shows what was observed once the froth had formed (after a minute).

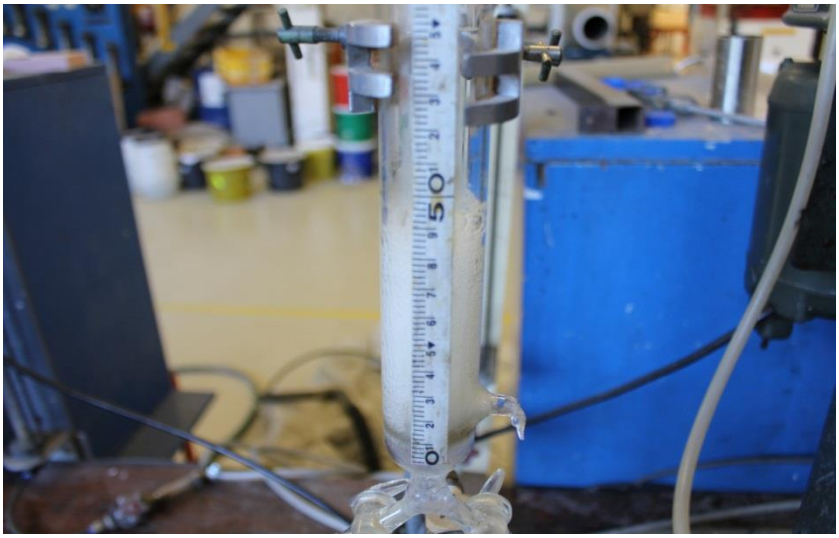

Figure 50: Froth generated within bubbler

The results for this calibration are shown in Figure 51:

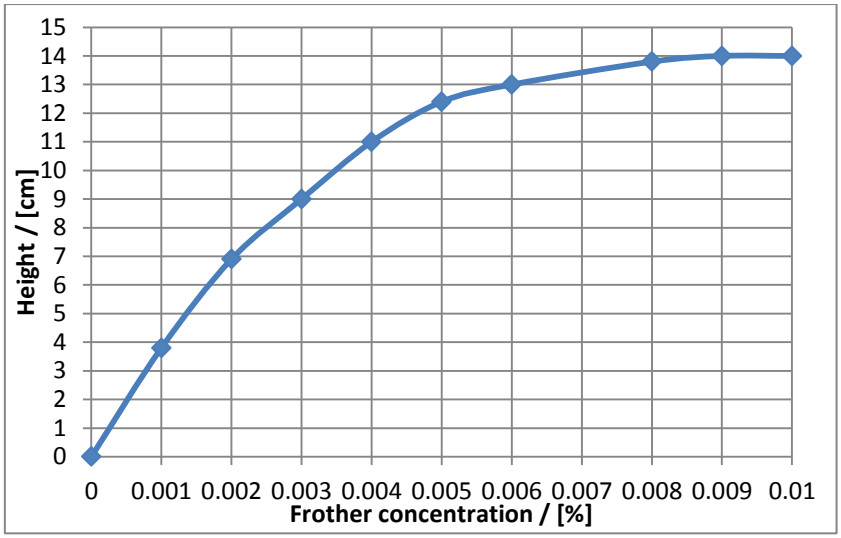

Figure 51: bubbler calibration at 2.5 L/min with 10 ml samples

Figure 51 shows the relationship between frother concentration and froth height, at a fixed air flow rate. This response is similar to what was observed in flotation tests. The graph shows that there is a tailing off in the rate of increase of the height when the concentration exceeded 0.007% (or 0.07 g/L). This means that there is a maximum froth height that can be achieved at any single air flow rate, irrespective of the frother concentration. This height is achieved, for this particular setup, at frother concentrations greater than 0.1 g/L. The data used to generate Figure 49 is available in Table 45, Appendix B, and Page 111.

It was decided to further investigate this device by including concentration data at an even more dilute range. This range refers to concentrations less than 0.02 g/L. It was found that the sensitivity of the bubbler, at the same conditions, was poor in this dilute range. The froth heights were indistinguishable at the various concentrations.

In an attempt to improve the sensitivity of the device, it was then decided to use 20 ml aliquots of frother solutions rather than the initial 10 ml aliquots. The aeration rate was increased to 3 L/min in an effort to increase the differences in the froth heights at various concentrations. The results are shown in the Figure 52:

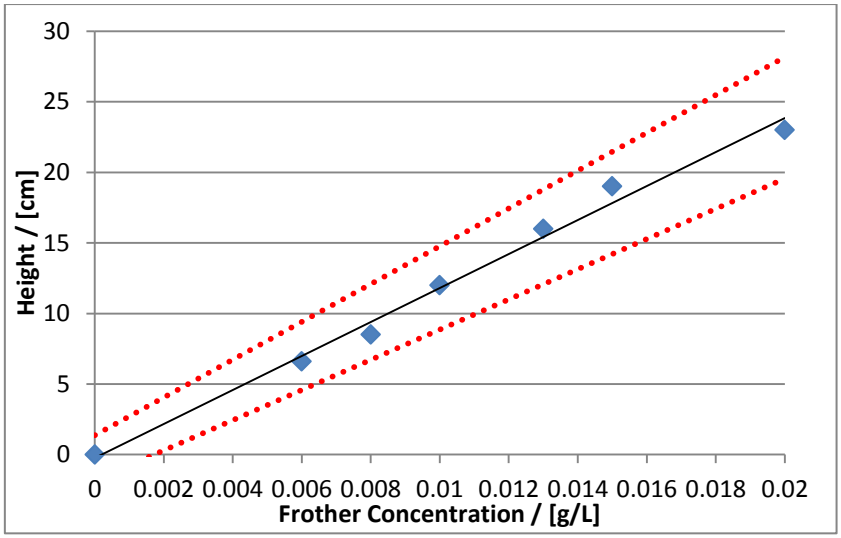

Figure 52: Bubbler calibration at 3 L/min with 20 ml samples

Figure 52 shows a linear trend with regards to the relationship between the froth height and the frother concentration. The froth height at 0.01 g/L is 12 cm. According to Figure 51, it was approximately 4 cm. Thus, the froth height was magnified at these new conditions. The data used to generate Figure 52 is available in Table 46, Appendix B, and Page 111.

The above calibration enabled the author to quantify the frother concentration of an unknown solution based on the froth height. This method was subsequently applied to all streams in the circuit shown in Figure 35. The experimental procedure was identical to the one used to generate Figure 52 with the exception that all samples were filtered before using the bubbler. (The solids content would obviously affect froth height.) Figure 53 shows typical frother concentrations in the various stages, given the additions of frother indicated. The mass balance on the frother was not calculated at this stage, as the amounts of water added had not been measured.

This updated circuit together with the concentrations of all the streams are indicated in Figure 53:

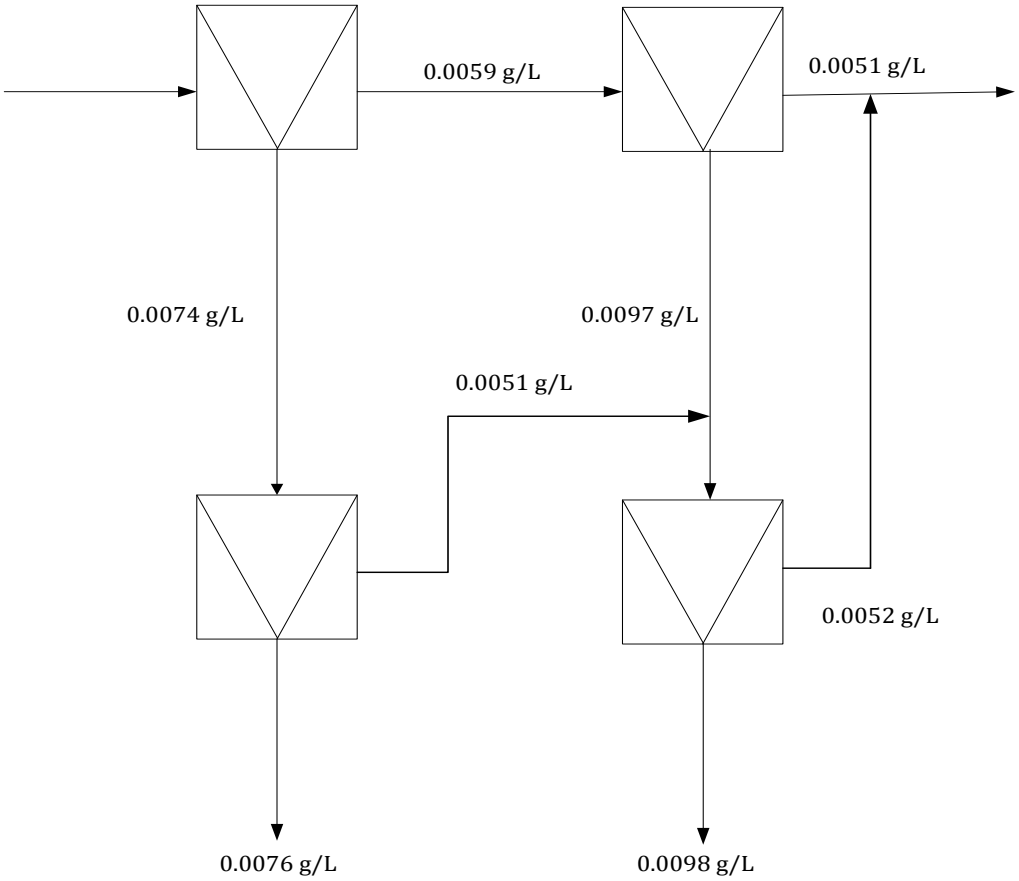

Figure 53: Updated bad ore circuit including frother concentrations

The next phase of experiments involved preparing standard solutions based on the figures shown above. These solutions, prepared using water and DOW 200, were used to maintain operating levels in each cell, rather than adding tap water. The rougher cell level was maintained with fresh water. The results from this cell remained unchanged using this new technique. The HG cleaner results differed with the introduction of this synthetic top-up water. The results are detailed in the next section.

5.3.3 NEW HG CLEANER DATA

The concentration of frother in the rougher concentrate, shown in Figure 53, was 0.0074 g/L. As mentioned previously, the total volume accounted for by the rougher concentrate was approximately 45% of the HG cleaner operating cell volume. The remainder of this volume was made up using a synthetic solution with the same concentration. This solution was also used to maintain the operating level during scraping. The first noticeable difference, compared to the previous HG cleaner scheme, was the froth structure.

Figure 54: Bad ore HG cleaner froth structure with water top-up

Figure 55: Bad ore HG cleaner froth structure with synthetic top-up

The above two pictures were taken at the commencement of each test. They present contrasting froth structures. Figure 54, where water was used to maintain the pulp level, indicates a brittle froth with bigger bubbles compared to Figure 55. From these images, one would expect the recovery of PGMs to be higher in Figure 55 compared to Figure 54. This was largely due to the difference in froth stability. However one would also expect the entrainment of gangue particles to be higher in Figure 55 compared to Figure 54. Selected results for the HG cleaner are shown in the Table 14:

Table 14: Comparison of HG cleaner results for bad ore

Top-up solution	Scrape Time / [min]	PGM recovery / [%]	Solids recovery / [%]
Water	7	62.8	1
Synthetic soln.	7	62.7	3.13

The results in Table 14 were based on previous depressant dosage of 5 g/t in the HG cleaner. The table shows the difference in flotation results obtained from a bulk test conducted over a period of 7 minutes. These tests were conducted using different top-up solutions hence the contrasting froth structures. Thus, dissimilar solids recoveries were obtained, but the recovery of PGM's was essentially the same.

The mass recovery was increased substantially when the synthetic top-up solution was used, probably due to entrainment. This was seen to have important practical implications.

Due to industrial smelting constraints, it is not feasible to process a solids recovery of 3 % from the HG cleaner. This is since it accounts for a mere 60 odd per cent PGM recovery. It

was decided to reduce the solids recovery target to 1% in the HG cleaner. This is in keeping with industrial solids recovery standards. Below are both the results and experimental conditions of bulk tests in which a 1 % solids recovery was targeted:

Table 15: Experimental conditions for HG cleaner at 0.0074 g/L

SIBX	g/t	0
DOW200	g/t	0
KU5	g/t	5
AIR FLOWRATE	$m.min^{-1}$	0.41 – 0.66
IMPELLER SPEED	Rpm	1000

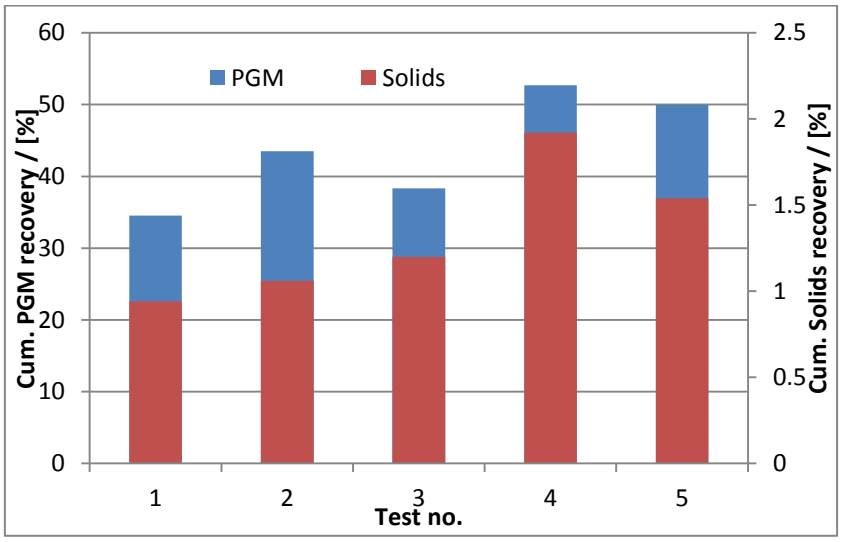

Figure 56: Solids recovery vs. PGM recovery in HG cleaner

Figure 56 shows both the PGM and solids recovery for several bulk tests conducted in the HG cleaner cell using synthetic make-up water. The PGM recoveries varied between 35-50 % depending on the solids recovery. It can thus be deduced that there exists a relationship between the solids recovery and PGM recovery.

In order to achieve the target mass pull in the HG cleaner, the air rate was reduced. Due to the synthetic make-up water, it is predicted that there will be more entrainment. A more stable froth reduces the natural drainage of entrained particles, implying a greater recovery of gangue minerals in the concentrate.

A greater amount of gangue would accompany the PGMs at each scrape interval compared to the previous setup. In order to achieve the same PGM recovery as the previous setup, one would have scrape for 7 minutes as shown in Table 14. This however would result in a solids recovery of over 3 %, due to additional gangue entrainment, which is not desirable.

The tests used to generate the results in Figure 56 were conducted over a period of 1 minute each. This meant that the resulting target recovery of 1 % solids was achieved in less time compared to the previous setup which took all of 7 minutes.

The air rate required was lower for synthetic top-up compared to water top-up as can be seen comparing Table 13 and Table 15. The concentration of frother is lower in a brittle froth compared to a stable froth. There is a loss of water that accompanies the solids in the concentrate. This water contains frother molecules. This means that these molecules are constantly being depleted in the cell. Synthetic top-up replenishes some of this loss of frother molecules whilst water top-up does not.

The air flux varied during the test however the results shown in Figure 56 refer to the cumulative recovery in 1 minute. The full set of data points showing the air flux velocity range can be found in Appendix B, Table 34, and Page 104.

5.3.4 EXPERIMENTAL OBSERVATIONS FROM HG CLEANER

The decision to design scrapers to skim less of the froth in the synthetic solution lies in the entrainment characteristics. A large amount of gangue minerals are present at the froth-pulp interface. In order to reduce the gangue entrainment, the scrapers were adjusted resulting in a froth depth of 2 cm.

It was observed that the use of synthetic frother method caused changes in the froth structure thus affecting the overall recovery of solids and PGMs. The flotation time, to acquire the same PGM recovery, differs as seen in the HG cleaner results. This meant that new flotation test work would be necessary to optimise the depressant dosage in the HG cleaner. Due to sample constraints, this was not possible.

It was ultimately decided that a 1% solids recovery be targeted in the HG cleaner. Even though this accounted for a relatively low PGM recovery, compared to the previous setup, it was assumed that the LG cleaner would be designed to recover all the remaining PGMs.

Another development in the experimental technique was the use of a scale that was placed underneath the concentrate trays during the flotation tests. This was used to target a consistent ‘wet’ mass in all concentrate streams. The word ‘wet’ refers to the mass of both the solids and water in the concentrate. The experimental setup including the scale and concentrate collection tray is shown in Figure 57:

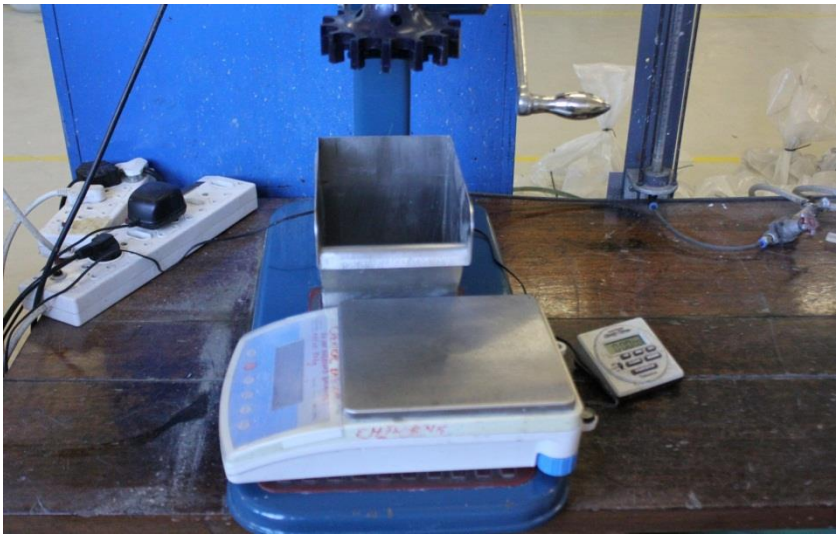

Figure 57: Experimental improvements made to HG cleaner setup

Figure 58 shows the new ‘wet’ mass targets for each of the concentrate streams in the HG cleaner and rougher cells:

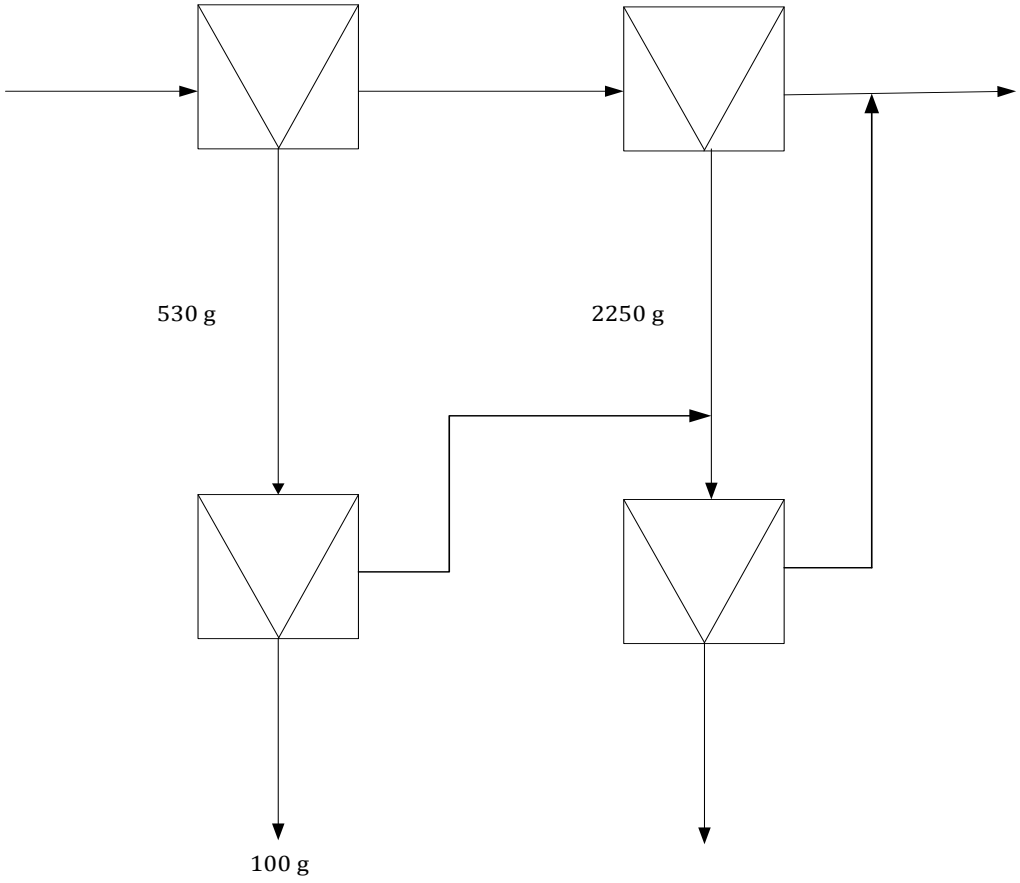

Figure 58: Wet mass targets for the rougher, scavenger and HG cleaner cells

These wet mass targets would only apply if the water-to-solids ratio (w/s) in the concentrates remained relatively constant. The scavenger concentrate accounted for a solids recovery of about 5.5-6%. According to the scale, this resulted in a wet mass of 2250 g and a w/s of 14:1. The rougher concentrate accounted for a solids recovery of about 4 % in a wet mass of 530 g and thus a w/s ratio of 4.3:1. The higher ratio of the rougher concentrate is due to the quality of concentrate.

The difference in these ratios was attributed to the water recovery in each cell. The rougher concentrate consists of fast floating material that is easily recovered. The scavenger cell consists of low grade material that is difficult to recover. Thus the scavenger cell has a higher degree of entrainment compared to the rougher cell. The water content is thus higher resulting in the difference in ratios.

The scavenger cell experimental conditions, using a synthetic frother top-up of 0.0059 g/L, are listed in Table 16:

Table 16: Experimental conditions for scavenger cell at 0.0059 g/L - bad ore

SIBX	g/t	0
DOW200	g/t	16
KU5	g/t	0
AIR FLOWRATE	$m.min^{-1}$	0.65 - 1.20
IMPELLER SPEED	Rpm	1200

The list of air flux velocities required to maintain constant froth stability is found in Table 35, Appendix B, and Page 104.

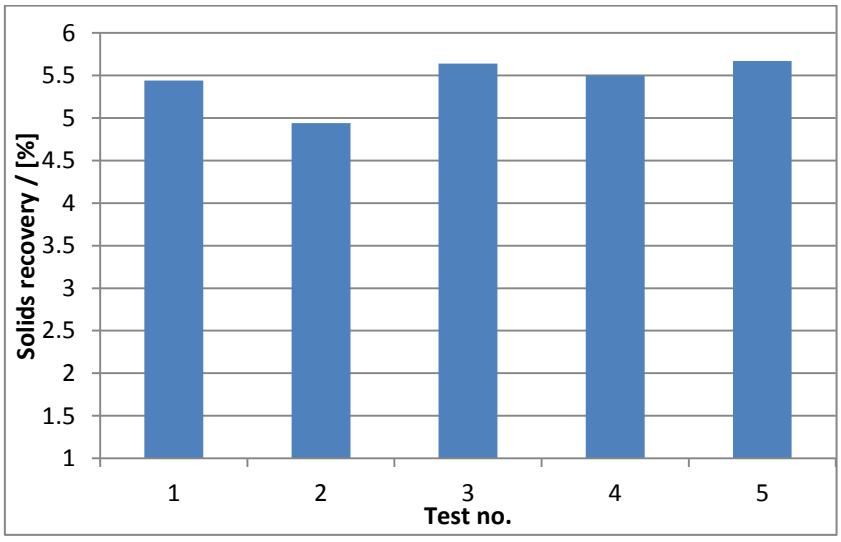

Figure 59: Solids recovery for scavenger tests at 0.0059 g/L- bad ore

Figure 59 shows the solids recovery for five tests performed using the experimental conditions listed in Table 16. The tests were all performed targeting a wet mass of 2250 g. This target was achieved after 20 minutes. Due to financial constraints, it was not possible to perform PGM analysis to determine the variability of PGM recovery.

It was noted that, according to results from the HG cleaner shown in Table 14, the PGM recovery using both the water and synthetic top-up was similar. This was true provided that the float time was the same. However, the use of a synthetic top-up resulted in a larger solids recovery due to entrainment. The objective of the scavenger cell is to recover as much of the PGMs as possible irrespective of the overall solids recovery.

It was assumed the same PGM recovery that was obtained in the previous setup, approx. 15%, was recovered using synthetic frother top-up. This recovery was obtained in approximately 5.5-6% solids recovery. Statistical analysis was performed on the sample set of data and summarized in Table 17 below.

Table 17: Statistical analysis on bad ore scavenger cell data

	Solids recovery
Mean	5.44
Standard Error	0.13
Median	5.50
Standard Deviation	0.29
Sample Variance	0.09
Kurtosis	3.01
Skewness	-1.68
Range	0.73
Minimum	4.94
Maximum	5.67
Sum	27.19
Count	5.00
Confidence Level (95.0%)	0.37

The excess recovery of gangue minerals in the scavenger concentrate was processed in the LG cleaner cell, which was the next phase of investigation.

5.3.5 LG CLEANER

This chapter details work performed with the LG cleaner cell. The feed to the LG cleaner consists of two different streams, shown in Figure 35. i.e. the tailings from the HG cleaner and the scavenger concentrate.

The quality of LG cleaner feed material is poor compared to that of the HG cleaner. The LG cleaner feed consists of composite particles and other slow floating minerals. The scavenger concentrate contains a large amount of chromite, recovered via entrainment, which causes downstream problems in the smelting process.

Prior to mixing the two streams, the concentration of frother in each was measured using the bubbler. The HG cleaner tailings had a frother concentration of 0.0059 g/L compared to the scavenger concentrate, whose frother concentration was 0.0097 g/L. In light of this significant difference in concentration, it was decided to design the LG cleaner to process for the worst case conditions viz. at the highest possible frother concentration of 0.0097 g/L. This is the highest possible concentration when the two streams are mixed.

The results from the HG cleaner showed that the higher the frother concentration, the greater the entrainment of solids. This causes a reduction of the concentrate grade. It was assumed that if one can attain a quality product at a frother concentration of 0.0097 g/L, then one should obtain a similar quality concentrate at lower frother concentrations. This can be done by making the necessary adjustments to the depressant dosage.

The HG tailings were filtered to remove all water and transferred to the LG cleaner cell. The scavenger concentrate was collected into the LG cleaner cell since it was at the desired frother concentration of 0.0097 g/L. A synthetic solution of 0.0097 g/L was used to maintain the flotation operating level.

In order to attain a good quality concentrate, it was decided to apply only the use of KU5 depressant in order to reduce the naturally floating gangue that would otherwise be recovered in the concentrate. Five different depressant dosages were investigated and the results and experimental conditions are listed below:

Table 18: Experimental conditions for LG cleaner at 0.0097 g/L- bad ore

SIBX	g/t	0
DOW200	g/t	0
KU5	g/t	8 – 32
AIR FLOWRATE	$m.min^{-1}$	0.59 – 1.33
IMPELLER SPEED	Rpm	1200

The superficial air flux velocity data required to maintain constant froth stability is found in Table 36, Appendix B, Page 104.

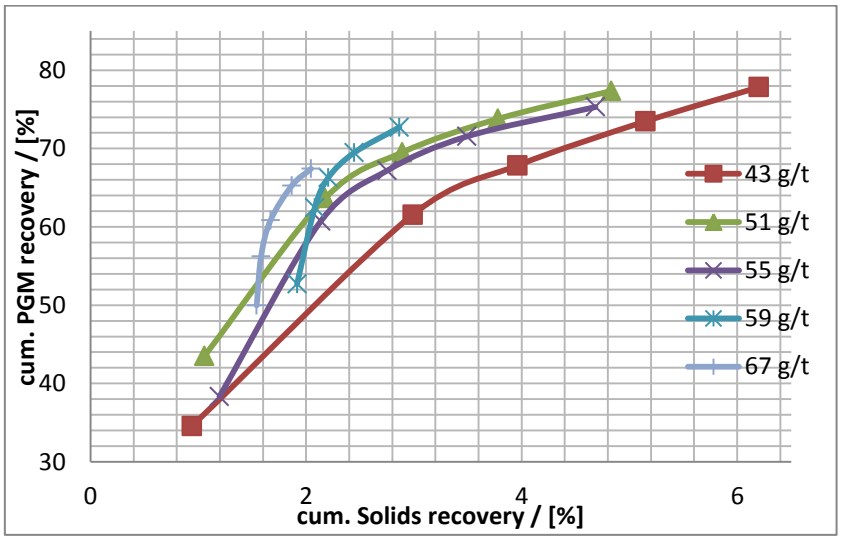

Figure 60: Combined PGM recovery vs. solids recovery for LG and HG cleaners at various KU5 dosages- bad ore

It was decided, in an effort to simplify the analysis, to combine the results for both the HG and LG cleaners. This meant that the KU5 dosages reflected are the ‘effective’ dosages

across the entire circuit. The PGM and solids recovery across both cleaners were combined and shown in Figure 60.

For example, one of the five dosages investigated in the LG cleaner cell itself, was 8 g/t. A fixed dosage of 30 g/t was added in the rougher whilst a further 5 g/t are added in the HG cleaner. No additional depressant was added in the scavenger cell. Hence, with the 8 g/t in the LG cleaner, this totals 43 g/t as seen in the figure above. Similarly, KU5 dosages of 16, 20, 24 and 32 g/t in the LG cleaner are reflected as effective dosages of 51, 55, 59 and 67 g/t respectively.

The PGM recovery was the highest at the highest solids content. This corresponds to the lowest depressant dosage of 43 g/t. This implied that an increase in depressant dosage caused a reduction in solids mass.

The PGM recovery, at a dosage of 43 g/t is 75% whilst the recovery is reduced to 67% at a dosage of 67 g/t. The effect of depressant on froth structure and talc recovery has been explained in the HG cleaner analysis section and it will not be reiterated here. The reasons for reduced PGM recovery at higher depressant dosages have also been described previously.

The solids target in the LG cleaner was 1%. Thus, effectively across both the HG and LG cleaners, the total solids recovery target was 2%. According to the above graph, the highest PGM recovery at this solids recovery target was 67%. This corresponded to a depressant dosage of 67 g/t. This was regarded as the optimum KU5 dosage to process this ore using in the circuit. However, this is a low PGM recovery compared to industrial standards.

The sensitivity of the ore with respect to depressant addition was highlighted by the reduction of PGM recovery from 70 to 67% with a slight increase in KU5 dosage from 59 to 67 g/t. This loss of PGMs implied that this ore was difficult to concentrate without risking the loss of PGMs. It was decided to investigate ways of improving the recovery of PGMs from this ore.

The froth structure of the LG cleaner at 67 g/t is shown in Figure 61:

Figure 61: Froth structure of LG cleaner at 67 g/t - bad ore

The picture shown in Figure 61 was taken at the commencement of the test. It has a different froth structure compared to the HG cleaner in Figure 55. Obviously, due to the different frother concentrations, the froth stability will differ. The LG cleaner had smaller bubbles, indicating greater froth stability. This was due to the higher frother concentration at the commencement of the test. Thus, one would expect a larger entrainment in the LG cleaner compared to the HG cleaner.

Two duplicate tests were performed at an effective depressant dosage of 67 g/t to determine the chromite content of this ore. The tests also served to check the reproducibility of results. The tests were conducted in an identical manner to the above, however only bulk samples were collected. They are combined results over both the LG and HG cleaners.

The results are summarized in Table 19:

Table 19: Summary of Results from bad ore investigation at 67 g/t KU5

	Original	Duplicate 1	Duplicate 2
PGM recovery / [%]	67.4	66.3	68.5
Cr_2O_3 content / [%]	3.9	3.9	3.9
Solids recovery / [%]	2.05	2.06	2.07

Table 20: Statistical analysis of bad ore test work

	PGM recovery	Cr_2O_3 content	Solids recovery
Mean	67.43	3.89	2.06
Standard Error	0.64	0.00	0.01
Median	67.42	3.89	2.06
Standard Deviation	1.11	0.01	0.01
Sample Variance	1.22	0.00	0.00
Skewness	0.04	1.73	0.00
Range	2.21	0.01	0.02
Minimum	66.33	3.89	2.05
Maximum	68.54	3.90	2.07
Count	3.00	3.00	3.00
Confidence Level (95.0%)	2.75	0.01	0.02
Mean	67.43	3.89	2.06

The above results show good repeatability for both the PGM and solids recovery. The Cr_2O_3 content is fairly similar between all these tests. The statistical analysis of this data was summarized in Table 20 above.

5.4 REGRINDING INVESTIGATION

Industrially, one would target a PGM recovery of at least 80% from the primary cleaners. The primary cleaners in this case refer to the HG and LG cleaners. The low PGM recovery was indicative of possible liberation problems in the ore.

Composite particles, as described earlier consist of both valuable PGMs and gangue minerals and are usually very difficult to recover. Thus, they can be considered slow floating species and are mainly concentrated in the scavenger concentrate. It was decided that regrinding of the rougher tailings would be investigated, in an effort to improve the liberation of PGMs from these composite particles. A grind of 90% passing 53µm was chosen since it was finer than the original grind of 80% -75µm. The rougher tailing was filtered and transferred to the mill, where filtrate was added back to prevent frother dilution. The scavenger cell thus comprised of the milled sample and the excess original filtrate.

The milling curve for this new grind is shown in the Figure 62:

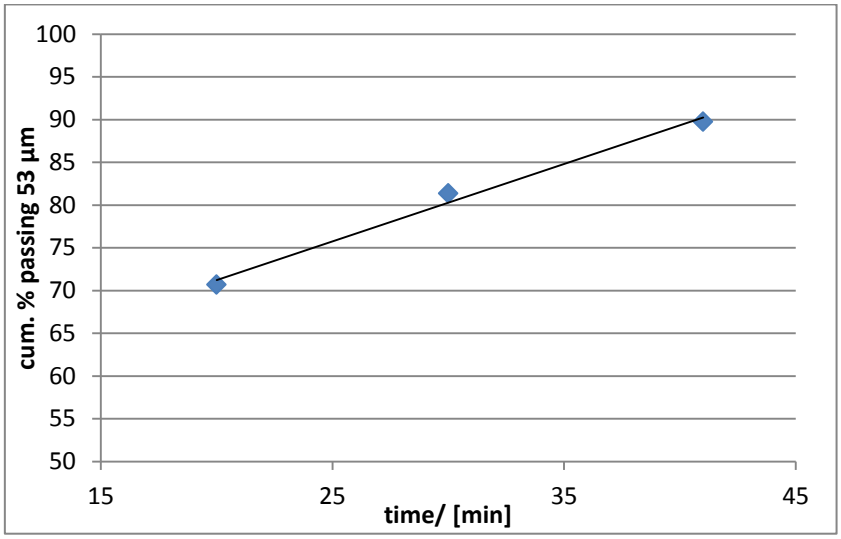

Figure 62: Milling curve for regrind investigation - bad ore

Figure 62 shows that the target grind was achieved at a time of 42 minutes. It was not possible to determine the initial feed % passing 53µm due to insufficient sample. It was important to note that the water that was originally associated with the rougher tailings was used in the mill. This ensured that the milling process introduced no additional dilution of the frother concentration. It was shown previously that this dilution affects the overall PGM recovery and concentrate grade.

Once the PGMs were liberated from the composite particles, their surfaces need to be made hydrophobic to ensure they are captured by bubbles. This required the addition of SIBX collector.

The experimental conditions for the scavenger cell are shown in Table 21:

Table 21: Experimental conditions for Scavenger cell with regrinding - bad ore

SIBX	g/t	76
DOW200	g/t	16
KU5	g/t	0
AIR FLOWRATE	$m.min^{-1}$	0.66 – 0.94
IMPELLER SPEED	Rpm	1200

The scavenger cell used the same frother dosage as with the previous setup. This was done in order to maintain a similar froth structure and solids recovery. The scraping was performed until the wet mass of 2250 g, as was the case with the previous setup, was obtained. The previous setup refers to that involving no regrind of the rougher tailings.

The time required to obtain this wet mass was reduced from 20 minutes to 14 minutes. The details of the air flux velocities required to maintain froth stability are found in Table 37, Appendix B, and Page 105. This can be attributed to the additional fast floating minerals liberated from the composite particles, which previously would not be captured easily. The three types of minerals obtained when composite particles are broken down include PGMs, talc and chromite. The first two of these minerals are recovered by true flotation whilst the latter is recovered via entrainment.

This means that faster floating material was present; hence more solids were recovered in a shorter time. This reduced the overall time required to achieve the same wet mass. It is also important to note that, due to the liberation of chromite from the composite particles, the chromite entrainment would be greater in this new setup as opposed to the previous setup.

The objective of the scavenger cell was to achieve as much solids recovery as possible. Hence the flotation test was performed until no solids were visible in the froth. This corresponded to a wet mass of approximately 2800g. This was achieved after 18 minutes. The froth was fairly white in colour at this point, portraying low solids content. This is shown in the image below:

Figure 63: Scavenger cell after 18 minutes - bad ore

There was an increase in the solids to water ratio compared to the previous scavenger experiment. This meant that there was less water recovered in the concentrate. Hence the frother concentration in the concentrate was higher than previously obtained. This concentration was 0.0135 g/L.

Due to financial constraints, it was not possible to perform any PGM or chromite analysis on the scavenger concentrate.

5.4.1 LG CLEANER WITH REGRINDING

The LG cleaner analysis was performed in much the same way as with the previous setup. A range of depressant dosages were utilised and their effects on both PGM and solids recovery were noted. The frother solution used to maintain the level was 0.0135 g/L. Experimental conditions are listed in Table 22:

Table 22: Experimental conditions for LG cleaner with regrinding - 0.0135 g/L bad ore

SIBX	g/t	0
DOW200	g/t	0
KU5	g/t	8 – 40
AIR FLOWRATE	$m.min^{-1}$	0.85 – 1.33
IMPELLER SPEED	Rpm	1200

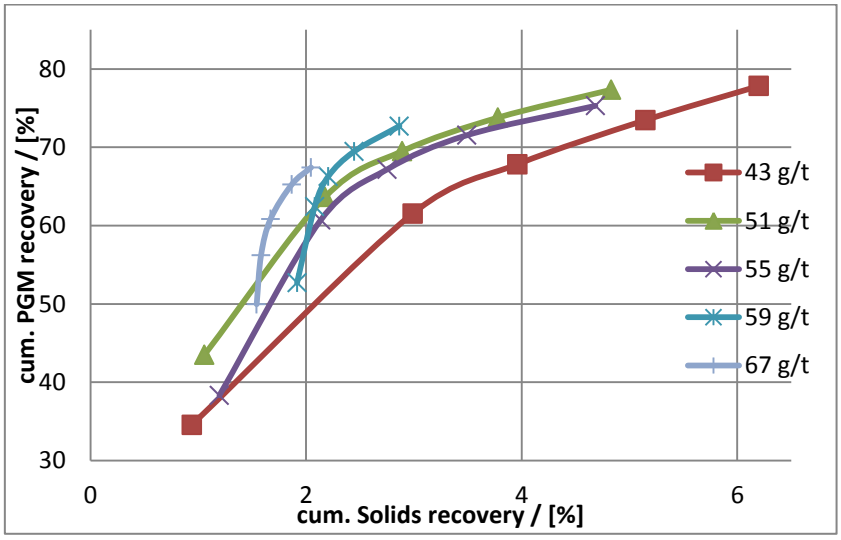

Figure 60: Combined PGM recovery vs. solids recovery for LG and HG cleaners at various KU5 dosages- bad ore (repeat)

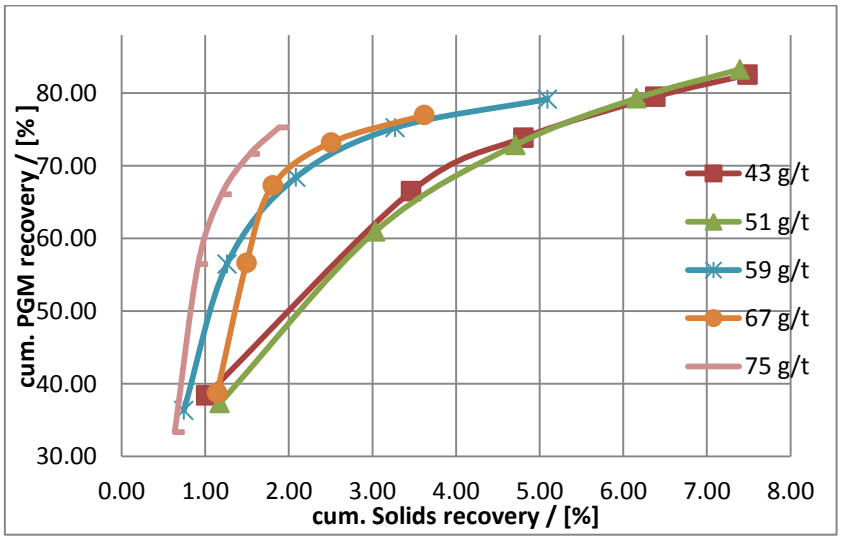

Figure 64: PGM vs. Solids recovery at various depressant dosages for combined HG and LG cleaners - bad ore regrind

Figure 64 was generated in the same way as Figure 60, with combined PGM and solids recovery data from the HG and LG cleaners. Figure 64 shows the relationship between the PGM and solids recovery at five different depressant dosages, ranging from 8 to 40 g/t in the LG cleaner. As explained previously, the dosages have been combined to denote an 'effective' depressant dosage across the entire circuit in order to simplify the analysis of results.

Considering the PGM recoveries, it can be seen that there is an improvement in the PGM recovery which can be attributed to the regrinding stage. This caused liberation of additional PGMs, in addition to other gangue minerals.

For example, if one compares the dosages of 43 g/t for each of Figure 60 and Figure 64, the PGM recovery improvement became more apparent. These tests were performed with near identical conditions, except for the regrinding of the rougher tailings. The overall PGM recovery has increased from 77 to 83 per cent. This was due to the liberation of additional PGMs from composite particles.

At the same time, one can see the solids recovery has increased from 6.2 to 7.5 %. It became apparent that regrinding had a negative impact. The word 'composite' refers to the fact that these particles consist of different minerals. As mentioned previously, they consist of PGMs and other gangue minerals including talc and chromite. Finer grinding implies the release of finer particles into the pulp phase. These finer particles report to the quiescent zone near the pulp-froth interface and are more likely to be entrained in the water, particularly Cr_2O_3. This implies a larger Cr_2O_3 content in the concentrate.

In fact, due to the increased amount of talc in the pulp phase, one would require a larger amount of depressant to suppress its flotation. The two circuits can be compared by analysing the PGM recovery at an approximate mass pull of 2 %. Regrinding increased the PGM recovery from about 67 to 76 per cent. The KU5 requirement to produce this final concentrate increased from 67 to 75 g/t. The regrinding required a further 42 minutes of milling. This is approximately double the rougher feed milling time. Hence there is approximately a doubling of the initial total energy costs.

The depressant had a profound effect on the froth structure for the LG cleaner. The image below was taken after adding 40 g/t depressant, for an effective dosage of 75 g/t, in the LG cleaner:

Figure 65: LG cleaner froth structure at 75 g/t - bad ore regrind

Figure 65 was taken at the commencement of the test. There are the particles that migrate to the launder and collect at the edge of the cell. Compared to Figure 61, one can notice the presence of more hydrophobic solids in this froth as a result of the regrind. The frother concentration in the LG cleaner with regrinding is 0.0135 g/L which is higher than that without regrinding, 0.0097 g/L. Thus one would expect the entrainment to be greater in the regrinding investigation. This entrainment was heightened due the excess liberation of chromite from composite particles.

The chromite content of the concentrate is of particular interest, particularly after regrinding. Hence, one of the main functions of the LG cleaner is rejection of entrained chromite from the scavenger stage. Figure 66 shows the compromise between PGM recovery and Cr_2O_3 content. The first data point refers to the HG concentrate.

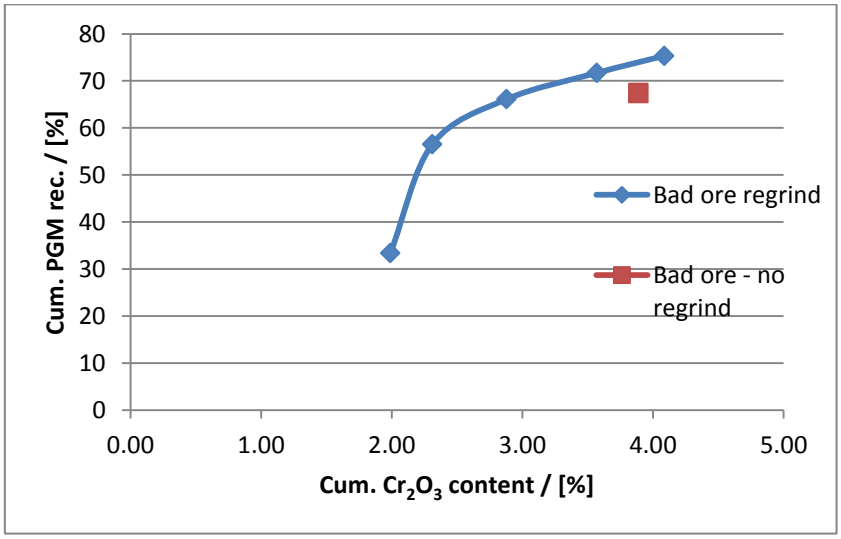

Figure 66: Cum. PGM recovery vs. Cum. Cr_2O_3 content at 75 g/t KU5 - bad ore regrind

The last point on Figure 66 showed the cumulative Cr_2O_3 content, 4.1 per cent, of the final concentrate. This was greater than the final concentrate of the bad ore with no regrind at 67 g/t, shown as a single point on Figure 66, which had a cumulative Cr_2O_3 content of 3.9 per cent.

As discussed earlier, there were differences in the LG cleaner top-up solutions used in both circuits. Frother concentration has a significant impact on the froth stability which, in turn, affects Cr_2O_3 entrainment. Thus, one can only speculate that this increased Cr_2O_3 content in the regrinding circuit was due to the additional liberation of chromite. However, more tests would be necessary to draw a definitive reason for these differences.

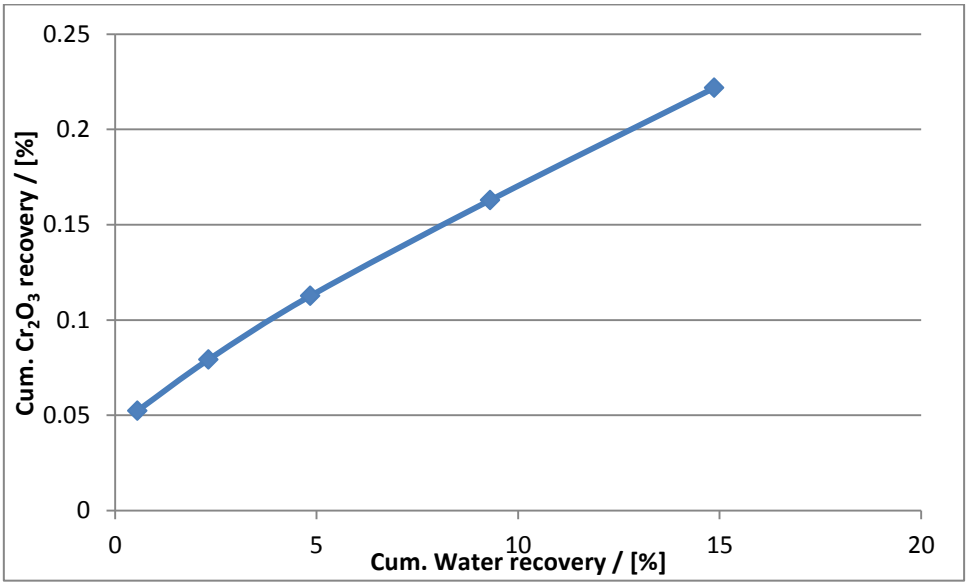

Figure 67: Cum. Cr_2O_3 recovery vs. Cum. water recovery at 75 g/t KU5 - bad ore regrind

Figure 67 shows that the relationship between Cr_2O_3 recovery and water is almost linear, indicating that the main mechanism is one of entrainment. Water is part of the froth structure. Chromite is entrained in the water. Thus as the water recovery increases one would expect the Cr_2O_3 recovery to increase.

A repeat bulk test was conducted to confirm the results obtained in the above test. The air flux velocities required to maintain a stable froth at 75 g/t KU5 are shown in Table 38, Appendix B, and Page 105.The results of that test are summarized in Table 23:

Table 23: Summary of results obtained in regrinding investigation at 75 g/t KU5

	Original	Duplicate
PGM recovery / [%]	76	75.4
Cr_2O_3 content / [%]	4.1	4.1
Solids recovery / [%]	2	1.9

5.5 GOOD ORE INVESTIGATION

The results from the bad ore investigation highlighted the processing difficulties associated with this kind of ore. It was decided to perform an investigation using ore with better flotation performance characteristics, aptly named “good ore”.

It was decided to use the circuit without a regrind stage, as shown in Figure 35. The same experimental techniques were used.

5.5.1 MILLING CURVE

The experimental procedure used for the bad ore, was used to determine the milling time for the good ore. A target grind of 80%-75µm was chosen. All other experimental conditions were the same. This includes, for example the rod distribution, feed water etc. The milling curve is shown in Figure 68:

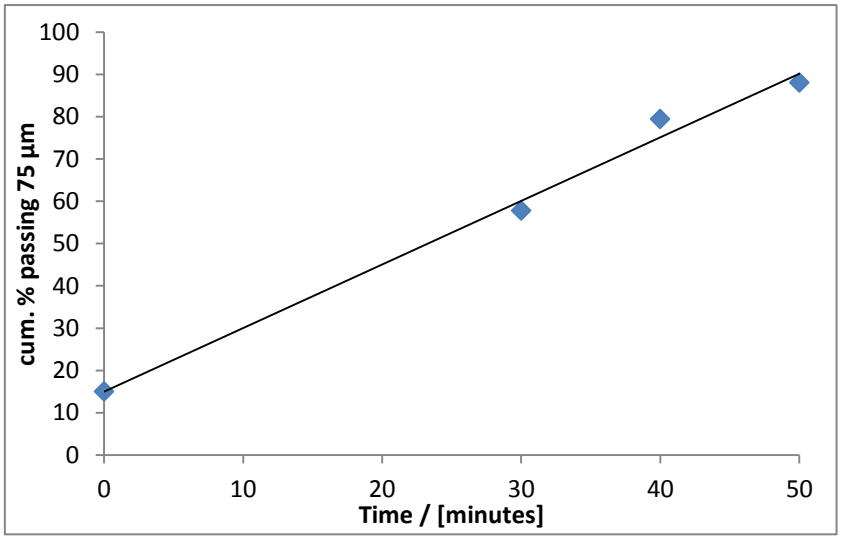

Figure 68: Good ore milling curve

From the above graph, it was seen that the target grind was achieved at approximately 42 minutes. It is also observed that the feed size was 15%-75µm. This was attained using the vibratory screening apparatus shown in Figure 25. This is slightly finer than the bad ore (20% -75 µm)

5.5.2 ROUGHER CELL

It was decided to use the same rougher concentrate wet mass as used previously of 530 g for all experiments. A similar process was undertaken with the depressant as was the case for the rougher cell in the bad ore investigation. 10 g/t increments were added until the froth structure was deemed suitable for flotation. This occurred after 30 g/t depressant and the froth structure, similar to Figure 41 is shown below:

Figure 69: Good ore rougher froth structure at 30 g/t KU5

The experimental conditions for the rougher cell are shown in Table 24:

Table 24: Experimental conditions for Rougher cell – good ore

SIBX	g/t	150
DOW200	g/t	20
KU5	g/t	30
AIR FLOWRATE	$m.min^{-1}$	0.73
IMPELLER SPEED	Rpm	1200

It was observed that the time required to obtain a wet mass of approximately 530 g was 2 minutes. This was a minute quicker than the time required to achieve the same wet mass in the rougher concentrate for the bad ore. One can only assume it is due to the good ore containing more fast floating PGM minerals compared to the bad ore. As with the bad ore investigation, water was used to control the operating cell level.

5.5.3 SCAVENGER CELL

It was assumed that recovery of PGM's would be easier in the scavenger cell. Frother was used to improve the solids recovery in the concentrate. Since this ore had less composite particles, it was felt that a reduction frother concentration in the cleaners would be beneficial. The experimental conditions are listed in the Table 25:

Table 25: Experimental conditions for Scavenger at 0.012 g/L – good ore

SIBX	g/t	0
DOW200	g/t	8
KU5	g/t	0
AIR FLOWRATE	$m.min^{-1}$	0.73 – 0.93
IMPELLER SPEED	Rpm	1200

The test was performed until a cumulative wet mass of 2800 g was obtained. The flotation time required to achieve this mass was 15 minutes. The details for the air flux velocities required to maintain a stable froth are given in Table 39, Appendix B, and Page 105. Again, it

was observed that the good ore achieved a larger wet mass in a quicker time compared to the bad ore. The fact that a lower amount frother and flotation time were required further highlights the positive flotation characteristics of the good ore. The bubbler was used to measure the synthetic top-up water necessary to maintain the flotation level. A frother solution of 0.012 g/L was used to maintain the scavenger cell operating level.

5.6 THICKENER INVESTIGATION

Thickeners have been used extensively in flotation plants, particularly on cleaner concentrates. One application has been a reduction in the water content, to reduce the size and maintenance costs of complex cleaner circuits. It has also enabled companies to achieve better overall control of the flotation process. The reduction of water implies an increase in the solids content of the slurry. Depending on the ore quality, an increase in the solids concentration could result in an improvement in the recovery of valuable minerals. However, for flotation of UG2 ore, this would have the effect of increasing the stability of the froth and an increase in the entrainment of chromite. The idea of thickening, followed by dilution using water with a lower frother concentration, appears to be a novel solution for reducing entrainment.

The results from the bad ore investigation, with particular reference to the HG cleaner cell, showed that a reduction of chromite entrainment in cleaner cells occurred when water was used to make up and maintain level. The frother concentration had been reduced by dilution. One way of achieving this in a plant, without increasing volumetric flow in the cleaners, would be to thicken the concentrate and then use make-up water to re-dilute the sedimented solids. The water from the thickener overflow could then be recycled to a suitable part of the circuit, where frother was required.

5.6.1 DILUTION INVESTIGATION

It was decided to investigate the maximum possible concentrate dilution under laboratory conditions. This test was performed on a sample of rougher concentrate obtained from previous work. This sample was used as a basis for the rest of the test work. It was transferred into a column and allowed to settle for 30 minutes. Industrially, this is analogous to the residence time used in designing a thickener. The concentrate separated into two phases after this time viz. water and solids. The experimental setup prior to the commencement is shown below:

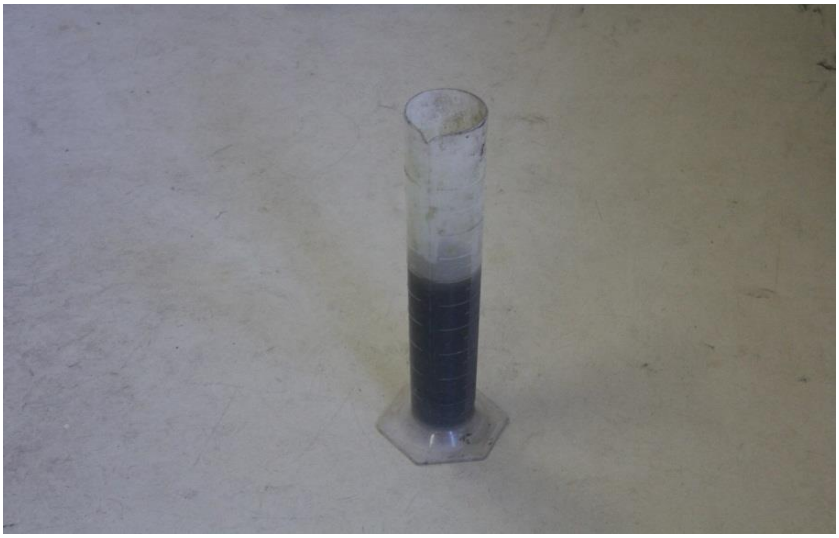

Figure 70: Thickener contents before separation

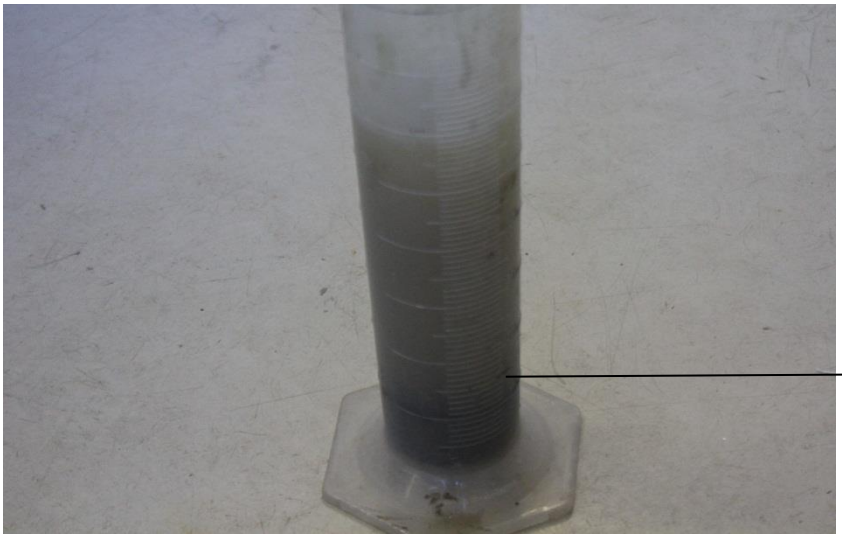

Figure 71: Thickener after 30 minutes showing two phase separation

The total volume occupied by the concentrate was 670 ml. After a settling time of half an hour, the separation of the solids and water occurred resulting in two different phases shown in Figure 71 above. According to the column reading, the volume occupied by the pulp was 140 ml.

The water was removed by slow decantation. This pouring was carefully performed such that no solids were allowed to leave with the water. The maximum allowable water removal corresponded to a level in the cylinder of 160 ml. The sedimented slurry was then dried to determine the mass/volume of associated water. The solids in the concentrate accounted for a mass of 100 g. This implied a volume of 33 ml. Hence the maximum water removal was calculated as follows:

Maximum water removal = $\frac{((670-33)-(160-33))ml}{(670-33)\,ml} * 100$ = 80.3 %

This means it is only possible to remove 80.3 % of the water from a concentrate without losing any solids and it depends upon the w/s ratio in that concentrate, or cleaner tails. This was relaxed by 5 % to include a safety factor for use of a continuous thickener. Thus it was decided to use 75 % as the maximum under laboratory conditions.

5.6.2 CLEANER CELLS

It was decided to investigate water removal from the stream entering in the HG cleaner only and then the feed to both cleaning stages. It was decided to utilize water removals of 55 % and 73% for the HG and LG cleaners respectively. This is a conservative approach to the benefit for the HG cleaner, in view of the possibility that tailings from a re-cleaner stage may have a relatively high solids content. Plant samples could be used to make realistic estimates of the fractional removal of water. The concentrations of frother calculated from the Bubbler measurements were reduced accordingly.

5.6.3 HG CLEANER

The HG cleaner experimental conditions are listed in the Table 26. There was, however a lack of adequate good ore sample. Hence it was decided to use the depressant dosage for the HG cleaner in the bad ore investigation. The LG cleaner would be used to optimise the PGM recovery/concentrate grade relationship.

Table 26: Experimental conditions for HG cleaner at 0.013 g/L –good ore

SIBX	g/t	0
DOW200	g/t	0
KU5	g/t	5
AIR FLOWRATE	$m.min^{-1}$	0.66
IMPELLER SPEED	Rpm	1000

A total of six tests were performed in this cell. The first two tests were done without resorting to any dilution of the cell contents. The bubbler was used to measure the frother concentration of the rougher concentrate. The solution used to maintain the levels in these two tests had a concentration of 0.013 g/L. The froth structure at the beginning of each of these two tests is shown below:

Figure 72: Froth structure of the HG cleaner at 0.013 g/L – good ore

The remaining four tests were performed using a thickener at the inlet of the HG cleaner. As mentioned before, a water removal of 55 % was investigated. This corresponded to a frother concentration of 0.006 g/L, as measured by the bubbler. It is significantly lower than the previous concentration due to the cell contents being diluted. The experimental conditions for these tests are listed in the Table 27.

Table 27: Experimental conditions for the HG cleaner at 0.006 g/L - good ore

SIBX	g/t	0
DOW200	g/t	0
KU5	g/t	5
AIR FLOWRATE	$m.min^{-1}$	0.82
IMPELLER SPEED	Rpm	1000

The froth structure corresponding to the above concentration is shown below, taken at the commencement of the each of the four tests.

Figure 73: Froth structure of HG cleaner at 0.006 g/L - good ore

Comparing the froth structures shown in Figure 72 and Figure 73, it was apparent that the 0.006 g/L froth had bigger bubbles compared to the 0.013 g/L froth. Evidently the 0.006 g/L froth structure was brittle hence it required a greater air flux to maintain a stable froth. The air rate required for the 0.006 g/L froth was 0.88 $m.min^{-1}$ compared to 0.66 $m.min^{-1}$ for the 0.013 g/L froth.

5.6.4 LG CLEANER

The tailings from the HG cleaner were filtered before being mixed with the concentrate from the scavenger cell. This represented the feed to the LG cleaner cell. Depressant was used to reduce the talc recovery in the LG cleaner concentrate. As with the HG cleaner, a total of six tests were performed. They were performed using two different synthetic frother top-up concentrations. The first concentration of 0.013 g/L corresponded to the first two tests performed without thickeners. The remaining four tests used 0.0033 g/L, based on a water removal of 73 % in the thickener. The experimental conditions for experiments conducted using each synthetic top-up solution are given in the tables below:

Table 28: Experimental conditions for LG cleaner at 0.0033 g/L - good ore

SIBX	g/t	0
DOW200	g/t	0
KU5	g/t	8 – 32
AIR FLOWRATE	$m.min^{-1}$	0.82 – 1.53
IMPELLER SPEED	Rpm	1200

Table 29: Experimental conditions for LG cleaner at 0.013 g/L - good ore

SIBX	g/t	0
DOW200	g/t	0
KU5	g/t	8 – 32
AIR FLOWRATE	$m.min^{-1}$	0.82 – 1.24
IMPELLER SPEED	Rpm	1200

Again, as with the HG cleaner in the previous section, similar trends were observed with regards to the air flux required in order to maintain froth stability. The required flux was higher in the experiments that used synthetic frother top-up solutions of 0.0033 g/L compared to 0.013 g/L. The reasons for this have been explained previously.

Three circuit configurations were used to perform flotation work on the good ore. They are shown in the figures below:

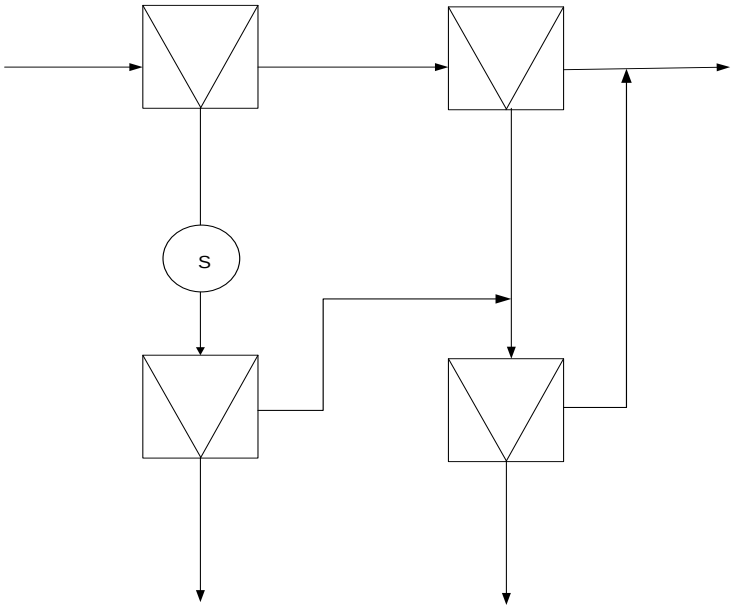

Figure 74: Circuit configuration A

Figure 74 shows the insertion of a thickener at the inlet to the HG cleaner only denoted by ‘S’. A 55% water removal was applied in this thickener. This resulted in a frother concentration of 0.006 g/L, measured by the bubbler. The concentration of frother was 0.013 g/L in the LG cleaner. Synthetic frother top-up solutions were made up to these concentrations and used to maintain the operating levels in the respective cells.

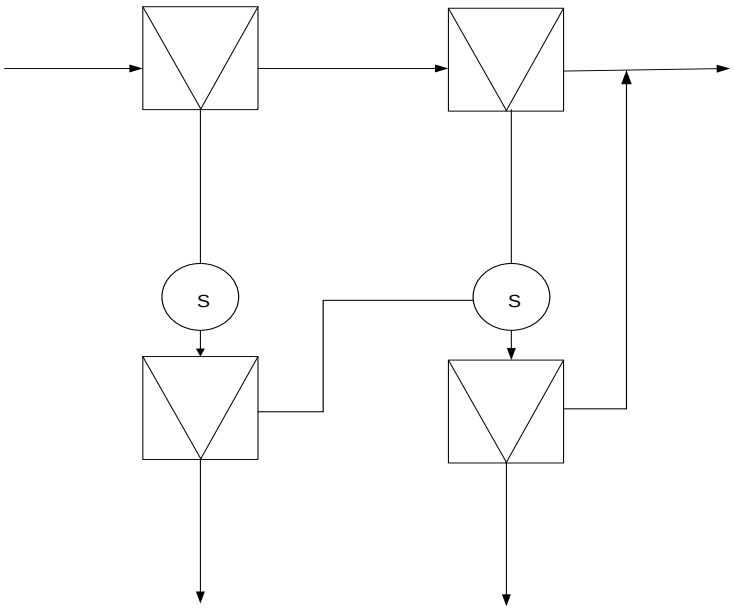

Figure 75: Circuit configuration B

Figure 75 shows the insertion of thickeners at the inlets of both the HG and LG cleaners denoted by ‘S’. The frother concentration of the top-up water was 0.006 g/L in the HG cleaner and 0.0033 g/L in the LG cleaner. Synthetic frother top-up solutions were made up to these concentrations and used to maintain the operating levels in the respective cells.

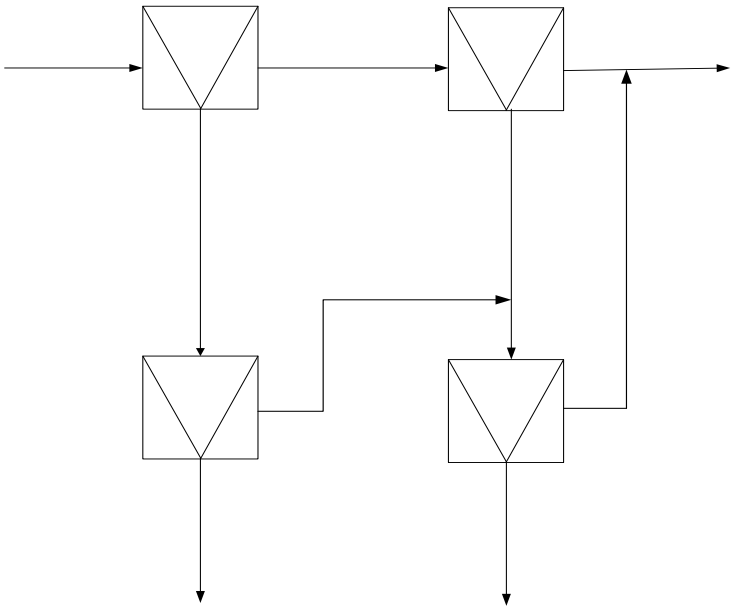

Figure 76: Circuit configuration C

Figure 76 is the base case for no thickeners at the inlets of either the HG or LG cleaners. In essence, this circuit resembles the circuit used to perform the bad ore investigation. The frother concentration of the top-up water was 0.013 g/L in both the HG and LG cleaners. Synthetic frother top-up solutions were made up to these concentrations and used to maintain the operating levels in the respective cells.

As mentioned previously, the above circuits were used to conduct a total of six experiments. The results were compiled in a similar manner to that used to analyse the bad ore. For simplicity sake, it was decided to combine the PGM, Cr_2O_3 and solids recovery results from both the HG and LG cleaners. The results from these experiments follow in the graphs below:

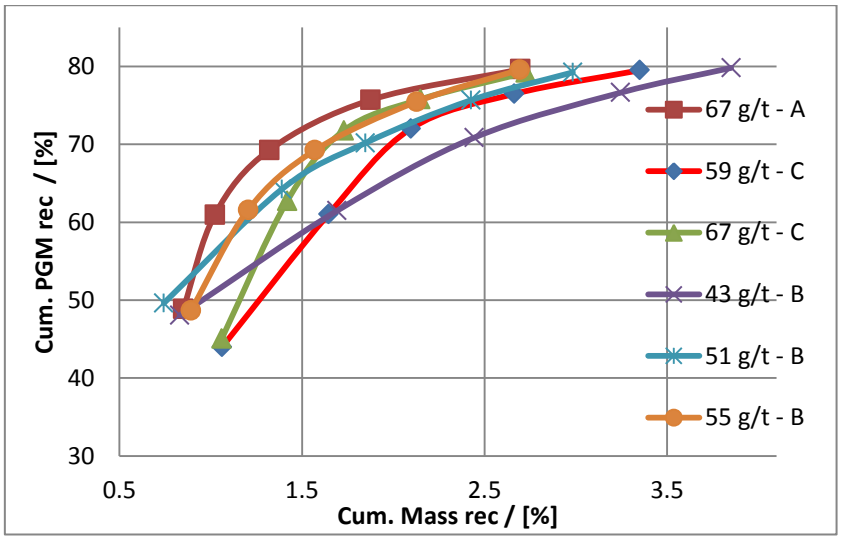

Figure 77: Cum. PGM recoveries vs. Cum. Solids recoveries at various depressant dosages - good ore

Figure 77 shows the combined cumulative solids and PGM recoveries across the LG and HG cleaners. The depressant dosages are listed for each individual curve. These dosages are the 'effective' dosages across the entire circuit. The letters next to each dosage refer to the circuit used to perform that specific experiment at that particular dosage. For example, '59 g/t – C' means that 24 g/t depressant was used in the LG cleaner cell with the entire test performed using circuit configuration C. The circuit configurations, along with their individual descriptions are given in Figure 74, Figure 75 and Figure 76.

Referring to Figure 77, one can observe the solids recovery is reduced as the depressant dosage increases. This is true for all depressant dosages used in the various circuits. The PGM recovery remained consistent at approximately 80% for all circuits irrespective of the depressant dosage. This implies that the ore could possibly have been treated with a higher depressant as it showed very little sensitivity, in terms of PGM recovery, at the various depressant dosages.

In particular, with reference to Figure 77 and Figure 60 (on Page 68), one can compare the good and bad ores in terms of their respective sensitivities to depressant addition. Circuit C used in Figure 77 is identical to that used to generate Figure 60. Again, one can only make valid comparisons at the same cumulative mass and if one compares 67 g/t – C from Figure 77 to the result for the bad ore, in Figure 60, the PGM recovery increases from 67% to about 75%.

From Figure 60, one can observe that the PGM recovery is reduced from 77 to 67% as the depressant dosage was increased from 43 to 67 g/t. At the same time, the solids recovery was reduced from 6.2 to 2 per cent. In comparison, Figure 77 showed that the PGM recovery changed minimally across all depressant dosages ranging from 43 to 67 g/t. The solids recovery was reduced from 4.8 to 3.1%.

This means that, in general, the good ore is less sensitive to depressant addition compared to the bad ore. This means that the use of higher depressant dosages in the good ore can produce lower solids recoveries whilst maintaining fairly consistent PGM recoveries. The froth, using the bad ore, depends on the presence of talc for stability. This was due to the comparably low amount of hydrophobic solids that are recoverable via flotation. They are difficult to recover due to the presence of composite particles.

If one considers the first points on each of the curves, they correspond to the cumulative recovery of both PGMs and solids in the HG cleaner. It is evident that all dosages involving circuits A and B have similar PGM/solids recoveries. Circuits A and B have thickeners at the inlets to the HG cleaner. They had similar froth structure hence similar PGM/solids recoveries were obtained.

Dosages used in conjunction with circuit C have higher solids recoveries in the HG cleaner compared to those used in circuits A and B. A higher synthetic make up water, in the HG cleaner, of 0.013 g/L was used in circuit C whilst 0.006 g/L was used in both circuits A and

B. A more stable froth was formed due to the higher frother concentration. This resulted in a larger entrainment of hydrophilic minerals, responsible for the difference in solids recovery. This entrainment can be justified according to analysis performed on the Cr_2O_3 content of the concentrate in the HG cleaner. This is a hydrophilic mineral that is recovered by entrainment. The graph is shown in Figure 78:

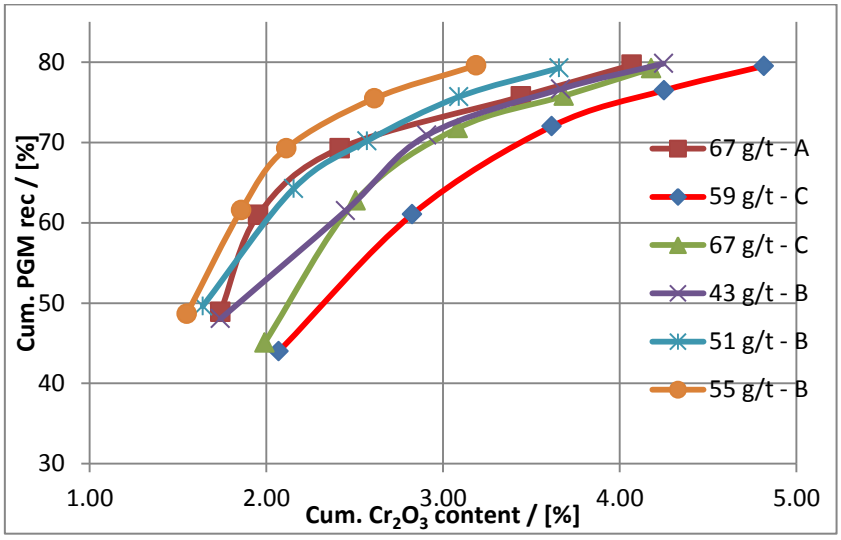

Figure 78: Cum. PGM recoveries vs. Cum. Cr_2O_3 content at various depressant dosages - good ore

Figure 78 shows the relationship between the Cr_2O_3 content and PGM recovery at various depressant dosages. Similar to Figure 77, the first point on each curve corresponded to the PGM recovery/ Cr_2O_3 content in the HG cleaner. The HG cleaner concentrate in Circuit C had much higher Cr_2O_3 contents compared to circuits A and B. This verified that the larger solids recovery of circuit C, shown in Figure 78, was attributed to the entrainment of Cr_2O_3. This was due to the higher frother concentration in the HG cleaner, which resulted in greater froth stability.

Figure 78 shows a decrease in the Cr_2O_3 content with an increase in depressant dosage. As the depressant dosage increases, the recovery of talc in the concentrate is reduced. Since talc is hydrophobic, it is necessary to maintain froth phase stability. Reduction in talc recovery results in decreased froth stability. This improves froth drainage characteristics thereby reducing the Cr_2O_3 recovery via entrainment.

The effect of circuit choice on the Cr_2O_3 content at different depressant dosages proved interesting. As expected, Circuit B had lower Cr_2O_3 contents than those associated with circuits A and C, due to reduced frother concentration in both cleaning stages. For example, at the end of each test, 55 g/t- B had Cr_2O_3 content of 3.2% compared to 67 g/t – A whose Cr_2O_3 content was 4.1%.

It is of particular interest to compare the experiments with circuits B and C, with depressant dosages of 55 g/t- B (orange) and 67 g/t- C (green). The two curves follow the same trajectory in the region of 2 % mass (Figure 77), but when one refers to the Cr_2O_3 content in Figure 78, the lower value of depressant is significantly better. This result is difficult to explain and further tests may be required.

There exists a relationship between the water and Cr_2O_3 recovery. Figure 79 depicts the relationship between these two variables:

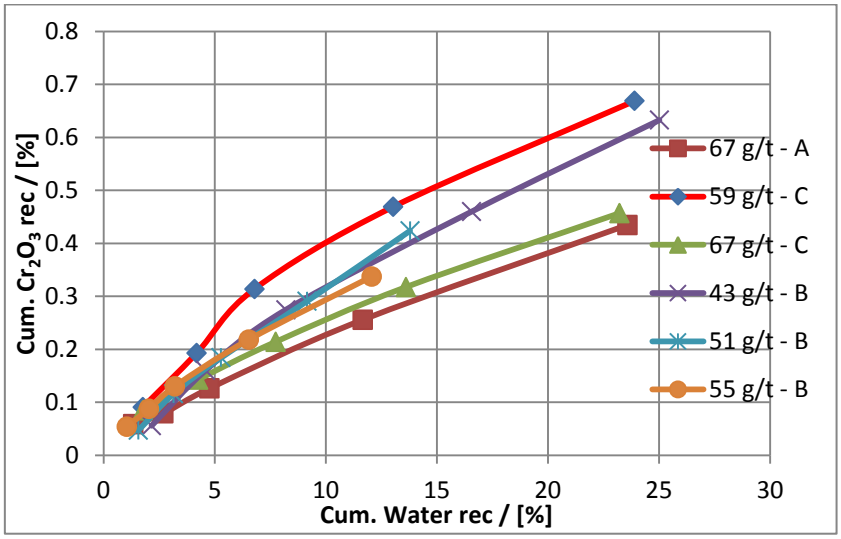

Figure 79: Cum. water vs. Cr_2O_3 recovery at various depressant dosages - good ore

Figure 79 shows the relationship between both the Cr_2O_3 and water recoveries at different depressant dosages. Water is not recovered by entrainment. It is part of the froth structure. Chromite is recovered to a large extent by entrainment in the water. Addition of depressant reduces flow of solids in the froth and hence the w/s ratio increases with time as the froth becomes 'barren'.

Comparing 55 g/t - B to 67 g/t – C, it was observed that the insertion of two thickeners significantly reduced both the water and Cr_2O_3 recoveries. Similar PGM recoveries were obtained in both cases. Furthermore, it was achieved at a lower depressant dosage, which implies a direct financial saving.

The recovery of Cr_2O_3 poses downstream processing problems in the smelters hence it is an important operational parameter. The response of the good ore to the inclusion of thickeners has validated the idea of using these tanks to reduce both the Cr_2O_3 and water recoveries.

6 SIGNIFICANCE OF RESULTS

This chapter has highlights some of the concerns faced by flotation technologists and how these were addressed in this thesis.

The chromite content in PGM concentrates is a major concern industrially. Besides reducing the overall flotation concentrate grades, it also affects downstream processing.

There is a trade-off between the chromite content and PGM recovery to the concentrate. Chromite is typically hydrophilic, hence one would expect little recovery in the concentrates. However due to its abundance in UG-2 ore, it is recovered largely by entrainment in water which forms part of the froth structure. This is the dilemma faced by UG-2 ore concentrators worldwide: How can one effectively reduce the chromite entrainment in the concentrate without risking the loss of PGMs to the tailings?

As mentioned in the theory section, increased chromite levels reduce the operating volume of the smelting furnace. This means that some PGMs are lost during the smelting process due to ineffective separation between the phases. Thus operating limits are imposed on the chromite content of the feed to the smelters.

According to Jones (1999), based on a solids recovery of 1%, typical UG-2 final concentrate grades and PGM recoveries are 430 g/t and 87% respectively. This ensures a reasonable profit is obtained. The Cr_2O_3 content limit for typical concentrates is 2.9%. This constraint can be increased to between 4-9% provided the grade of the product is improved to about 1000 g/t. In light of this, it is apparent that the concentrates obtained in this investigation raise certain concerns since the Cr_2O_3 contents were significantly greater than 2.9%.

The results obtained in this thesis can be used to solve an industry wide problem. Industrial concentrator plants consist of many different flotation circuits that treat various ore bodies i.e. good and bad ores. Thus they produce various grades of concentrates depending on the ore quality and flotation characteristics. These concentrates ultimately combine to form the smelting process feed. These form a single concentrate with an ‘effective’ grade which is a combination of all the concentrate grades. This analogy is best expressed using Figure 80:

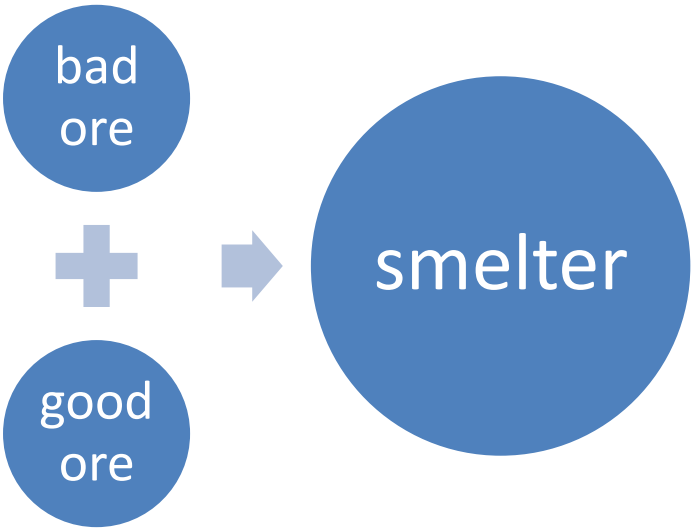

Figure 80: Block diagram showing different smelter feeds (Jones, 1999)

In this investigation, it was found that the good and bad ores produced different chromite grades. Figure 80 shows how the two concentrates combine to form the smelting feed. The installation of thickeners and re-routing of certain tailing streams to the milling circuit can prove to be advantageous. If, for any reason, the smelter feed contains too much chromite, then perhaps the plant can switch to process ore using thickeners in the cleaner feeds. This was shown to significantly reduce the chromite content. If the PGM recoveries are too low, then one can consider regrinding the bad ore rougher tailings to increase the PGM liberation.

The results obtained from the good ore investigation showed potential for the chromite content to be reduced whilst maintaining similar PGM recoveries. The use of thickeners was shown to reduce the chromite entrainment by reducing the frother concentration thereby affecting the froth structure.

The purpose of lab test work is to obtain preliminary experimental conditions which are then used as the basis for larger scale pilot plants. However this thesis highlighted the shortcomings of regular laboratory procedures, particularly in the cleaner cells. Due to insufficient volume of concentrate obtained in the rougher concentrate, the remaining cleaner cell operating volume is usually made up by using tap water. However the use of synthetic frother produced significantly different solids recoveries, due to entrainment in the water of the froth structure. The use of synthetic make-up water replicates the continuous operation of pilot plants. This is seen as a significant step in making laboratory tests more ‘realistic’.

It is hoped that this thesis provides some insight into ways to improve the flotation laboratory procedure, so that these results match those obtained from pilot plant and larger scale operations. It is believed that certain improvements proposed in this thesis can be utilized by the technologist to solve problems typically faced on a UG-2 ore flotation concentrating plant.

7 CONCLUSIONS

The flotation of two UG-2 ore types was investigated using laboratory scale equipment. The procedure was made more realistic, by using four stages of flotation, rather than just two, to mimic a typical platinum flotation plant. Attention was also given to the fact that water is often added to the second stage of flotation, to make up the level in a 'cleaner' test. Experiments showed that this dilution, which does not take place in practice, had a significant impact on overall efficiency. For example, with reference to the bad ore, the use of tap water to make-up the HG cleaner operating volume reduced the solids recovery from 3.1 to 1 per cent.

A method of measuring frother concentration was developed and used to determine the realistic level of frother in cleaning tests. The device, nicknamed the 'bubbler' was able to measure the frother concentration of any stream in the circuit. Tests at these levels of frother concentration showed that significant improvements could be made to plant performance, by making use of a thickener to reduce the frother concentration in the cleaner stages. For example, a water removal of 55 % in the HG cleaner reduced the overall frother concentration from 0.013 to 0.006 g/L.

The improved test procedure was used on both good and bad ores and the effect of regrinding was investigated. These tests provided insight on how to improve performance on a platinum flotation plant, particularly when floating the bad ore.

Initial tests on the rougher cell and primary cleaner cell were used to optimise these stages. However, for the sake of simplicity, the following PGM and solids recoveries refer to the combination of both cleaner concentrates and referred to as a single concentrate. The depressant dosage which produced the most favourable result for each ore type and circuit configuration is described. The following conclusions were drawn from the bad ore investigation:

At a combined depressant dosage of 67 g/t over the entire circuit, the PGM and solids recoveries were 67 and 2 per cent respectively. The addition of a regrinding stage, which reduced the rougher tailings to 90%-53µm, improved the PGM recovery to 76 per cent at a solids recovery of 2 per cent. This was achieved at the expense of an additional 8 g/t depressant. However, the Cr_2O_3 content increased from about 3.9 to 4.1 per cent. It is believed that these increases could be attributed to regrinding and differences in top-up frother concentrations in the LG cleaner.

Whilst regrinding did improve the overall performance of this bad ore in terms of PGM liberation, the ore was particularly sensitive to depressant addition. The results showed that both the PGM and solids recovery were reduced significantly with the use of depressant.

With no regrinding, the solids recovery was reduced from 6 to 2 per cent whilst the PGM recovery was reduced from 78 to 67 per cent at the expense of an additional 24 g/t KU5. Regrinding the rougher tails reduced the solids recovery from 7 to 2 per cent whilst the PGM recovery was reduced from 83 to 75 per cent at the expense of an additional 32 g/t KU5.

This investigation illustrated that simple changes in the circuit could be used to improve results. The good ore was used to investigate the effects of reducing frother concentration in the cleaners by using thickeners and dilution with fresh water. Three different circuit configurations were tested, namely A, B and C and the following conclusions were drawn:

Circuit C involved the use of no thickeners. The PGM and solids recoveries of the combined final concentrate were 79.2 and 2.7 and per cent respectively at an effective depressant dosage of 67 g/t. The Cr_2O_3 content at this dosage was 4.2 per cent.

The use of thickeners involved water removals of 55 and 73 per cent in the HG and LG cleaners respectively.

The use of a single thickener in the HG cleaner was investigated in Circuit A. The PGM and solids recoveries of the combined final concentrate were 79.6 and 2.7 per cent respectively at an effective depressant dosage of 67 g/t. The Cr_2O_3 content was reduced to 4.1 per cent.

The use of two thickeners was investigated in Circuit B. The PGM and solids recoveries of the combined final concentrate were 79.6 and 2.7 per cent respectively. Perhaps the most significant finding was that an effective depressant dosage of a mere 55 g/t was required to reduce the Cr_2O_3 content to 3.2 per cent.

Good ore tests conducted using Circuit B produced the lowest Cr_2O_3 content in the concentrates as described above. However it involved the use of two thickeners for each of the cleaner cells. This implies the additional capital investment to install these tanks. In a similar fashion, the regrinding of the bad ore rougher tails, though it improved the liberation and recovery of PGMs, also implies an additional milling energy utility compared to the circuit with no regrinding. It would thus be difficult to select the optimum circuit without conducting a detailed economic analysis on the various circuits, taking into account all the associated costs.

8 RECOMMENDATIONS

I. The superficial air flux velocity data, located from Table 31 to Table 41, can be used as a guideline to map appropriate air flux as a function of solids concentration. This model can subsequently be utilized in developing control schemes for maintaining cell levels in industrial cells.

II. It is suggested that samples of plant water and water associated with concentrates be taken to evaluate the potential for using thickeners improve plant performance.

III. It is recommended that regrinding of high grade cleaner tailings be investigated to improve the PGM liberation. The data obtained from tests on the bad ore showed that residual PGMs were not liberated.

IV. It is suggested that additional work be done on the ‘bubbler’, to develop it into a reliable on-line device.

V. It is suggested that a continuous flotation test be done, using a pilot plant, be conducted using the experimental conditions listed in this work. These results can be used to verify the effectiveness of the laboratory method.

9 REFERENCES

APLAN, F. F. & FUERSTENAU, D. 1962. In: Fuerstenau, D.W. (Ed),*Froth Flotation 50th anniversary*, New York, AIME.

ATA, S. 2012. Phenomena in the froth phase of flotation — A review. *International Journal of Mineral Processing,* 102–103, 1-12.

BEATTIE, D. A., HUYNH, L., KAGGWA, G. B. & RALSTON, J. 2006. Influence of adsorbed polysaccharides and polyacrylamides on talc flotation. *International Journal of Mineral Processing,* 78, 238-249.

BRADSHAW, D. J., OOSTENDORP, B. & HARRIS, P. J. 2005. Development of methodologies to improve the assessment of reagent behaviour in flotation with particular reference to collectors and depressants. *Minerals Engineering*, 18, 239-246.

BRYSON, M. A. W. 1998. New Technologies in the concentration of PGM values from UG-2 ores. *The South African Institute of Mining and Metallurgy*, 104, 311-313.

ÇILEK, E. C. & YıLMAZER, B. Z. 2003. Effects of hydrodynamic parameters on entrainment and flotation performance. *Minerals Engineering*, 16, 745-756.

CORIN, K. C. & HARRIS, P. J. 2010. Investigation into the flotation response of a sulphide ore to depressant mixtures. *Minerals Engineering*, 23, 915-920.

CROZIER, R. D. 1992. *Flotation : theory, regents and ore testing,* Oxford, Pergamon Press.

DEGLON, D. A. 2005. The effect of agitation on the flotation of platinum ores. *Minerals Engineering*, 18, 839-844.

EKMEKÇI, Z., BRADSHAW, D. J., ALLISON, S. A. & HARRIS, P. J. 2003. Effects of frother type and froth height on the flotation behaviour of chromite in UG2 ore. *Minerals Engineering*, 16, 941-949.

HADLER, K. & CILLIERS, J. J. 2009. The relationship between the peak in air recovery and flotation bank performance. *Minerals Engineering*, 22, 451-455.

HAY, M. P. 2010. A case study of optimising UG2 flotation performance part 2: Modelling improved PGM recovery and Cr_2O_3 rejection at Northam's UG2 concentrator. *Minerals Engineering*, 23, 868-876.

HAY, M. P. & ROY, R. 2010. A case study of optimising UG2 flotation performance. Part 1: Bench, pilot and plant scale factors which influence Cr_2O_3 entrainment in UG2 flotation. *Minerals Engineering*, 23, 855-867.

IVES, K. J. 1984 *The scientific basis of flotation*, The Hague : Nijhoff

JAN, L. 1982. *Surface chemistry of froth flotation*, New York : Plenum Press

JONES, R. T. 1999. Platinum Smelting in South Africa. *South African Journal of Science*, 95, 525-534.

KOH, P. T. L. & SMITH, L. K. 2011. The effect of stirring speed and induction time on flotation. *Minerals Engineering*, 24, 442-448.

LIU, G., FENG, Q., OU, L., LU, Y. & ZHANG, G. 2006. Adsorption of polysaccharide onto talc. *Minerals Engineering*, 19, 147-153.

LOTTER, N. O. & BRADSHAW, D. J. 2010. The formulation and use of mixed collectors in sulphide flotation. *Minerals Engineering*, 23, 945-951.

LOTTER, N. O., BRADSHAW, D. J., BECKER, M., PAROLIS, L. A. S. & KORMOS, L. J. 2008. A discussion of the occurrence and undesirable flotation behaviour of orthopyroxene and talc in the processing of mafic deposits. *Minerals Engineering*, 21, 905-912.

LOVEDAY, B. K. & HEMPHILL, A. L. 2006. Optimisation of a multistage flotation plant using survey data. *Minerals Engineering*, 19, 627-632.

MAILULA, T. D., BRADSHAW, D. J. & HARRIS, P. J. 2003. The effect of copper sulphate addition on the recovery of chromite in the flotation of UG2 ore. *The South African Institute of Mining and Metallurgy,* 103, 143-146.

MARTYN P, H. 2010. A case study of optimising UG2 flotation performance part 2: Modelling improved PGM recovery and Cr_2O_3 rejection at Northam's UG2 concentrator. *Minerals Engineering,* 23, 868-876.

MEGRAW, H. A. 1916. *The Flotation Process*, 239 West Street, New York, New York : McGraw-Hill.

MUGANDA, S., ZANIN, M. & GRANO, S. R. 2011. Influence of particle size and contact angle on the flotation of chalcopyrite in a laboratory batch flotation cell. *International Journal of Mineral Processing,* 98, 150-162.

NAVE, R. 2012. *HyperPhysics Capillary Action [Online]*. Georgia State University: Department of Physics and Astronomy. Available: http://hyperphysics.phy-astr.gsu.edu/hbase/hph.html [Accessed 10 September 2012].

OUDHOFF K.A , BUITENHUIJS F.A , WIJNEN P.H , SCHOENMAKERS P.J & W.T, K. 2004. Determination of the degree of substitution and its distribution of carboxymethylcelluloses by capillary zone electrophoresis. *Carbohydrate Research,* 339, 1917-1924.

PAROLIS, L. A. S., VAN DER MERWE, R., GROENMEYER, G. V. & HARRIS, P. J. 2008. The influence of metal cations on the behaviour of carboxymethyl celluloses as talc depressants. *Colloids and Surfaces A: Physicochemical and Engineering Aspects,* 317, 109-115.

ROSS, V. E. 1997. Particle-bubble attachment in flotation froths. *Minerals Engineering,* 10, 695-706.

SCHUBERT, H. 1999. On the turbulence-controlled microprocesses in flotation machines. *International Journal of Mineral Processing*, 56, 257-276.

SHORTRIDGE, P. G., HARRIS, P. J., BRADSHAW, D. J. & KOOPAL, L. K. 2000. The effect of chemical composition and molecular weight of polysaccharide depressants on the flotation of talc. *International Journal of Mineral Processing,* 59, 215-224.

SOPHOCLEOUS, M. 2009. Understanding and explaining surface tension and capillarity:an introduction to fundamental physics for water professionals. *Hydrogeology Journal,* 18, 811-821.

SURVEY, U. G. 2012a. *Capillary action* [Online]. Water Science for Schools. Available: http://ga.usgs.gov/edu/capillaryaction.html [Accessed 10 September 2012].

SURVEY, U. G. 2012b. *Surface Tension* [Online]. Water Science for Schools. Available: http://ga.water.usgs.gov/edu/surface-tension.html [Accessed 10 September 2012].

THORPE, T. 2002. *Lake Foam* [Online]. Winter 2002 Waterline Newsletter of the LMVP: Lakes of Missouri Volunteer Program. Available: http://www.lmvp.org/Waterline/winter2002/foam.html [Accessed 10 September 2012].

VAN DER WESTHUIZEN, A. P. & DEGLON, D. A. 2007. Evaluation of solids suspension in a pilot-scale mechanical flotation cell: The critical impeller speed. *Minerals Engineering,* 20, 233-240.

WAGNER, P. A. 1973. *The platinum deposits and mines of South Africa,* Cape Town : Struik

WESSELDIJK, Q. I., REUTER, M. A., BRADSHAW, D. J. & HARRIS, P. J. 1999. The flotation behaviour of chromite with respect to the beneficiation of UG2 ore. *Minerals Engineering,* 12, 1177-1184.

WIESE, J., HARRIS, P. & BRADSHAW, D. 2011. The effect of the reagent suite on froth stability in laboratory scale batch flotation tests. Minerals Engineering, 24, 995-1003.

WIESE, J. G., HARRIS, P. J. & BRADSHAW, D. J. 2010. The effect of increased frother dosage on froth stability at high depressant dosages. *Minerals Engineering*, 23, 1010-1017.

WILLS, B. A. & NAPIER-MUNN, T. 2005. 12 - Froth flotation. *Wills' Mineral Processing Technology (Seventh Edition*). Oxford: Butterworth-Heinemann.

XIAO, Z. & LAPLANTE, A. R. 2004. Characterizing and recovering the platinum group minerals—a review. *Minerals Engineering*, 17, 961-979.

YANG, X.-S. & ALDRICH, C. 2006. Effects of impeller speed and aeration rate on flotation performance of sulphide ore. *Transactions of Nonferrous Metals Society of China*, 16, 185-190.

ZHMUD, B. V., TIBERG, F. & HALLSTENSSON, K. 2000. Dynamics of capillary rise. *Journal of Colloid and Interface Science*, 228, 263-269.

10 APPENDIX A – SAMPLE CALCULATIONS

10.1 MILLING SAMPLE CALCULATIONS

The individual masses of the rods are summarized in Table 30:

Table 30: Mass of various rods

Rod diameter(mm)	Mass(g)
5	64
10	180
15	463
20	717

A single set of rods (i.e. comprising of one of each of the rods) = (64+180+463+717) g

= 1425 g

Mill dimensions

Diameter (d) = 0.2 m

Length (l) = 0.3m

Volume = $\pi\frac{d^2}{4}$*l

= 9.42 litres (L)

Assuming 40% of this volume is occupied by the total charge into the mill

Charge Volume (V_c) = 0.4*9.42 L= 3.77 L

Assuming 60% of the V_c represents the media volume (V_m)

V_m = 0.6*3.77L = 2.26 L

Density of stainless steel = 8000kg/m^3

Mass of media (M) = 8kg/L*2.26L =18.09 kg

Thus no. of each rod = 18.09/1.425 = 12.5

Hence 12 of each rod were used.

10.2 BAD/GOOD ORE

It was decided to use only the 10, 15 and 20 mm rods in these investigations. The masses of these rods are given in Table 30.

A single set of rods (i.e. comprising of one of each of the rods) = (180+463+717) g

= 1360 g

The total internal volume of the mill was calculated before as 9.42 L.

Assuming 50% of this volume is occupied by the total charge into the mill

Charge Volume (V_c) = 0.5*9.42 L= 4.71 L

Assuming 60% of the V_c represents the media volume (V_m)

V_m = 0.6*4.71 L = 2.826 L

Density of stainless steel = 8000kg/m^3

Mass of media (M) = 8kg/L* 2.826 L =22.608 kg

Thus no. of each rod = 22.608/1.360 = 16.62

Hence 16 of each rod were used.

10.3 SUPERFICIAL AIR FLUX VELOCITY DATA

The calculation for superficial air flux velocity is as follows:

The formula is given as: $v_a = \frac{Q}{A}$

Where Q is the air flow rate in $m^3.min^{-1}$

And A is the cross sectional area of the cell.

This area is based on the square dimensions of the cell base. It is known that there exists a cell lip at the top of the cell. For the purposes of this investigation, this additional area of the lip has been ignored. It is assumed therefore that the cross sectional area is the same at all points in the cell including the base.

The dimensions at the base of each cell are given below:

- **8 L cell**
  Length - 18.5 cm
  Breadth - 18.5 cm
- **2.5 L cell**
  Length - 13 cm
  Breadth - 13 cm
- **1 L cell**
  Length - 11 cm
  Breadth - 11 cm

Thus if the value of the rotameter tube reading is 13.5 initially in the large 8 L cell, the calculation for the v_a is as follows:

Initially, the calibration chart, found in Figure 82, was used to convert from the tube reading to the air flow rate. The corresponding flow rate at a tube reading of 13.5 is 26 l/min.

Thus the $Q = \frac{26}{1000}\ m^3.min^{-1}$

$Q = 0.026\ m^3.min^{-1}$

$A = 18.5 * 18.5 = 342\ cm^2 = 0.0342\ m^2$

Hence $v_a = \frac{0.026}{0.0342}$

$v_a = 0.73\ m.min^{-1}$

A similar type of calculation was undertaken to calculate all the v_a values for the various cells listed in the tables below.

10.4 FLOTATION SAMPLE CALCULATIONS

The following example is based on test work done on the good ore. It is based on circuit configuration B, shown in Figure 75. A version of this circuit is attached below with stream labels.

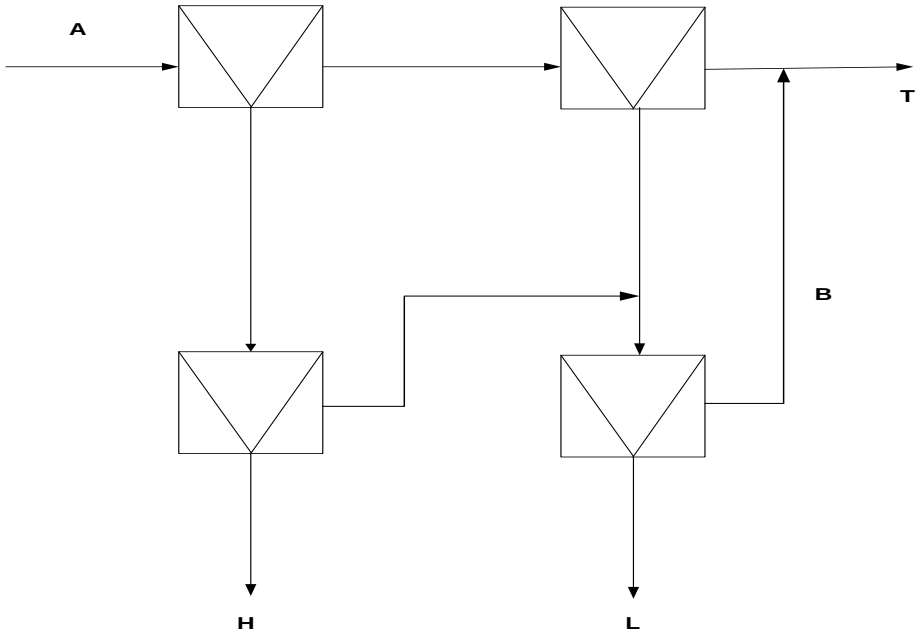

Figure 81: Circuit with stream labels

The sample was split using the riffle splitter, shown in Figure 23, and weighed to a 2.5 kg sample. This sample was subsequently ground to 80%-75µm according to the manner described in Section 4.1. The flotation circuit procedure was described in Section 4.4. The rougher float was conducted according to the methods outlined in these sections. The experimental conditions are given in Table 24.

The concentrate obtained from this was transferred to the HG cleaner for processing. The HG cleaner cell, according to this circuit configuration, possessed a thickener. The bubbler was used to obtain the frother concentration of the concentrate from the rougher cell.

Frother concentration of feed concentrate (G_o) = 0.013 g/L

Initial volume of concentrate (V_o) = 670 ml

Assuming 100 g of solids were obtained, volume of solids (S_o) = 100/3 = 33 ml

Remaining liquid volume = 670 - 33 = 637 ml

<u>Assuming a 55% removal of water volume</u>

Volume of liquid after removal = (1- 0.55)*637 = 287 ml

Hence final calculated concentration (C_c) after dilution back up to original 637 ml in apparatus:

$C_c = \frac{0.013*287}{637}$ = 0.00585 g/L

Measured concentration (C_m) using bubbler apparatus = 0.006 g/L.

Percentage error(E_r) associated with bubbler $= \frac{0.006-0.00585}{0.00585} * 100$

E_r =2.5 %.

Hence it was decided to measure all concentrations using the bubbler due to the low percentage error.

A synthetic solution was made up to this concentration of 0.006 g/L and used to maintain the cell operating level. The experimental conditions for the cell are listed in Table 27. This calculation was based upon a 5 g/t KU5 depressant addition.

A concentrate was obtained from this cell. It was dried overnight in the oven and weighed subsequently to record a dry mass (M_{HG}) of 22.4 g. This concentrate was bagged and sent for PGM and Cr_2O_3 analysis.

The tailings from the rougher cell were transferred to the scavenger cell. Conditioning was allowed for according to the experimental conditions listed in Table 25. The frother concentration was determined using the bubbler as 0.012 g/L. A solution was prepared according to this concentration and used to maintain the operating level. The tailings of the HG were filtered before being transferred to the LG cleaner cell.

The concentrate obtained from the scavenger cell was measured using the bubbler to determine the frother concentration viz. 0.013 g/L. This concentrate was combined with the tailings from the HG cleaner to form the complete feed to the LG cleaner cell. The tailings were dried then subsequently weighed before being sent for further PGM and Cr_2O_3 analysis.

According to this circuit, the insertion of another thickener was necessary. A water removal of 73% was selected. In a calculation similar to that with the HG cleaner, the following was obtained based on a concentrate volume of 2000 ml:

The frother concentration was measured using the bubbler as 0.0033 g/L.

The calculated value was 0.003314 g/L. Hence the error was minimal.

A top-up solution was prepared using a concentration of 0.0033 g/L and used to maintain the operating level of the LG cleaner cell. The other experimental details for the LG cleaner cell are listed in Table 28. This calculation was based upon a 55 g/t KU5 depressant addition. Samples were taken at various collection points and a rate plot was obtained. The dry mass of these samples was obtained and they were sent for further PGM and Cr_2O_3 analysis.

The data and results were summarized and presented in Table 47. The table is labelled according to the combined depressant dosage, followed by circuit B, used across the entire circuit viz. 55 g/t. This was the method used in to describe all subsequent data tables.

The PGM, solids and Cr_2O_3 recoveries were based on the amount present in the feed. For example, if one considers the PGM recovery for the 1st minute in stream L:

Data: PGM grade : 177 g/t

Mass : 7.9 g

Feed Data: PGM grade : 4.3 g/t

Mass : 2514.9 g

Hence the PGM recovery $= \frac{177*7.9}{4.3*2541.9} * 100\ \%$

$= 12.92\ \%$.

For the 2nd point of stream L, at 3 minutes, a PGM recovery of 7.67% was obtained. The solid mass obtained was 9.2 g. Hence the cumulative PGM recovery, after 3 minutes, was calculated as follows:

Cum. PGM recovery = 12.92 + 7.67 = 20.59 %.

Similar calculations were undertaken for all experiments and used to generate various PGM, Cr_2O_3 and solids graphs.

11 APPENDIX B. SUMMARY OF RAW DATA

11.1 AIR FLUX VELOCITY DATA

Table 31: Air flux velocities for Preliminary Sample - Rougher

TUBE READING	AIR FLOW RATE / [$m^3.min^{-1}$]	TIME / [min]	SUPERFICIAL FLUX VELOCITY / [$m.min^{-1}$]
6.2	0.014	0	0.410
8.0	0.017	3	0.495
10.0	0.020	5	0.589
12.0	0.023	7	0.683
15.0	0.028	10	0.824
18.0	0.033	17	0.965
22.5	0.040	20	1.177
6.2	0.014	0	0.410
8.0	0.017	3	0.495

Table 32: Air flux velocities for Preliminary Sample / bad ore - Scavenger

TUBE READING	AIR FLOW RATE / [$m^3.min^{-1}$]	TIME / [min]	SUPERFICIAL FLUX VELOCITY / [$m.min^{-1}$]
13.5	0.026	0	0.730
14.5	0.027	1	0.801
15.0	0.028	3	0.824
17.0	0.031	4	0.918
18.5	0.034	7	0.989
20.0	0.036	10	1.059
22.0	0.039	17	1.153
23.5	0.042	30	1.240

Table 33: Air flux velocity for bad ore - HG cleaner

TUBE READING	AIR FLOW RATE / [$m^3.min^{-1}$]	TIME / [min]	SUPERFICIAL FLUX VELOCITY / [$m.min^{-1}$]
0.6	0.005	0	0.410
3.0	0.009	1	0.734
6.0	0.014	3	1.134
7.0	0.015	5	1.267
9.0	0.019	6	1.533
10.0	0.020	7	1.666
15.0	0.028	15	2.331
20.0	0.036	30	2.996

Table 34: Air flux velocities for bad ore - HG cleaner at 0.0074 g/L

TUBE READING	AIR FLOW RATE / [$m^3.min^{-1}$]	TIME / [min]	SUPERFICIAL FLUX VELOCITY / [$m.min^{-1}$]
0.6	0.0050	0	0.410
1.0	0.0057	15 s	0.468
2.0	0.0073	30 s	0.601
2.4	0.0080	1	0.660

Table 35: Air flux velocity bad ore at 0.0059 g/L- Scavenger cell

TUBE READING	AIR FLOW RATE / [$m^3.min^{-1}$]	TIME / [min]	SUPERFICIAL FLUX VELOCITY / [$m.min^{-1}$]
11.5	0.0226	0	0.659
13.0	0.0250	1	0.730
14.0	0.0266	3	0.777
14.5	0.0274	5	0.801
15.5	0.0290	7	0.848
16.0	0.0298	10	0.871
17.0	0.0314	13	0.918
19.0	0.0346	16	1.012
21.0	0.0379	17	1.106
21.5	0.0387	19	1.130
23.0	0.0411	20	1.200

Table 36: Air flux velocity for bad ore at 0.0097 g/L- LG cleaner cell

TUBE READING	AIR FLOW RATE / [$m^3.min^{-1}$]	TIME / [min]	SUPERFICIAL FLUX VELOCITY / [$m.min^{-1}$]
3.7	0.0100	0	0.593
4.5	0.0113	1	0.669
5.0	0.0121	3	0.716
7.0	0.0153	5	0.907
8.0	0.0169	6	1.002
8.5	0.0177	7	1.050
10.0	0.0202	10	1.193
11.0	0.0218	11	1.288
11.4	0.0224	12	1.326

Table 37: Air flux velocity bad ore - Scavenger regrinding investigation

TUBE READING	AIR FLOW RATE / [$m^3.min^{-1}$]	TIME / [min]	SUPERFICIAL FLUX VELOCITY / [$m.min^{-1}$]
11.5	0.0226	0	0.659
12.0	0.0234	1	0.683
12.5	0.0242	3	0.707
13.5	0.0258	5	0.754
15.0	0.0282	8	0.824
15.5	0.0290	10	0.848
16.0	0.0298	12	0.871
16.5	0.0306	13	0.895
17.5	0.0322	14	0.942

Table 38: Air flux velocity bad ore - 0.0135 g/L- LG cleaner regrinding investigation

TUBE READING	AIR FLOW RATE / [$m^3.min^{-1}$]	TIME / [min]	SUPERFICIAL FLUX VELOCITY / [$m.min^{-1}$]
6.5	0.0145	0	0.859
7.0	0.0153	1	0.907
8.5	0.0177	3	1.050
9.0	0.0185	4	1.097
10.0	0.0202	6	1.193
11.0	0.0218	8	1.288
11.5	0.0226	10	1.336

Table 39: Air flux velocity good ore - 0.012 g/L- Scavenger

TUBE READING	AIR FLOW RATE / [$m^3.min^{-1}$]	TIME / [min]	SUPERFICIAL FLUX VELOCITY / [$m.min^{-1}$]
13.0	0.025	0	0.730
14.0	0.027	3	0.777
14.5	0.027	5	0.801
15.5	0.029	8	0.848
16.0	0.030	12	0.871
17.5	0.032	15	0.942

Table 40: Air flux velocity good ore – LG cleaner at 0.013 g/L

TUBE READING	AIR FLOW RATE / [$m^3.min^{-1}$]	TIME / [min]	SUPERFICIAL FLUX VELOCITY / [$m.min^{-1}$]
6.0	0.014	0	0.812
6.5	0.015	1	0.859
7.0	0.015	3	0.907
7.5	0.016	6	0.955
9.0	0.019	9	1.097
10.0	0.020	10	1.193
10.5	0.021	11	1.240
11.0	0.022	12	1.288

Table 41: Air flux velocity good ore– LG cleaner at 0.013 g/L

TUBE READING	AIR FLOW RATE / [$m^3.min^{-1}$]	TIME / [min]	SUPERFICIAL FLUX VELOCITY / [$m.min^{-1}$]
6.0	0.014	0	0.812
7.0	0.015	1	0.907
8.0	0.017	3	1.002
9.5	0.019	5	1.145
10.5	0.021	9	1.240
11.0	0.022	12	1.288
12.0	0.023	14	1.383
13.5	0.026	15	1.526

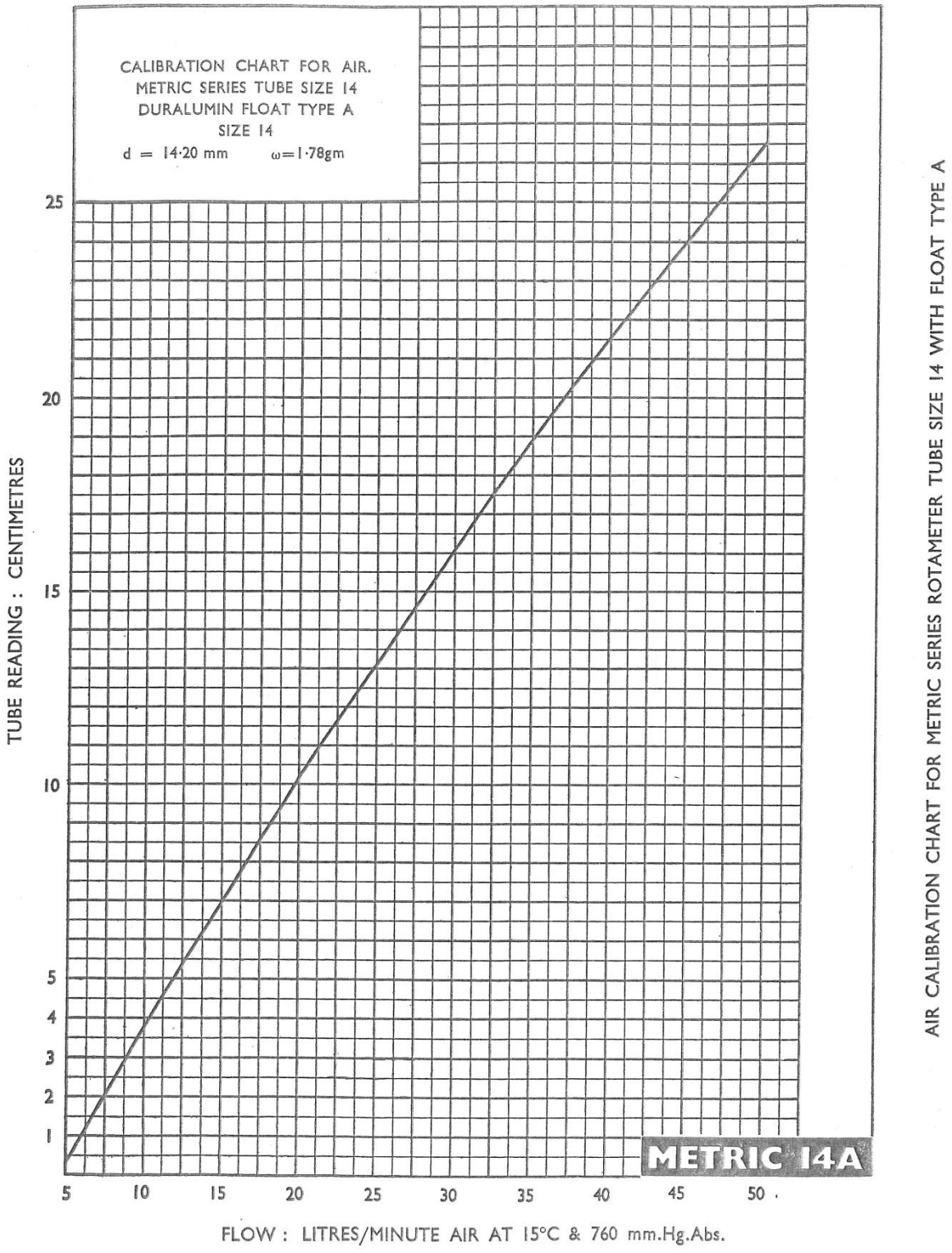

Figure 82: Air rotameter calibration chart

11.2 FROTHER INVESTIGATION

Table 42: Raw data for liquid heights at various frother concentrations

Liquid height / [mm]		
Experimental values	Arithmetic mean	Frother Concentration / [%]
48.67 48.66 48.68	48.67	0
46.32 46.37 46.27	46.32	0.1
46.48 46.5 46.46	46.48	0.2
44.08 44.04 44.12	44.08	0.3
48.005 47.68 48.33	48.005	0.4
44.05 44 44.1	44.05	0.5
41.88 41.9 41.86	41.88	0.6
44.055 44.02 44.09	44.055	0.7
45.58 45.59 45.57	45.58	0.8
41.9 41.85 41.95	41.9	0.9
41.67 41.7 41.64	41.67	1

Table 43: Raw data for frother calibration using capillary method

Frother concentration / [%]	Beaker mass before / [g]	Beaker mass after/ [g]	Capillary tube mass/[g]	Solution mass/[g]
0	19.783	19.57	0.155	0.058
0.1	19.541	19.325	0.16	0.056
0.2	20.991	20.778	0.157	0.056
0.3	19.668	19.461	0.155	0.052
0.4	20.765	20.559	0.154	0.052
0.5	20.779	20.561	0.165	0.052
0.6	19.942	19.737	0.155	0.05
0.7	19.758	19.549	0.159	0.05
0.8	20.785	20.568	0.159	0.05
0.9	19.791	19.584	0.159	0.048
1	19.872	19.663	0.156	0.047

Table 44: Raw data for frother calibration using capillary method in dilute solution

Frother concentration / [%]	Capillary Tube mass / [g]	Beaker mass before/ [g]	Beaker mass after/[g]	Solution mass/ [g]	Arithmetic mean / [g]
0.000	0.158	20.838	20.621	0.059	0.059
	0.158	20.838	20.620	0.060	
	0.158	20.837	20.619	0.059	
0.010	0.156	19.374	19.159	0.059	0.059
	0.156	19.373	19.158	0.059	
	0.156	19.372	19.158	0.059	
	0.156	19.366	19.150	0.060	
	0.156	19.364	19.146		
	0.156	19.363	19.145		
0.020	0.155	19.638	19.430		0.057
	0.155	19.638	19.429		
	0.155	19.637	19.428		
	0.155	19.626	19.416		
	0.155	19.624	19.412	0.056	
	0.155	19.622	19.410	0.057	
0.030	0.159	19.390	19.178		0.056
	0.159	19.389	19.179		
	0.159	19.389	19.177		
	0.159	19.379	19.164	0.056	
	0.159	19.377	19.163		
	0.159	19.377	19.162		
0.040	0.154	19.837	19.629		0.055
	0.154	19.836	19.627		
	0.154	19.835	19.626	0.055	
0.050	0.160	19.528	19.314	0.055	0.055
	0.160	19.527	19.313		
	0.160	19.526	19.313		
0.060	0.155	19.619	19.408		0.056
	0.155	19.617	19.407		
	0.155	19.616	19.405	0.056	
0.070	0.160	19.710	19.496		0.055
	0.160	19.709	19.495		
	0.160	19.708	19.493	0.055	
0.080	0.159	20.804	20.589	0.056	0.055
	0.159	20.802	20.589	0.054	
	0.159	20.802	20.588	0.055	

N/B: All outlier points have been omitted from the calculation of the arithmetic mean in the above table.

Table 45: Raw data - bubbler calibration- 10 ml aliquots

Concentration/ [$g.L^{-1}$]	Height/[cm]
0	0
0.01	3.8
0.02	6.9
0.03	9
0.04	11
0.05	12.4
0.06	13
0.08	13.8
0.09	14
0.1	14

Table 46: Raw data- bubbler calibration - 20 ml aliquots

Concentration/ [$g.L^{-1}$]	Height/[cm]
0	0
0.006	6.6
0.008	8.5
0.01	12
0.013	16
0.015	19
0.02	23

Table 47: Raw data- good ore- 55 g/t – B

Stream	Time	SOLIDS				PGM				Cr_2O_3			
		Mass	Cum. Mass	Cum.Mass distribution	Mass rec	Grade	Distribution	Cum. Recovery	Cum. Grade	Grade	Distribution	Cum. Recovery	Cum.Content
	Min	g	g	%	%	g/ton	%	%	g/ton	%	%	%	%
T		2360.50	2360.50	93.86	93.86	0.58	12.65	12.65	0.58	26.65	98.35	98.35	26.65
A		2514.90	2514.90	100.00	100.00	4.30	100.00	100.00	4.30	25.43	100.00	100.00	25.43
H	1	22.40	22.40	0.89	0.89	235.00	48.65	48.65	0.00	1.55	0.05	0.05	1.55
L	1	7.90	7.90	0.31	0.31	177.00	12.92	12.92	177.00	2.73	0.03	0.03	2.73
	3	9.20	17.10	0.68	0.37	90.20	7.67	20.59	130.30	2.95	0.04	0.08	2.85
	7	14.00	31.10	1.24	0.56	48.10	6.22	26.82	93.30	4.02	0.09	0.16	3.38
	15	14.20	45.30	1.80	0.56	31.30	4.11	30.93	73.86	5.36	0.12	0.28	4.00
B		86.70	86.70	3.45	3.45	9.69	7.77	7.77	9.69	9.82	1.33	1.33	9.82

Table 48: Raw data- good ore- 51 g/t - B

Stream	Time	SOLIDS				PGM				Cr_2O_3			
		Mass	Cum. Mass	Cum.Mass distribution	Mass rec	Grade	Distribution	Cum. Recovery	Cum. Grade	Grade	Distribution	Cum. Recovery	Cum.Content
	min	g	g	%	%	g/ton	%	%	g/ton	%	%	%	%
T		2330.00	2330.00	93.58	93.58	0.65	13.49	13.49	0.65	27.00	98.12	98.12	27.00
A		2489.90	2489.90	100.00	100.00	4.51	100.00	100.00	4.51	25.75	100.00	100.00	25.75
H	1	18.50	18.50	0.74	0.74	301.00	49.62	49.62	0.00	1.64	0.05	0.05	1.64
L	1	16.10	16.10	0.65	0.65	102.00	14.63	14.63	102.00	2.75	0.07	0.07	2.75
	3	11.40	27.50	1.10	0.46	58.40	5.93	20.56	83.93	3.83	0.07	0.14	3.19
	7	14.40	41.90	1.68	0.58	42.80	5.49	26.06	69.79	4.75	0.11	0.24	3.73
	15	13.90	55.80	2.24	0.56	28.90	3.58	29.64	59.61	6.12	0.13	0.38	4.32
B		85.60	85.60	3.44	3.44	9.51	7.25	7.25	9.51	10.90	1.46	1.46	10.90

Table 49: Raw data- good ore- 43 g/t - B

Stream	Time	SOLIDS				PGM				Cr_2O_3			
		Mass	Cum. Mass	Cum.Mass distribution	Mass rec	Grade	Distribution	Cum. Recovery	Cum. Grade	Grade	Distribution	Cum. Recovery	Cum.Content
	Min	g	g	%	%	g/ton	%	%	g/ton	%	%	%	%
T		2315.00	2315.00	94.14	94.14	0.79	16.56	16.56	0.79	27.00	98.31	98.31	27.00
A		2459.00	2459.00	100.00	100.00	4.49	100.00	100.00	4.49	25.86	100.00	100.00	25.86
H	1	20.40	20.40	0.83	0.83	260.00	48.03	48.03	0.00	1.74	0.06	0.06	1.74
L	1	21.20	21.20	0.86	0.86	70.00	13.44	13.44	70.00	3.13	0.10	0.10	3.13
	3	18.50	39.70	1.61	0.75	56.10	9.40	22.84	63.52	3.94	0.11	0.22	3.51
	7	19.70	59.40	2.42	0.80	32.30	5.76	28.60	53.17	5.98	0.19	0.40	4.33
	15	14.90	74.30	3.02	0.61	23.60	3.18	31.79	47.24	7.37	0.17	0.58	4.94
B		49.30	49.30	2.00	2.00	8.10	3.62	3.62	8.10	13.60	1.05	1.05	13.60

Table 50: Raw data- good ore- 67 g/t - A

Stream	Time	SOLIDS				PGM				Cr_2O_3			
		Mass	Cum. Mass	Cum.Mass distribution	Mass rec	Grade	Distribution	Cum. Recovery	Cum. Grade	Grade	Distribution	Cum. Recovery	Cum.Content
	min	g	g	%	%	g/ton	%	%	g/ton	%	%	%	%
T		2321.90	2321.90	93.46	93.46	0.63	13.66	13.66	0.63	26.50	98.15	98.15	26.50
A		2484.40	2484.40	100.00	100.00	4.31	100.00	100.00	4.31	25.23	100.00	100.00	25.23
H	1	21.10	21.10	0.85	0.85	248.00	48.88	48.88	0.00	1.74	0.06	0.06	1.74
L	1	4.30	4.30	0.17	0.17	301.00	12.09	12.09	301.00	3.00	0.02	0.02	3.00
	3	7.40	11.70	0.47	0.30	120.00	8.29	20.38	186.52	4.00	0.05	0.07	3.63
	7	13.80	25.50	1.03	0.56	50.00	6.44	26.83	112.64	5.88	0.13	0.20	4.85
	15	20.40	45.90	1.85	0.82	20.70	3.94	30.77	71.78	5.50	0.18	0.38	5.14
B		95.50	95.50	3.84	3.84	7.50	6.69	6.69	7.50	9.32	1.42	1.42	9.32

Table 51: Raw data - good ore- 59 g/t - C

Stream	Time	SOLIDS				PGM				Cr_2O_3			
		Mass	Cum. Mass	Cum.Mass distribution	Mass rec	Grade	Distribution	Cum. Recovery	Cum. Grade	Grade	Distribution	Cum. Recovery	Cum.Content
	Min	g	g	%	%	g/ton	%	%	g/ton	%	%	%	%
T		2335.40	2335.40	93.95	93.95	0.69	15.79	15.79	0.69	25.30	98.53	98.53	25.30
A		2485.90	2485.90	100.00	100.00	4.11	100.00	100.00	4.11	24.12	100.00	100.00	24.12
H	1	26.40	26.40	1.06	1.06	170.00	43.98	43.98	0.00	2.07	0.09	0.09	2.07
L	1	14.50	14.50	0.58	0.58	120.00	17.05	17.05	120.00	4.20	0.10	0.10	4.20
	3	11.20	25.70	1.03	0.45	100.00	10.98	28.03	111.28	6.50	0.12	0.22	5.20
	7	14.10	39.80	1.60	0.57	32.40	4.48	32.50	83.34	6.60	0.16	0.38	5.70
	15	17.10	56.90	2.29	0.69	18.10	3.03	35.54	63.73	7.00	0.20	0.58	6.09
B		67.20	67.20	2.70	2.70	7.13	4.70	4.70	7.13	11.60	1.30	1.30	11.60

Table 52: Raw data - good ore- 67 g/t - C

Stream	Time	SOLIDS				PGM				Cr_2O_3			
		Mass	Cum. Mass	Cum.Mass distribution	Mass rec	Grade	Distribution	Cum. Recovery	Cum. Grade	Grade	Distribution	Cum. Recovery	Cum.Content
	min	g	g	%	%	g/ton	%	%	g/ton	%	%	%	%
T		2337.90	2337.90	94.25	94.25	0.65	14.87	14.87	0.65	26.00	98.36	98.36	26.00
A		2480.60	2480.60	100.00	100.00	4.12	100.00	100.00	4.12	24.91	100.00	100.00	24.91
H	1	26.30	26.30	1.06	1.06	175.00	45.05	45.05	0.00	1.99	0.08	0.08	1.99
L	1	8.90	8.90	0.36	0.36	203.00	17.68	17.68	203.00	4.03	0.06	0.06	4.03
	3	7.70	16.60	0.67	0.31	120.00	9.04	26.73	164.50	5.73	0.07	0.13	4.82
	7	10.40	27.00	1.09	0.42	39.40	4.01	30.74	116.31	6.16	0.10	0.23	5.33
	15	14.30	41.30	1.66	0.58	24.40	3.42	34.16	84.49	6.02	0.14	0.37	5.57
B		75.10	75.10	3.03	3.03	8.05	5.92	5.92	8.05	9.71	1.18	1.18	9.71

Table 53: Raw data 67 g/t bad ore

Stream	Time	**SOLIDS**				**PGM**				**Cr_2O_3**			
		Mass	Cum. Mass	Cum.Mass distribution	Mass rec	Grade	Distribution	Cum. Recovery	Cum. Grade	Grade	Distribution	Cum. Recovery	Cum.Content
	Min	g	g	%	%	g/ton	%	%	g/ton	%	%	%	%
T		2238.60	2238.60	90.33	90.33	0.58	18.90	18.90	0.58	25.60	97.54	97.54	25.60
A		2478.30	2478.30	100.00	100.00	2.75	100.00	100.00	2.75	23.61	100.00	100.00	23.61
H	1	38.20	38.20	1.54	1.54	89.08	49.96	49.96	0.00	1.94	0.07	0.07	1.94
L	1	1.00	1.00	0.04	0.04	425.00	6.24	6.24	425.00	0.00	0.00	0.00	0.00
	3	2.20	3.20	0.13	0.09	144.00	4.65	10.89	231.81	0.00	0.00	0.00	0.00
	7	4.90	8.10	0.33	0.20	61.40	4.42	15.31	128.72	0.00	0.00	0.00	0.00
	15	4.40	12.50	0.50	0.18	33.20	2.14	17.45	95.10	5.78	0.08	0.08	5.78
B		189.00	189.00	7.63	7.63	4.93	13.68	13.68	4.93	6.18	2.17	2.17	6.18

Table 54: Raw data 51 g/t bad ore

Stream	Time	**SOLIDS**				**PGM**			
		Mass	Cum. Mass	Cum.Mass distribution	Mass rec	Grade	Distribution	Cum. Recovery	Cum. Grade
	min	g	g	%	%	g/ton	%	%	g/ton
T		2276.40	2276.40	91.06	91.06	0.65	16.70	16.70	0.65
A		2500.00	2500.00	100.00	100.00	3.54	100.00	100.00	3.54
H	1	26.40	26.40	1.06	1.06	146.00	43.49	43.49	146.00
L	1	28.00	28.00	1.12	1.12	63.80	20.16	20.16	63.80
	3	17.90	45.90	1.84	0.72	29.00	5.86	26.02	50.23
	7	22.20	68.10	2.72	0.89	17.10	4.28	30.30	39.43
	15	26.30	94.40	3.78	1.05	12.00	3.56	33.86	31.79
B		102.80	102.80	4.11	4.11	5.13	5.95	5.95	5.13

Table 55: Raw data - 43 g/t - bad ore

Stream	Time	SOLIDS				PGM			
		Mass	Cum. Mass	Cum.Mass distribution	Mass rec	Grade	Distribution	Cum. Recovery	Cum. Grade
	Min	g	g	%	%	g/ton	%	%	g/ton
T		2263.90	2263.90	90.56	90.56	0.64	16.78	16.78	0.64
A		2500.00	2500.00	100.00	100.00	3.45	100.00	100.00	3.45
H	1	23.50	23.50	0.94	0.94	127.00	34.56	34.56	127.00
L	1	51.20	51.20	2.05	2.05	45.50	26.97	26.97	45.50
	3	24.30	75.50	3.02	0.97	22.40	6.30	33.28	38.07
	7	29.70	105.20	4.21	1.19	16.40	5.64	38.91	31.95
	15	26.30	131.50	5.26	1.05	14.30	4.35	43.27	28.42
B		81.10	81.10	3.24	3.24	5.75	5.40	5.40	5.75

Table 56: Raw data - 55 g/t - bad ore

Stream	Time	SOLIDS				PGM			
		Mass	Cum. Mass	Cum.Mass distribution	Mass rec	Grade	Distribution	Cum. Recovery	Cum. Grade
	min	g	g	%	%	g/ton	%	%	g/ton
T		2258.90	2258.90	90.36	90.36	0.72	18.49	18.49	0.72
A		2500.00	2500.00	100.00	100.00	3.49	100.00	100.00	3.49
H	1	29.90	29.90	1.20	1.20	112.00	38.33	38.33	112.00
L	1	23.50	23.50	0.94	0.94	83.20	22.38	22.38	83.20
	3	15.40	38.90	1.56	0.62	36.70	6.47	28.85	64.79
	7	18.50	57.40	2.30	0.74	20.60	4.36	33.21	50.55
	15	29.80	87.20	3.49	1.19	11.00	3.75	36.96	37.03
B		124.00	124.00	4.96	4.96	4.38	6.22	6.22	4.38

Table 57: Raw data - 59 g/t - bad ore

Stream	Time	SOLIDS				PGM			
		Mass	Cum. Mass	Cum.Mass distribution	Mass rec	Grade	Distribution	Cum. Recovery	Cum. Grade
	Min	g	g	%	%	g/ton	%	%	g/ton
T		2312.75	2312.75	92.51	92.51	0.75	20.07	20.07	0.75
A		2500.00	2500.00	100.00	100.00	3.46	100.00	100.00	3.46
H	1	47.90	47.90	1.92	1.92	95.10	52.70	52.70	95.10
L	1	4.10	4.10	0.16	0.16	205.00	9.72	9.72	205.00
	3	3.15	7.25	0.29	0.13	106.00	3.86	13.59	161.99
	7	6.00	13.25	0.53	0.24	45.80	3.18	16.77	109.37
	15	10.50	23.75	0.95	0.42	26.70	3.24	20.01	72.82
B		115.60	115.60	4.62	4.62	5.40	7.22	7.22	5.40

Table 58: Raw data - 43 g/t - bad ore regrind

Stream	Time	SOLIDS				PGM			
		Mass	Cum. Mass	Cum.Mass distribution	Mass rec	Grade	Distribution	Cum. Recovery	Cum. Grade
	min	g	g	%	%	g/ton	%	%	g/ton
T		2237.20	2237.20	89.51	89.51	0.58	14.27	14.27	0.58
A		2499.40	2499.40	100.00	100.00	3.64	100.00	100.00	3.64
H	1	25.30	25.30	1.01	1.01	138.00	38.39	38.39	138.00
L	1	61.30	61.30	2.45	2.45	41.70	28.11	28.11	41.70
	3	33.50	94.80	3.79	1.34	20.00	7.37	35.47	34.03
	7	39.50	134.30	5.37	1.58	13.00	5.65	41.12	27.85
	15	27.50	161.80	6.47	1.10	10.00	3.02	44.14	24.81
B		75.10	75.10	3.00	3.00	3.88	3.20	3.20	3.88

Table 59: Raw data -51 g/t - bad ore regrind

Stream	Time	SOLIDS				PGM			
		Mass	Cum. Mass	Cum.Mass distribution	Mass rec	Grade	Distribution	Cum. Recovery	Cum. Grade
	min	g	g	%	%	g/ton	%	%	g/ton
T		2200.70	2200.70	89.16	89.16	0.45	12.75	12.75	0.45
A		2468.30	2468.30	100.00	100.00	3.15	100.00	100.00	3.15
H	1	29.00	29.00	1.17	1.17	100.00	37.33	37.33	100.00
L	1	45.90	45.90	1.86	1.86	40.00	23.64	23.64	40.00
	3	41.40	87.30	3.54	1.68	22.30	11.88	35.52	31.61
	7	35.70	123.00	4.98	1.45	14.00	6.43	41.95	26.50
	15	30.50	153.50	6.22	1.24	10.10	3.97	45.92	23.24
B		85.10	85.10	3.45	3.45	3.65	4.00	4.00	3.65

Table 60: Raw data – 59 g/t – bad ore regrind

Stream	Time	SOLIDS				PGM			
		Mass	Cum. Mass	Cum.Mass distribution	Mass rec	Grade	Distribution	Cum. Recovery	Cum. Grade
	Min	g	g	%	%	g/ton	%	%	g/ton
T		2237.20	2237.20	89.51	89.51	0.60	15.24	15.24	0.60
A		2499.40	2499.40	100.00	100.00	3.52	100.00	100.00	3.52
H	1	18.60	18.60	0.74	0.74	172.00	36.33	36.33	172.00
L	1	12.90	12.90	0.52	0.52	137.50	20.14	20.14	137.50
	3	20.60	33.50	1.34	0.82	50.90	11.91	32.05	84.25
	7	29.70	63.20	2.53	1.19	20.30	6.85	38.90	54.20
	15	45.50	108.70	4.35	1.82	7.63	3.94	42.84	34.70
B		134.90	134.90	5.40	5.40	3.65	5.59	5.59	3.65

Table 61: Raw data - 67 g/t - bad ore regrind

Stream	Time	SOLIDS				PGM			
		Mass	Cum. Mass	Cum.Mass distribution	Mass rec	Grade	Distribution	Cum. Recovery	Cum. Grade
	min	g	g	%	%	g/ton	%	%	g/ton
T		2217.20	2217.20	92.81	92.81	0.59	18.57	18.57	0.59
A		2388.90	2388.90	100.00	100.00	2.95	100.00	100.00	2.95
H	1	27.30	27.30	1.14	1.14	100.00	38.75	38.75	100.00
L	1	8.40	8.40	0.35	0.35	150.00	17.88	17.88	150.00
	3	7.50	15.90	0.67	0.31	100.00	10.65	28.53	126.42
	7	16.70	32.60	1.36	0.70	25.00	5.93	34.46	74.46
	15	26.60	59.20	2.48	1.11	10.00	3.78	38.23	45.50
B		85.20	85.20	3.57	3.57	3.68	4.45	4.45	3.68

Table 62: Raw data - 75 g/t - bad ore regrind

Stream	Time	SOLIDS				PGM				Cr_2O_3			
		Mass	Cum. Mass	Cum.Mass distribution	Mass rec	Grade	Distribution	Cum. Recovery	Cum. Grade	Grade	Distribution	Cum. Recovery	Cum.Content
	Min	g	g	%	%	g/ton	%	%	g/ton	%	%	%	%
T		2229.80	2229.80	89.12	89.12	0.54	13.43	13.43	0.54	26.40	97.51	97.51	26.40
A		2502.10	2502.10	100.00	100.00	3.58	100.00	100.00	3.58	24.13	100.00	100.00	24.13
H	1	15.90	15.90	0.64	0.64	188.00	33.34	33.34	188.00	1.99	0.05	0.05	1.99
L	1	7.00	7.00	0.28	0.28	296.00	23.11	23.11	296.00	3.04	0.04	0.04	3.04
	3	7.00	14.00	0.56	0.28	123.00	9.60	32.71	209.50	4.74	0.05	0.09	3.89
	7	8.50	22.50	0.90	0.34	58.80	5.57	38.29	152.57	6.00	0.08	0.17	4.69
	15	8.70	31.20	1.25	0.35	37.50	3.64	41.93	120.48	6.37	0.09	0.27	5.16
B		225.20	225.20	9.00	9.00	4.50	11.30	11.30	4.50	5.81	2.17	2.17	5.81

Single stage batch flotation was used for the preliminary test work. Rate tests were conducted at various times according to the following labels for each concentrate: RC1, RC2 et al. The rougher tails, collected at the end of the test, was labelled as RT.

Table 63: Preliminary ore - Test 1

Stream	Time	Mass	Cum. Mass	Mass distribution	Cum. Mass rec
	min	G	G	%	%
RC1	1	58.50	58.50	4.29	4.29
RC2	3	34.20	92.70	2.51	6.80
RC3	7	38.30	131.00	2.81	9.61
RC4	20	44.40	175.40	3.26	12.86
RT		1188.20	1363.60	87.14	100.00
Total (cal.)		1363.60			
Total (meas.)		1427.50			
Variance		4.48%			

Table 64: Preliminary ore - Test 2

Stream	Time	Mass	Cum. Mass	Mass distribution	Cum. Mass rec
	min	G	g	%	%
RC1	1	62.10	62.10	4.54	4.54
RC2	3	32.20	94.30	2.35	6.89
RC3	7	39.70	134.00	2.90	9.79
RC4	20	45.90	179.90	3.36	13.15
RT		1188.20	1368.10	86.85	100.00
Total (cal.)		1368.10			
Total (meas.)		1427.50			
Variance		4.16%			